

**Estimation of groundwater recharge in the context of future climate
change in the White Volta River Basin, West Africa**

Dissertation

zur

Erlangung des Doktorgrades (Dr. rer. nat)

der

Mathematisch-Naturwissenschaftlichen Fakultät

der

Rheinischen Friedrich-Wilhelms-Universität Bonn

vorgelegt von

EMMANUEL OBUOBIE

aus

GHANA

Bonn 2008

1. Referent: Prof Dr. B. Dieckrüger

2. Referent: Prof. Dr. B. Reichert

Tag der Promotion: 21.11.2008

Erscheinungsjahr: 2008

Diese Dissertation ist auf dem Hochschulschriftenserver der ULB Bonn
http://hss.ulb.uni-bonn.de/diss_online elektronisch publiziert

ABSTRACT

The White Volta River Basin is one of the major sub-basins of the Volta River Basin of West Africa. It covers about 106,000 km², and the major riparian countries are Burkina Faso and Ghana. The basin has enough water resources to meet current demands but there are many challenges including high spatial and temporal variability in rainfall, global climate change, deforestation, land degradation, and high population growth rate. These challenges put immense pressure on the water resources. The basin experiences a prolonged dry season when many rivers and streams dry up. As a result, surface water supplies are unreliable and insufficient to meet the water demands for socio-economic development in many places in the basin, thereby making groundwater sources the preferred and most cost-effective means of supplying water to the largely rural and dispersed population in the basin. A key prerequisite for efficient and sustainable management of the groundwater resource is the understanding and quantification of the groundwater recharge.

This study estimates the total amount and spatial distribution of the groundwater recharge at different scales in the White Volta Basin using the chloride mass balance, water table fluctuation, and hydrological modeling with the Soil and Water Assessment Tool (SWAT). In addition, the study evaluates the impact of future climate change on the shallow groundwater recharge.

The chloride mass balance method was applied in the northeastern part Ghana (Upper East Region of Ghana), within the basin, to estimate the long-term recharge. Based on the variation of chloride concentrations measured in groundwater samples taken from 11 wells in 2006, the estimated long-term annual groundwater recharge in the region ranged from 34.0 to 182.0 mm, with an area-weighted mean of 82.0 mm. The mean annual recharge represents 8 % of the long-term mean annual rainfall of 990 mm.

The water table fluctuation method was used in the south of the basin (commonly called the White Volta Basin of Ghana) to evaluate the seasonal and annual variations in water level rise and to estimate the groundwater recharge. The results show that annual water level rise ranged from 1238 to 5000 mm in 2006 and from 1594 to 6800 mm in 2007. Based on standard values of specific yield and the measured water level rise, the estimated annual recharge ranged from 28.0 to 150.0 mm in 2006 and from 32.0 to 204.0 mm in 2007. The area-weighted mean recharge was 70.0 mm in 2006, representing 8 % of the annual rainfall (870 mm), and 92.0 mm in 2007, representing 7 % of the annual rainfall (1294 mm).

The SWAT model was calibrated (1986-1999) and validated (1992-1999) at Nawuni for the whole White Volta River Basin. The simulated mean recharge to the shallow groundwater was 59.0 mm, about 7 % of the mean annual rainfall (824 mm). Using SWAT-simulated water balance for the present time period (1991-2000) as the basis for comparison, the simulated future (2030-2039) water balance in the White Volta Basin shows important increases in the mean annual discharge, surface runoff and shallow groundwater recharge as a result of future climate change in the basin. The shallow groundwater recharge is expected to increase by about 29 %.

KURZFASSUNG

Grundwassererneuerung vor dem Hintergrund des zukünftigen Klimawandels im Becken des Weißen Voltas, Westafrika

Das Weiße Voltabecken ist eines der wichtigsten Unterbecken des Voltabeckens in Westafrika. Die Fläche beträgt ca. 106,000 km², und die wichtigsten Anrainerstaaten sind Burkina Faso und Ghana. Die Wasserressourcen können den gegenwärtigen Bedarf decken, aber die hohe räumliche und zeitliche Niederschlagsvariabilität, der globale Klimawandel, Abholzung, Bodendegradation sowie starkes Bevölkerungswachstum führen zu einem enormen Druck auf die Wasserressourcen. Im Becken gibt es eine lange Trockenzeit wo viele Flüsse und Bäche austrocknen. Dadurch ist die Versorgung mit Oberflächenwasser unzuverlässig und reicht nicht, um den Wasserbedarf für die soziale und wirtschaftliche Entwicklung in vielen Gegenden des Beckens zu erfüllen. Das Grundwasser ist daher die bevorzugte und am kosteneffektivste Möglichkeit, die größtenteils ländliche und verteilte Bevölkerung im Becken mit Wasser zu versorgen. Am wichtigsten für ein effizientes und nachhaltiges Management der Grundwasserressourcen sind Kenntnisse über die Grundwasserneubildung sowie deren Quantifizierung.

Diese Studie untersucht die gesamte Höhe und räumliche Verteilung der Grundwasserneubildung im Weißen Voltabecken in unterschiedlichen Maßstäben mit den Methoden Chloridmassenbilanz, Grundwasserspiegel-Fluktuation, sowie hydrologische Modellierung mit dem Soil and Water Assessment Tool (SWAT). Außerdem bewertet die Studie die Auswirkungen des erwarteten Klimawandels auf die Neubildung von oberflächennahem Grundwasser.

Die Chloridmassenbilanz-Methode wurde im nordöstlichen Teil von Ghana (Upper East Region of Ghana) angewandt, um die langfristige Grundwasserneubildung zu ermitteln. Auf der Grundlage der Variation der Chloridkonzentrationen in Grundwasserproben aus 1100 Brunnen in 2006 lag die langfristige jährliche Grundwasserneubildung in der Region zwischen 34.0 und 182.0 mm, mit einem area-weighted Mittel von 82.0 mm. Die mittlere jährliche Neubildung stellt 8 % des langjährigen mittleren jährlichen Niederschlags von 990 mm dar.

Die Grundwasserspiegel-Fluktuationmethode wurde im Süden des Beckens eingesetzt (genannt Weißes Voltabecken von Ghana), um die saisonalen und jährlichen Variationen bei Grundwasseranstieg und Grundwasserneubildung zu ermitteln. Die Ergebnisse zeigen, dass der jährliche Anstieg des Grundwasserspiegels zwischen 1238 und 5000 mm in 2006 und zwischen 1594 und 6800 mm in 2007 lag. Auf der Grundlage der Standardwerte des spezifischen Ertrags und der gemessene Anstieg des Grundwassers betrug die jährliche Grundwasserneubildung zwischen 28.0 und 150.0 mm in 2006 und zwischen 32.0 und 204.0 mm in 2007. Die area-weighted mittlere Neubildung war 70.0 mm in 2006, und damit 8 % des jährlichen Niederschlags (870 mm), und 92.0 mm in 2007, die 7 % (1294 mm) darstellen.

Das SWAT-Modell wurde kalibriert (1986-1999) und validiert (1992-1999) in Nawuni für das ganze Weiße Voltabecken. Die simulierte mittlere Grundwasserneubildung im oberflächennahen Grundwasser betrug 59.0 mm, das sind ca. 7 % des mittleren jährlichen Niederschlags (824 mm). Mit der SWAT-simulierten

Wasserbilanz für den Zeitraum (1991-2000) als Vergleichsgrundlage zeigt die simulierte zukünftige (2030-2039) Wasserbilanz eine bedeutende Zunahme des durchschnittlichen jährlichen Niederschlags, Abflusses, Oberflächenabflusses und der Neubildung von oberflächennahem Grundwasser als Folge des zukünftigen Klimawandels im Becken. Es wird erwartet, dass die oberflächennahe Grundwasserneubildung um ca. 29 % zunehmen wird.

TABLE OF CONTENTS

1	INTRODUCTION.....	1
1.1	Overview of freshwater resources	1
1.2	Background of the study	3
1.3	Study objectives.....	6
1.4	Structure of the thesis	7
2	LITERATURE REVIEW.....	8
2.1	Groundwater recharge	8
2.2	Definition and concepts of groundwater recharge.....	8
2.3	Recharge estimation methods.....	10
2.4	Limitations and errors in estimating groundwater recharge.....	14
2.5	Recharge methods commonly used in semi-arid regions.....	15
2.6	Recharge estimates in the Volta Basin and other semi-arid areas in Africa.....	18
3	THE STUDY AREA.....	21
3.1	Introduction	21
3.2	Location	21
3.3	Topography	22
3.4	Climate	23
3.4.1	Rainfall.....	25
3.4.2	Temperature	25
3.4.3	Evapotranspiration	26
3.5	River runoff	26
3.6	Geology	28
3.7	Soils	30
3.8	Land-cover and -use	32
3.9	Hydrogeology	34
3.10	Demography	35
3.11	Groundwater resource utilization and problems.....	36
4	WATER TABLE FLUCTUATION METHOD FOR ESTIMATING GROUNDWATER RECHARGE.....	41
4.1	Overview	41
4.2	Method.....	42
4.2.1	Description of study area	42
4.2.2	Water level measurement.....	44
4.2.3	Estimation of water level rise (Δh)	45
4.2.4	Specific yield	47
4.3	Results and discussions	49
4.3.1	Water level rise	49
4.3.2	Recharge estimates.....	53

5	THE CHLORIDE MASS BALANCE METHOD FOR ESTIMATING GROUNWATER RECHARGE.....	56
5.1	Introduction	56
5.2	Study area	57
5.3	Data.....	58
5.3.1	Water sampling and chloride analysis	59
5.3.2	Rainfall measurements.....	59
5.4	Results and discussions	59
5.4.1	Chloride concentrations in rainfall.....	59
5.4.2	Chloride concentrations in groundwater.....	61
5.4.3	Recharge estimates.....	63
6	RECHARGE ESTIMATION USING THE SOIL AND WATER ASSESSMENT TOOL (SWAT).....	67
6.1	Introduction	67
6.2	SWAT hydrology	68
6.2.1	Precipitation	69
6.2.2	Surface runoff	71
6.2.3	Peak runoff rate.....	73
6.2.4	Surface runoff lag	74
6.2.5	Transmission losses	75
6.2.6	Evapotranspiration	75
6.2.7	Soil water	76
6.2.8	Groundwater	80
6.2.9	Reservoir	85
6.2.10	Flow routing.....	86
6.3	Sensitivity analysis	86
6.4	Model calibration and performance evaluation	88
6.5	Baseflow separation.....	92
6.6	SWAT input data preparation	92
6.6.1	Digital elevation model (DEM)	92
6.6.2	Land-use/ -cover data.....	93
6.6.3	Soil data	95
6.6.4	Climate data	98
6.6.5	River discharge data.....	100
6.6.6	Reservoir data	102
6.6.7	Other data.....	103
6.7	Results and discussion	103
6.7.1	White Volta Basin SWAT setup and sensitivity analysis.....	103
6.7.2	Effects of the number of rainfall stations and landuse on model output.....	105
6.7.3	Model calibration	106
6.7.4	Model validation	111
6.7.5	Annual water balance.....	115
6.7.6	Distribution of surface runoff and baseflow	118
6.7.7	SWAT recharge estimates.....	118

7	IMPACTS OF FUTURE CLIMATE CHANGE ON WATER RESOURCES.	120
7.1	Introduction	120
7.2	Climate change scenarios of MM5/ECHAM4	121
7.3	Frequency statistics of MM5 and measured rainfall series	123
7.4	Impacts of measured and generated climate series on water balance	126
7.5	Impacts of future climate change scenario on water resources	128
7.6	Comparison of study results with previous studies	133
8	CONCLUSIONS AND RECOMMENDATIONS.....	136
8.1	Introduction	136
8.2	Chloride mass balance method for estimating groundwater recharge.....	136
8.3	Water table fluctuation method for estimating groundwater recharge.....	137
8.4	Hydrological modeling and recharge estimation with SWAT	137
8.5	Impacts of future climate change on water resources	138
8.6	Final conclusions	139
8.7	Recommendations	139
9	REFERENCE.....	141

LIST OF ACRONYMS AND ABBREVIATIONS

AET	Actual Evapotranspiration
AGCM	Atmospheric Global Climate Models
AI	Agreement Index
AOGCM	Atmosphere-Ocean Global Climate Models
CMB	Chloride Mass Balance
CI	Continental Interclaire
CRU	Climate Research Unit (East Anglia)
CT	Complex Terminal
CV	Coefficient of Variation
DANIDA	Danish International Development Agency
DGH	Direction Générale des l’Hydraulique
ECHAM	European Centre Hamburg Model
FAO	Food and Agriculture Organization
GCM	Global Climate Model
GFDL	Geophysical Fluid Dynamics Laboratory (NOAA US)
GMSD	Ghana Meteorological Services Department
HADCM	Hadley Center Model
HAP	Hydrological Assessment Project of the Northern Regions of Ghana
HRU	Hydraulic Response Unit
IPCC	Intergovernmental Panel on Climate Change
LARS-WG	Long Ashton Research Station Weather Generator
LPIU	Livestock Planning and Information Unit (Ghana)
MOFA	Ministry of Food and Agriculture (Ghana)
MM5	Mesoscale Model
MRC	Master Recession Curve
MWH	Ministry of Works and Housing (Ghana)
NASA	United States National Aeronautics and Space Administration
NGA	National Geospatial-Intelligence Agency
NSE	Nash-Sutcliff model Efficiency
OGCM	Oceanic Global Climate Models

PET	Potential Evapotranspiration
PRECIS	Providing REgional Climates for Impacts Studies
R ²	Coefficient of determination
REMO	Regional MOdel
RCM	Regional Climate Model
SAGA	System for Automated Geo-Scientific Analysis
SRTM	Shuttle Radar Topography Mission
SWAT	Soil and Water Assessment Tool
UNEP	United Nations Environmental Programme
UNESCO	United Nations Educational, Scientific and Cultural Organization
USGS	United States Geological Survey
WASIM	Water flow and balance SIMulation Model
WEAP	Water Evaluation And Planning System
WRI	Water Research Institute (Ghana)
WTF	Water Table Fluctuation
ZEF	Center for Development Research (Germany)

1 INTRODUCTION

1.1 Overview of freshwater resources

The importance of water, particularly freshwater, has been recognized since the beginning of man. In every human society anywhere on the planet earth, water is said to be life because all aspects of life depend on it. Freshwater constitutes less than 3 % of the world's water resources but it is one of the world's most important natural resources and an indispensable part of all terrestrial ecosystems. It is a necessary input for many sectors of the global economy. In many world regions, particularly in developing regions like Africa, availability and access to freshwater largely determines patterns of economic growth and social development (Odada, 2006). Freshwater resources are pivotal to key economic and social activities such as water supply and sanitation, agriculture, industry, urban development, hydropower generation, inland fisheries, transportation and recreation among others. These activities provide employment and generate revenue that sustains many economies of the world. Besides its economic value, freshwater plays an important role in addressing issues of health, poverty and hunger and has been rightly recognized in the formulation of the United Nations' millennium development goals.

The importance of freshwater is increasing very rapidly due to the fast growth in the world's population, which has resulted in increased demand for the resource world-wide. Notwithstanding the increasing demand, the amount of freshwater available on the earth is limited. Its distribution is quite varied; many locations have plenty of it while others have very little. A UNEP (2002) study reveals that about one third of the world's population lives in countries with moderate to high water stress with disproportionately high impacts on the poor. The same study observes that, with the current projected human population growth, industrial development and expansion of irrigated agriculture in the next two decades, water demand will rise to levels that will make the task of providing water for human sustenance more difficult. Africa in general and West Africa in particular will be among the regions that are most likely to be affected.

Africa as a continent has an immense supply of rainfall, with an average annual of 744 mm, and relatively low withdrawals of water for its three major water sectors, namely agriculture, community water supply and industry (FAO, 2003).

However, natural phenomena such as rainfall variability and global climate change, and human factors such as over-exploitation and pollution, create a serious threat to the sustainability of Africa's freshwater resources, and hence the livelihood of the many poor that inhabit the continent.

Rainfall intensities and amount in Africa, particularly in western and central Africa, have high spatial and temporal variability within and between countries and river basins (UN-Water/Africa, 2006) with frequent events of drought and flood. Such natural variability has resulted in uneven distribution of surface and groundwater resources across the continent. While places like Comoros, Mauritius, Madagascar, Seychelles and the southern to the tropic belt of mid Africa have abundant freshwater resources, places like northern Africa, Sub-Saharan Africa including the Sahara and Kalahari deserts with severe aridity have very limited freshwater resources (Odada, 2006).

Global climate change puts further constraint on the already limited and unevenly distributed freshwater resources in Africa. In equatorial Africa, the climate is expected to become warmer with an average temperature increase of 1.4°C by 2050 (IPCC, 2001). Predicted hydrological changes associated with the expected increase in temperature include (1) an increase in precipitation of 5 to 30% from December to February and 5 to 10 % from June to August and (2) greater runoff (Joubert and Hewitson, 1997; Arnell, 1999; Nelson, 2005). In West Africa, Kunstmann and Jung (2003) among others, have predicted changes in rainfall patterns with a general increase in rainfall amount and an increase in the mean temperature of about 1.2°C in 2030-2039. Despite this, statistical analysis of long-term (1951-1991) observed rainfall and river discharge data in the Volta Basin of West Africa show significant reductions in both rainfall and river discharge in most areas of the basin (Opoku-Ankomah and Amisigo, 1996; Opoku-Ankomah, 2000; Gyau-Boakye and Tumbulto, 2006). Similar statistical analysis of observed rainfall from the 1960s and 1970s in other areas in West Africa found significant reductions in rainfall amounts and river discharges (Servat et al., 1997, Lebarbé and Lebel, 1997; Amani, 2001). Observations made on major rivers in the West African region since the early 1970s show a mean decline of 40-60 % in discharge (Niasse et al., 2004). Recharge to groundwater aquifers in the region have also

decreased noticeably. This is attributed to the decline in rainfall and runoff (Niasse et al., 2004).

Based on the above discussions, it is clear that wise management measures are required to address the many challenges that confront the sustainability of freshwater resources in West Africa in order to guarantee present and future provision of water for human sustenance.

1.2 Background of the study

The Volta River Basin is one of the 80 internationally shared lake and river basins in Africa. It is located in West Africa and shared by six riparian countries. The basin's water resource has been a very important input for the economic growth and development in the riparian countries. With the basin's population currently growing at an annual rate of 2.5 % (Andah et al., 2003), the demand for water will continue to increase significantly and will put immense pressure on the limited available water resources, which are concentrated in streams and rivers and groundwater aquifers.

The Volta Basin is fairly well watered with a mean annual rainfall ranging from 1600 mm in the humid southern parts to 600 mm in the extreme northern areas (VBRP, 2002). However, the rainfall is highly variable between the wet and dry seasons as well as from one place to another. The basin experiences a prolonged dry season of about 7 months in most areas, and as a result many of the rivers and streams are ephemeral in nature. Surface water supplies are unreliable, subject to high evaporative losses and insufficient to meet the water demand for socio-economic development everywhere in the basin. Besides, many of the surface water sources, particularly those used by small towns and rural communities have serious health risks with regard to water-related diseases such as bilharzias, cholera and guinea worm (MWH, 1998). Groundwater sources have become the preferred and cost-effective means of supplying water to meet the growing demand of the largely rural and dispersed population in the basin. Generally, the chemical and microbiological quality of groundwater is better than that of surface water. Additionally, groundwater sources respond more slowly to changes in rainfall, which makes it less vulnerable to drought compared to surface water.

Groundwater resources are used mainly for domestic and municipal water supply, as well as for watering of livestock and dry season irrigation of vegetables in many places in the basin. Over the past three decades, the exploitation of groundwater in the Volta Basin has increased substantially, particularly in the middle to north-eastern parts (Figure 1.1), which encompass large cities like Ouahigouya, Ouagadougou, and Bolgatanga (all within the White Volta sub-basin). Abstraction of groundwater in the basin is done mainly using boreholes fitted with hand pumps and mechanised boreholes connected to piping systems (Figure 1.2). An estimate made by Martin and van de Giesen (2005) reveals that about 44 % of the basin's total population depends on groundwater supply from both mechanised and hand-pump-equipped boreholes as well as from modern hand-dug wells. This figure is expected to increase as the population grows and water demand increases, leading to further exploitation of the groundwater resource. This could result in problems should the groundwater exploitation not be well managed.

Already, there are cases of groundwater depletion in some areas of the basin within Ghana. Gyau-Boakye and Tumbulto (2000) mentioned increased abstraction as the cause of the depletion. Over-abstraction of groundwater is said to be the reason for the diminishing yields of boreholes within a relatively short time and depletion of rivers in close proximity to areas of high borehole concentration (Water Research Institute-WRI, 2002). Open wells and some deeper boreholes in the basin are frequently experiencing reduced yields, sometimes drying up completely in the dry season (WRI/DANIDA, 1993; Martin and van de Giesen, 2005). During the drought of the 1980s, observation of groundwater levels showed pronounced drops (Wardrop Engineering, 1987 and Thierry, 1990), which is an indication of the impact of climate change on the groundwater resources in the basin.

Therefore, the development of groundwater resources in the Volta Basin must be well managed particularly in areas where the sustainability of the resources could be threatened by over-exploitation and contamination, as well as by climate change. A basic prerequisite for efficient and sustainable management of groundwater resource is the groundwater recharge (Lerner et al., 1990; Scanlon and Cook, 2002, Chand et al., 2005). Quantification of the recharge is needed, for example, to estimate the sustainable

yield of the groundwater aquifers (Sanford, 2002; Sophocleous and Schloss, 2000) and for rational and sustainable exploitation of the resource.

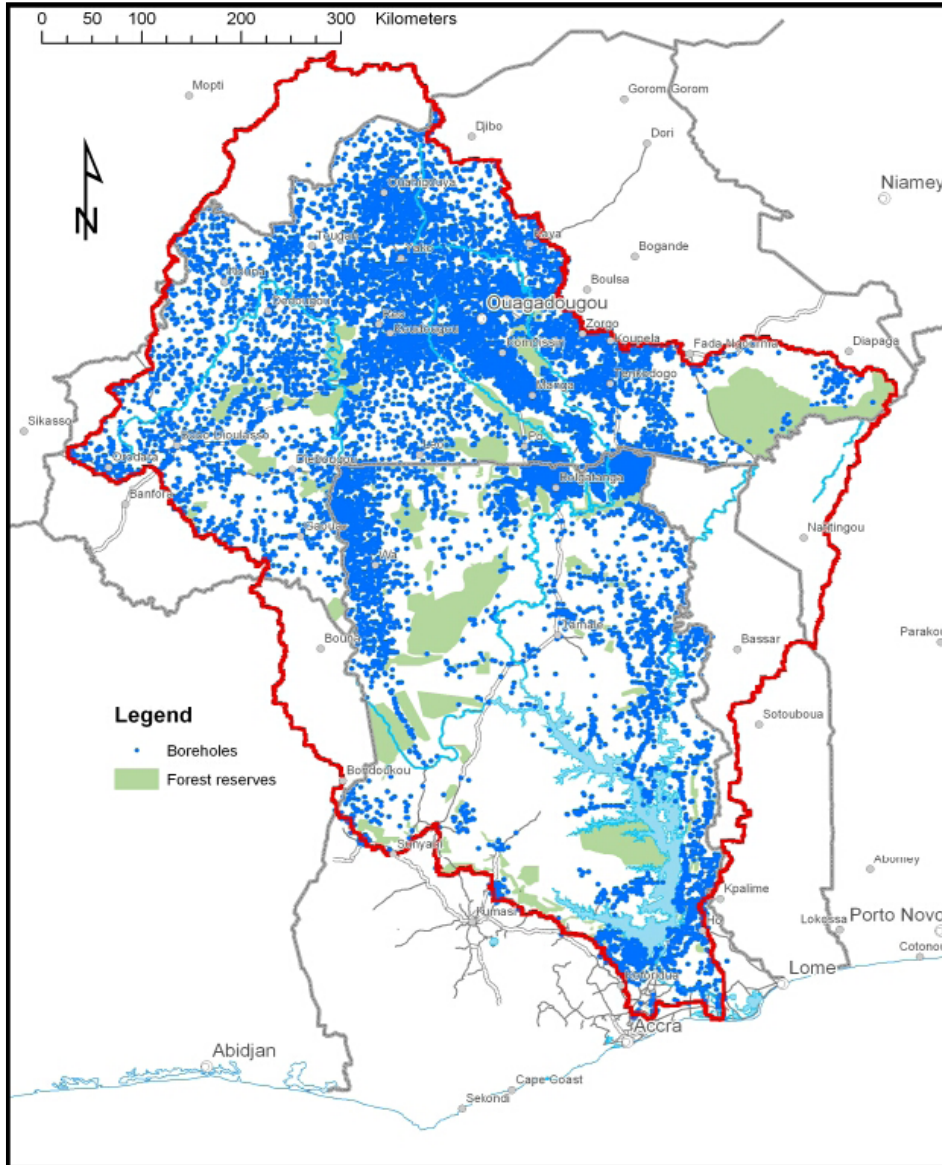


Figure 1.1 Location of hand-pump-equipped boreholes in the Volta River Basin of West Africa (Source: Martins, 2005)

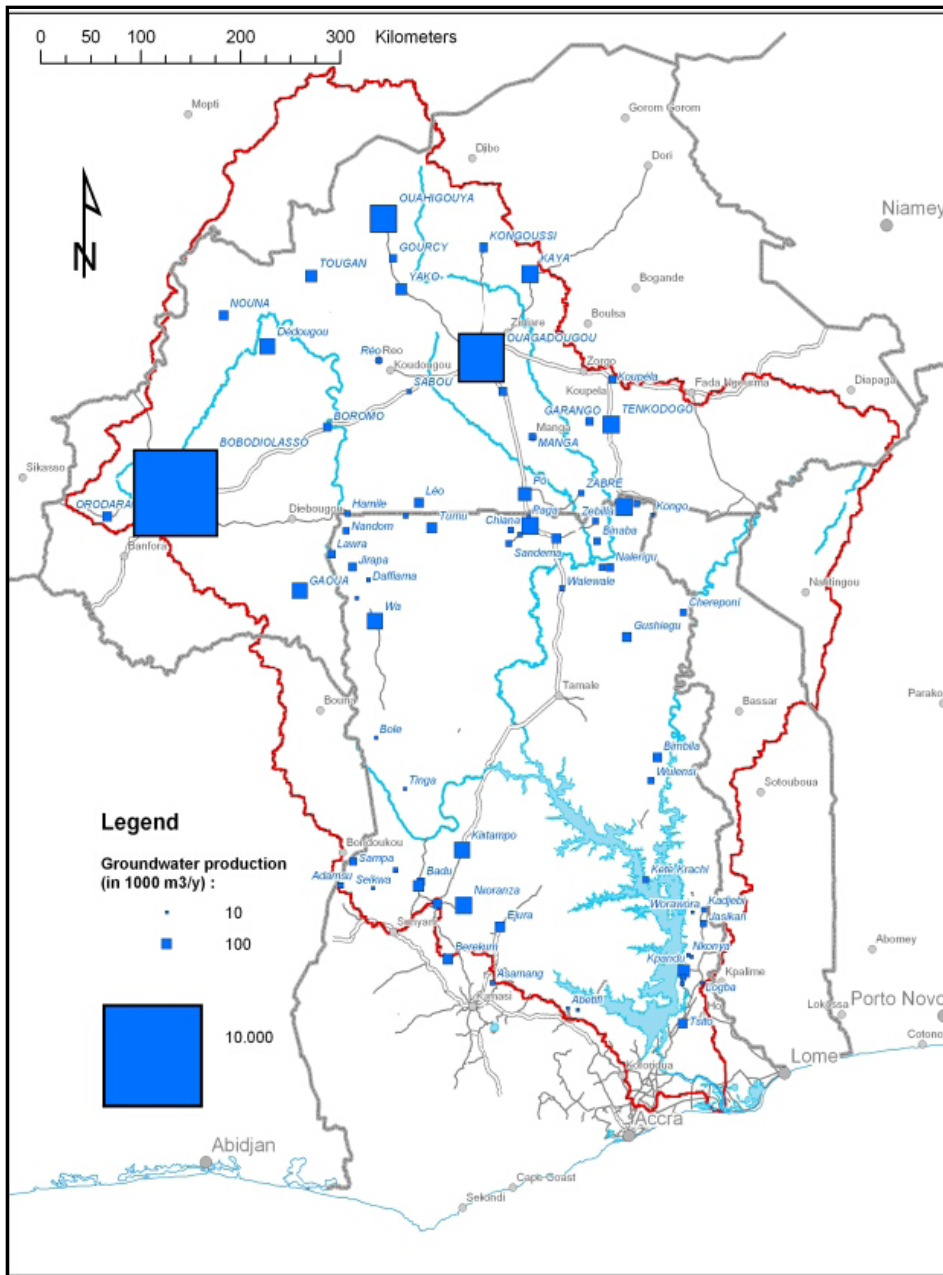


Figure 1.2 Groundwater-based Town water supply systems in the Volta River Basin of West Africa (Source: Martins, 2005)

1.3 Study objectives

This study seeks to contribute to the sustainable management of water resources in the Volta Basin by investigating the recharge to groundwater and the impact of future climate change on the hydrology and water resources in the White Volta sub-basin of the Volta Basin.

The specific objectives are to:

1. Estimate the total amount and spatial distribution of groundwater recharge in the White Volta Basin;
2. Evaluate the ability of a regional scale hydrological model, i.e., the Soil and Water Assessment Tool (SWAT), to reproduce the hydrological variables in the White Volta Basin;
3. Evaluate the impact of future (2030-2039) climate change on the water resources in the White Volta Basin.

1.4 Structure of the thesis

The first of the eight chapters of this thesis gives a general introduction and defines the context within which the study was done. It also outlines the objectives that guided the study. Chapter 2 presents a review of relevant literature on the mechanisms of groundwater recharge, of methods for estimating recharge and examples of recharge estimates from previous studies in arid and semi-arid areas. Chapter 3 provides a detailed description of the Volta River basin of which the study area, i.e., the White Volta Basin, is a major sub-basin. Chapter 4 discusses groundwater recharge estimation in the downstream part of the study area, using the water table fluctuation (WTF) method. Strengths and weaknesses of the WTF method are outlined. Besides the WTF method, the chloride mass balance (CMB) method for estimating groundwater recharge was applied to a smaller area within the downstream part of the study area. Chapter 5 elaborates on the CMB method and compares recharge estimates from the WTF and CMB methods.

Chapter 6 deals with modeling of watershed hydrology and groundwater recharge using the Soil and Water Assessment Tool (SWAT) model. The results of model calibration and validation, sensitivity analysis and model performance evaluation are discussed. Impacts of future climate change, mainly changes in rainfall and temperature, on the water resources in the study area are examined in Chapter 7. In the final Chapter, 8, the major conclusions of the study are discussed and recommendations for further studies given.

2 LITERATURE REVIEW

2.1 Groundwater recharge

Groundwater use is of fundamental importance and often the key to economic and social development in many areas world-wide, particularly in arid and semiarid areas where surface water supplies are unreliable and poorly distributed. The evaluation of the groundwater resources involves several factors of which the groundwater recharge is a key. An understanding of the recharge processes and the quantification of natural recharge rate are basic prerequisites for efficient and sustainable management of the groundwater resources (Foster, 1988; Scanlon and Cook, 2002, Chand et al., 2005). Quantification of the recharge is needed to estimate the sustainable yield of groundwater aquifers. Knowledge of aquifer sustainable yield is important for rational and sustainable exploitation of the groundwater resources (Sanford, 2002; Sophocleous and Schloss, 2000; Gonfiantini, et al, 1998; Scanlon, et al., 2002).

2.2 Definition and concepts of groundwater recharge

In a broader sense, groundwater recharge is defined by Lerner (1997) as water that reaches an aquifer from any direction, i.e., down, up, or laterally. In arid- and semi-arid- regions of the world, which include the White Volta Basin, recharge by downward flow of water through the unsaturated zone is generally the most important mode of recharge (Xu and Beekman, 2003). Therefore, groundwater recharge as used in this study refers to the downward flow of water reaching the water table from the unsaturated zone (Freeze and Cherry, 1979; Lerner et al., 1990). Recharge may occur naturally from precipitation, rivers, canals and lakes, and man-induced through activities of irrigation and urbanization (Lerner et al., 1990). This study is focused on recharge from precipitation, since it is the most important category of recharge in the White Volta Basin (Martin, 2005; Kortatsi, 1994). The recharge to groundwater is controlled by factors such as the rate and duration of precipitation or irrigation, the antecedent moisture condition of the soil profile, geology, soil properties, the depth to water table and aquifer properties, vegetation and land use, topography and landform.

The basic mechanisms of groundwater recharge in arid- and semi-arid- areas are reasonably well known. However, estimation of the various processes of the hydrological cycle in order to quantify the recharge is a difficult task (Lerner et al.,

1990). The two major flow mechanisms in arid- and semi-arid- areas are piston or uniform flow, and preferential flow. Often, in many locations both types of flow mechanisms occur simultaneously, though one may dominate (Figure 2.1). When water is supplied to the soil surface, some of the arriving water penetrates the surface and is absorbed into the soil, while some may fail to penetrate and instead accrues or flows over the surface. The water that does penetrate is itself later partitioned into the amount that returns to the atmosphere by evapotranspiration and that which seeps downward, with some of the latter re-emerging as stream flow while the remainder recharges the groundwater reservoir. The water that recharges the groundwater reservoir may later on re-emerge as stream flow.

Recharge can be expressed as a percentage of the annual precipitation or as an average rate of water in millimeters per year. The volume of recharge, expressed as cubic meters per year, can be obtained by multiplying the recharge rate by the land area under consideration.

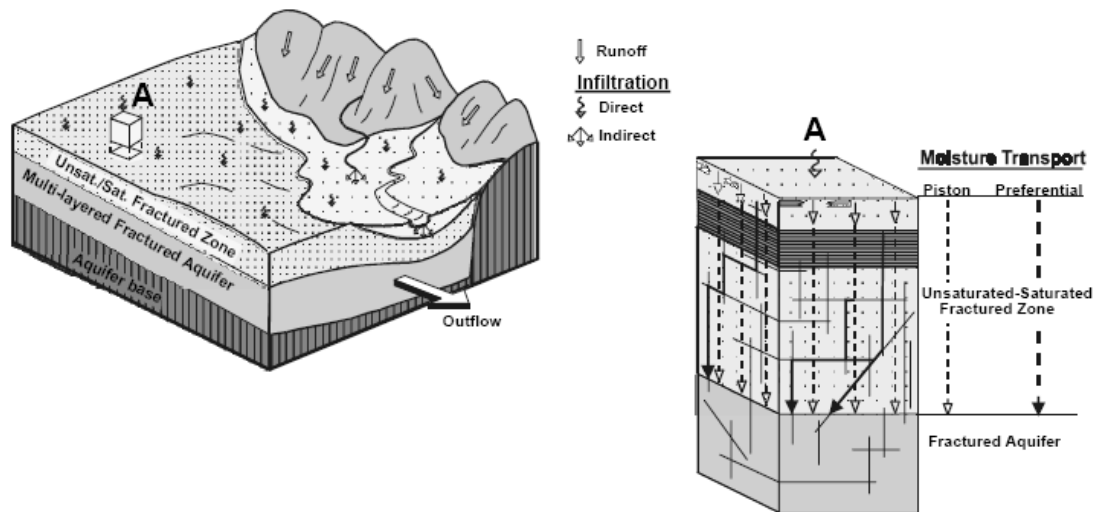


Figure 2.1 Mechanisms of infiltration and moisture transport that are likely to occur in arid- and semi-arid- areas (Beekman et al., 1996)

Recharge to groundwater can be classified as (i) direct or indirect on the basis of the origin of the recharging water, (ii) piston or preferential flow on the basis of the flow process through the unsaturated zone, (iii) point, line or areal recharge on the basis of the area on which it acts, and (iv) present-day, short-term or long-term recharge on

the basis of the time scale during which it occurs (Table 2.1) (Beekman et al., 1999; Lerner et al., 1999; Lerner et al., 1990). Again, recharge can be classified as actual, which refers to water that has infiltrated and reaches the water table, or potential, which refers to infiltrated water that may or may not reach the water table because of the unsaturated zone processes or the ability of the saturated zone to accept recharge (Rushton, 1997). In many locations, a combination of the recharge categories occurs.

Table 2.1: Definitions of categories of groundwater recharge

Category of recharge	Definition
<i>On the basis of origin of water:</i>	
Direct	Water added to the groundwater in excess of soil moisture deficits and evaporation by direct vertical percolation of precipitation through the unsaturated zone
Indirect	Percolation to water table following runoff and localization in joints, as ponding in low lying areas and lakes, or through the beds of surface watercourses
<i>On the basis of flow mechanism through the unsaturated zone:</i>	
Piston flow	precipitation stored in the unsaturated zone is displaced downwards by the next infiltration/percolation event without disturbance of the moisture distribution
Preferential flow	Flow via preferred pathways/macro-pores, which are sites (e.g., abandoned root channels, burrows, fissures) or zones (e.g., stream beds) in the unsaturated zone with a relatively high infiltration and/or percolation capacity
<i>On the basis of area on which it acts:</i>	
Point recharge	Recharge at a site, with no areal extent
Line recharge	Recharge from a line source e.g., drainage feature or river
Area recharge	Recharge over an area
<i>On the basis of time scale during which recharge occurs:</i>	
Present-day recharge	Recharge occurring within a time frame of days/months
Short-term recharge	Recharge covering a short period in the past or predicted for the near future within a time frame of months/years
Long-term recharge	Recharge over a longer period in the past (palaeo-recharge) or predicted for the future (accounting for climate change) within a time frame of tens up to thousands of years

2.3 Recharge estimation methods

Estimating groundwater recharge in arid- and semi-arid- regions can be difficult, since in such areas the recharge is generally low compared to the average annual rainfall or

evapotranspiration, and thus difficult to determine precisely (Scanlon et al., 2002; Beekman, 1999). Recharge processes vary from one place to another, and there is no guarantee that a method developed and used for one locality will give reliable results when used in another. Therefore, it is necessary to identify the probable flow mechanisms and the important features influencing the recharge in a locality before deciding on the recharge method to use (Lerner et al., 1990). The recharge to a groundwater aquifer cannot be easily measured directly, and usually estimated by indirect means (Lerner, 1990). The accuracy of the indirect estimates is usually difficult to determine, and therefore it is recommended that recharge should be estimated using multiple methods to obtain more reliable values (USGS, 2008; Scanlon et al., 2002; Lerner, 1990). A wide variety of methods exists for estimating groundwater recharge, which have been designed to represent the actual physical processes of the recharge.

Recharge estimation methods can be classified according to (i) hydrogeological provinces (Lerner et al., 1990), (ii) hydrologic zones (Scanlon et al., 2002; Beekman et al., 1999; Bredenkamp et al., 1995), (iii) physical, numeric modeling, and (iv) tracer techniques (Scanlon et al., 2002; Lerner et al., 1990; Kinzelbach et al., 2002). Scanlon et al. (2002) classified recharge methods on the basis of three hydrologic zones of studies namely surface water, unsaturated zone and saturated zone. Each of these zones provides a different set of data that can be used to estimate the groundwater recharge. Within each of the hydrologic zones, the recharge techniques were further classified into physical techniques, tracers and numerical modeling.

Recharge estimation methods based on surface water studies include physical methods e.g., channel-water budget, seepage meters and baseflow discharge; tracer methods e.g., stable isotopes of oxygen and hydrogen; numerical modeling methods e.g., deep percolation model, SWAT model and water budget equation. Methods based on the unsaturated zone studies include physical methods e.g., lysimeters, Darcy's law and zero-flux plane; tracer techniques e.g., bromide, ^3H , and visible dyes, ^{36}Cl , and Cl ; numerical modeling methods e.g., soil water storage routing, quasi-analytical approaches and numerical solutions to the Richards equation. Recharge estimation methods based on the saturated zone studies are physical methods e.g., water table fluctuation and Darcy's law; groundwater dating using traces such as CFC, $^3\text{H}/^3\text{He}$, and ^{14}C ; and groundwater flow modeling. A detailed description of each of the above-

mentioned techniques can be found in Scanlon et al. (2002), Scanlon et al. (2003) and Lerner (1990).

Based on several literatures, Scanlon et al. (2002) observed that recharge methods differ in terms of the typical quantity measured, the range of recharge values that can be expected, and the spatial and temporal scales that the recharge represents. Generally, techniques based on surface-water and unsaturated-zone studies provide recharge rates that are only potential, because the estimated recharge flux has not yet reached the water table and there may be losses during the flow process through the unsaturated zone. As such, the recharge rates estimated are sometimes less reliable compared to the estimates based on techniques of the saturated zone studies, which are actual recharge rates because the recharge flux reaches the water table. Techniques like historic tracers (e.g. $^3\text{H}/^3\text{He}$) applied in the unsaturated zone require a minimum recharge rate to transport the tracer through the unsaturated zone. Again, if the same tracer is applied in the saturated zone, it requires a yearly minimum of about 30 mm to confine the ^3He (Scanlon et al., 2002). Such techniques do not give reliable estimates when used in localities where the expected recharge rate is smaller. Environmental tracers like chloride, on the other hand, are often used to reliably estimate small recharge rates (e.g., Sami and Hughes, 1996; Wood and Sanford, 1995).

The spatial and temporal scale represented by recharge rates varies with the different methods. Unsaturated-zone methods often provide point or local-scale estimates of the recharge, whereas methods based on saturated-zone studies provide recharge estimates from local- to regional- scale. Additionally, tracer and physical methods usually provide point to local estimates with numerical modeling methods giving local to regional estimates. Large-scale integrated recharge estimates are often very useful in water-resource assessments, whereas detailed point to local-scale studies are useful for understanding aquifer vulnerability to potential contaminations. Surface water techniques such as seepage meters and streamflow gain/loss measurements, and unsaturated zone methods such as lysimeters, zero-flux plane, and applied tracers, and saturated-zone techniques, such as water-table fluctuations, give recharge estimates that represent a short time span, from instantaneous to any time period over which data are monitored (Scanlon et al., 2002). Modeling techniques such as watershed models and

deep percolation models can be used to estimate recharge over a long time scale, ranging from hours to years.

The use of modeling techniques has the added advantage that it can be used for the purpose of forecasting recharge. Forecasting groundwater recharge has become important because of the impact of envisaged climate change and increased demand for groundwater resources in the future (Kirchner, 2003). Recharge techniques that have great potential to forecast recharge are those that have established relationships between rainfall, abstraction and water levels (Xu and Beekman, 2003); models mostly have such established relationships.

Recharge methods differ also in terms of the ease of use, data needs and the associated cost (Table 2.2) (USGS, 2008).

Table 2.2 Comparison of selected recharge estimation methods (USGS, 2008)

Method	Temporal scale	Ease of use	Data needs	Relative cost
Chloride	Years	Easy	Moderate	Moderate
Chlorofluorocarbons	Month to Years	Difficult	Moderate	High
Deep percolation model	Day to Years	Moderate	Moderate	Moderate
Groundwater modelling	Month to Years	Moderate	High	High
Seepage meters	Event to Months	Moderate	Low	Low
Stream baseflow	Years	Easy	Low	Low
Tritium	Month to Years	Moderate	Moderate	High
Watershed models	Days to Years	Moderate	High	High
Water table fluctuation	Day to Years	Easy	Low	Low
Zero-flux plain	Day to Years	Difficult	High	High
Zero-tension lysimeters	Day to Years	Difficult	Low	High
Streamflow measurements	Instantaneous	Easy	Low	Low

On the basis of the differences among the recharge estimation methods as discussed above, the choice of appropriate methods for a recharge study requires the considerations of several factors such as the goal of the recharge study, the required accuracy and reliability, space and time scale, the range of the expected recharge estimates, the time to be spent on the study, and the financial resources available. These factors have been discussed in detail in Lerner et al. (1990), and Scanlon et al. (2002).

According to Lerner et al. (1990), a ‘good’ recharge estimation method should have five essential characteristics. First, the method should explicitly account for the water that does not become recharge in order to reduce the possibility of over-estimating the recharge. Second, with the exception of few methods that do not rely on knowledge of the recharge mechanism, a good method should reveal whether the conceptual model underlying it is incorrect. Third, it should be insensitive to parameters that are difficult to estimate accurately in order to provide estimates with low error. Fourth, the method should be easy to use and not require unusual or expensive data. Finally, the method should be able to use readily available data to extrapolate recharge over a long time scale.

2.4 Limitations and errors in estimating groundwater recharge

Estimating the recharge to groundwater is often achieved using indirect methods, because it is difficult to measure directly. The use of indirect methods is associated with various limitations, which make the recharge rates prone to large uncertainties and errors. For instance, unsaturated-zone methods are mostly founded on the principle of mass balance. An important underlying assumption of such recharge methods is that recharge occurs through a diffuse process or piston flow of water and, therefore, recharge flux through preferred pathways is often not accounted for. Meanwhile, in many arid- and semi-arid- areas, particularly in Sub-Saharan Africa, recharge flux via preferred pathways is the rule rather than the exception and, therefore, recharge estimates from unsaturated-zone methods can be questionable (Xu and Beekman, 2003; Tonder and Bean, 2003).

Lerner (1990) identified four types of errors associated with indirect estimation of the recharge. They are (i) incorrect conceptual model, (ii) neglect of spatial and temporal variability, (iii) measurement errors, and (iv) calculation errors. Incorrect conceptual model is the most serious and most common error type and arises when the recharge process is over-simplified or not properly understood. For instance, estimating recharge in semiarid areas using a water budget technique with monthly data can result in a zero recharge rate, which signifies no recharge, whereas occasional wet conditions can overcome soil moisture deficit and result in some recharge.

Most recharge processes have a non-linear relationship with time and space due to the variability of precipitation and evapotranspiration as well as soil and aquifer properties. For instance, an amount of rainfall over a period of time may result in no recharge due to high rate of evapotranspiration, but the same amount of rainfall spread over a shorter time period could be sufficient to saturate the soil and cause some recharge. Therefore, errors are likely to occur when the temporal and spatial variability in factors that control the recharge is neglected. Measurement errors are associated with equipment used to make measurements and are usually considered. Calculation errors, for instance, can result from the use of wrong units of the input parameters.

2.5 Recharge methods commonly used in semi-arid regions

Basically, the hydrological processes in arid- and semi-arid- climatic regions are not different from those in any other climatic region in the world. According to Lloyd (1986) cited in Lerner (1990), the only difference is that in some situations, the interrelationships between the different processes of the hydrological cycle are more emphasized under arid conditions. For instance, rainfall, a key hydrological process, is highly variable both spatially and temporally in arid- and semi-arid- areas, making the recharge rates also highly variable. Rainfall events in semi-arid areas usually have short duration and occur as intensive rainstorms. These influence the infiltration process by reducing the amount of direct recharge while increasing the amount of indirect recharge through pools of accumulated runoff, intermittent streams and preferential pathways (Lerner et al., 1990; HAPS, 2006).

Evapotranspiration, another key hydrological process, dominates the water budget in arid- and semi-arid- areas contrary to the situation in humid areas, where precipitation dominates. Therefore, many simplifying assumptions inherent in some of the recharge methods may not be valid for arid and semiarid areas. The water balance method, for instance, is widely used in all climatic regions, because it is simple to use and the required data are easily obtainable. However, the use of such technique is not always appropriate under arid conditions, because recharge in such areas constitutes a smaller proportion of the water budget, and the recharge term accumulates the errors in all the other terms of the equation (Gee and Hillel, 1988; Lerner, 1990; HAP, 2006).

Unsaturated-zone techniques such as lysimeters, zero-flux plane, historical tracers (e.g., ^{36}Cl and ^3H), environmental tracers (e.g., Cl) and numerical modeling are the most widely used methods for estimating groundwater recharge in arid- and semi-arid regions (Scanlon et al., 2002). Saturated-zone techniques such as Darcy's law and water table fluctuation have also been used widely in semi-arid areas, where the groundwater table is shallow.

Xu and Beekman (2003) reviewed literatures on recharge estimation methods used in a number of southern African countries (Botswana, Zimbabwe, Namibia and South Africa) and came up with a list of commonly used methods (Table 2.3). The list indicates that the chloride mass balance, cumulative rainfall departure, extended model for aquifer recharge and moisture transport through unsaturated hard rock, water table fluctuation, groundwater dating and modeling, historical tracers (e.g., ^3H) and the zero flux plane have often been used with high accuracy in the Southern African countries.

Table 2.3: Recharge estimation methods applied in arid- and semi-arid- Southern Africa (Beekman and Xu, 2003)

Zone	Method	Principle	References
Surface water	Hydrograph separation	Stream hydrograph separation: outflow, evapotranspiration and abstraction balances recharge	10
	Channel water budget	Recharge derived from difference in flow upstream and downstream accounting for evapotranspiration, in- and outflow and channel storage change	4
	Watershed modeling	Numerical rainfall-runoff modeling; recharge estimated as a residual term	5
Unsaturated	Lysimeter	Drainage proportional to moisture flux / recharge	2
	Unsaturated flow modeling	Unsaturated flow simulation e.g. by using numerical solutions to Richards equation	2, 4
	Zero-flux plane	Soil moisture storage changes below zero flux plane (zero vertical hydraulic gradient) proportional to moisture flux/recharge	2, 3, 6
	Chloride mass balance	Chloride Mass Balance Profiling: drainage inversely proportional to Cl in pore water	1, 2, 3, 6
	Historical tracers	Vertical distribution of tracer as a result of activities in the past (3H)	1, 2, 3, 6
Unsaturated - saturated	Cumulative rainfall departure	Water level response from recharge proportional to cumulative rainfall departure	2, 9
	Extended model for aquifer recharge and moisture transport through unsaturated hard rock	Lumped distributed model simulating water level fluctuations by coupling climatic, soil moisture and groundwater level data	3, 7
	Water table fluctuation	Water level response proportional to recharge / discharge	2
	Chloride mass balance	Amount of Cl into the system balanced by amount of Cl out of the system for negligible surface runoff/run on	1, 2, 3, 6
Saturated	Groundwater modeling	Recharge inversely derived from numerical modeling groundwater flow and calibrating on hydraulic heads /groundwater ages	2, 3
	Saturated volume fluctuation	Water balance over time based on averaged groundwater levels from monitoring boreholes	2
	Equal volume-spring flow	Water balance at catchment scale	2
	Groundwater dating	Age gradient derived from tracers, inversely proportional to recharge; Recharge unconfined aquifer based on vertical age gradient (^3H , CFCs, $^3\text{H}/^3\text{He}$); Recharge confined aquifer based on horizontal age gradient (^{14}C)	1, 6, 8

¹Beekman et al. (1996); ²Bredenkamp et al. (1995); ³Gieske (1992); ⁴Lerner et al. (1990); ⁵Sami and Hughes (1996); ⁶Selaolo (1998); ⁷van der Lee and Gehrels (1997); ⁸Weaver and Talma (1999); ⁹Xu and Van Tonder (2001); ¹⁰Xu et al. (2002)

2.6 Recharge estimates in the Volta Basin and other semi-arid areas in Africa

Recharge estimates from specific areas in the Volta Basin and its major riparian countries are reviewed in this section. In addition, recharge values from other areas in Africa with climatic condition and geology similar to what exists in the Volta Basin, were reviewed. These estimates have been obtained mostly as part of water balance and groundwater resource evaluation studies in research projects.

Gischler (1976), cited in Lerner et al. (1990) carried out a study on the aquifers of the Continental Interclaire (C.I.) and the Complex Terminal (C.T.) underlying the western areas of the Sahara desert. The C.I. aquifer extends over 600,000 km² with an average thickness of 250-600 m, transmissivity of 0.001-0.050 m²/s, and effective porosity of 20 %. Annual recharge to the C.I. aquifers is mainly by infiltration of runoff water and amounts to about 2.7 x 10⁸ m³ (0.45 mm). The C.T. aquifer covers an area of 350,000 km² with an average thickness of 100-400 m. The annual recharge was estimated to be 5.8 x 10⁸ m³, which is equivalent to 16.7 mm. Margat (1982) cited in Lerner et al. (1990) studied the multi-layer aquifer of the sedimentary basin underlying Mali, Niger and Nigeria. The aquifer consists of sand, sandstone and argillaceous sand with an average thickness of 240-300 m in Nigeria and 500 m in Niger. The basin has an average annual rainfall of 0-50 mm. The annual groundwater recharge in the basin was estimated to be 8.5 x 10⁸ m³.

Houston (1982) estimated the recharge to the Precambrian dolomitic limestone aquifer in a semiarid climate at Kabwe in Zambia using a modified version of the groundwater recharge model developed by Penman for temperate regions. The mean annual precipitation in the Kabwe area varies between 640 and 1470 mm. The aquifer has a high specific yield of about 14 % and an average transmissivity of about 1000 m²/d. The model was run for the period 1965-80 and under different conditions of vegetative cover. The annual recharge ranged from 26 to 771 mm under bare-soil vegetative cover, and from 0 to 534 mm under open forest.

In Zimbabwe, Huston (1988) studied the recharge to the groundwater aquifer in the Victoria Province as part of a programme on drought relief, commissioned by the Government of Zimbabwe and the European Economic Community. The area studied covers 22,000 km² and is underlain by basement granite and gneisses. The major aquifer in the area is a composite of weathered regolith of low permeability and high storage,

and the overlying fissured bedrock of high permeability and low storage. Three different recharge estimation techniques were applied in the study, and they all estimated a recharge of 2-5 % of the annual rainfall.

In Ethiopia, the annual groundwater recharge in the entire country is about 28,000 Mm³ (24.8 mm), while annual production is in the order of 18 Mm³ (0.02 mm) (Ketema and Tadesse, 2003). The natural recharge to groundwater in 14 major river basins in Ethiopia has also been estimated. This was done via baseflow separation using river discharge records from 17 selected river gaging stations (Ayenew et al., 2006). The estimated recharge ranges from 10 mm in the Mereb, Barka, Red sea, Gulf of Aden, Ogaden, and Danakil basins to 120 mm in the Baro-Akobo basin.

An FAO (1995) study in Burkina Faso shows that the annual recharge to the water table is about 5 mm in the northern part of the country, and 50 mm in the south. The same study estimated the total groundwater recharge for the whole of Burkina Faso to be 9.5 billion m³ (34.6 mm). Thierry (1988), cited in Leners (1990) used a lumped parameter hydrological model to examine the recharge to the fractured granites near Ouagadougou, the capital of Burkina Faso. The area has an average annual rainfall of 690 mm (1978-1985). The model was calibrated using water level data obtained from the monitoring of a well (20 m depth) drilled in the study area. The estimated annual recharge was between 23 and 45 mm (3.3 - 6.5 % of the annual rainfall).

At a smaller scale in south-eastern Burkina Faso, Sandwidi (2007) investigated the recharge to groundwater in the Kompienga Dam Basin, which has a semi-arid climate with mean annual rainfall of 830 mm (1959-2005). The basin is underlain by crystalline rocks of granite and amphibolites that have poor water storage capacity. Recharge to the groundwater is mostly by piston flow of the rainfall though preferential flow is dominant in a few places. Using the water balance, chloride mass balance and the water table fluctuation techniques, the recharge to the basin was estimated to be about 44 mm, representing 5.3 % of the basin's long-term mean annual rainfall.

As part of an investigation to design well fields in parts of Ghana, Bannerman and Ayibotele (1984) monitored water level in the Upper East and Upper West Regions of Ghana, all in the Volta Basin. Fluctuations of 0.3-5.4 m were observed between the dry and wet seasons for the period 1976 - 1979, and a recharge rate of 2.5 % of the mean annual rainfall (1075 mm) was used for designing the well field in the Upper West

Regional capital (Wa). In the Upper East Region, the groundwater recharge to the well field in Bawku was estimated to be 3-4 % of the mean annual rainfall (1000 mm) (Apambire, 1996).

Martin (2005) conducted a detailed recharge study in the Atankwidi basin in the semi-arid Sudan-Savanna climate zone of Ghana. The basin covers 275 km² and has a mean annual rainfall of 990 mm. The principal aquifer in the basin is the regolith aquifer that is found in the weathered mantle. Three methods, namely, water table fluctuation, isotope analysis and the chloride mass balance were used to estimate the recharge to groundwater in the basin. The results show considerable variation in recharge, not only between wet and dry years but also from one location to another. The recharge ranged from 2 to 13 % of the mean annual rainfall; the long-term mean was obtained to be 6 %.

In the Volta Basin, Friesen et al. (2005) investigated the water balance and the recharge to groundwater in the entire basin. The basin has a mean annual rainfall of 1002 mm. The net recharge was taken to be equal to the discharge of groundwater across the basin boundary i.e., baseflow. Recharge to the basin was estimated to be 5 % of the mean annual rainfall.

3 THE STUDY AREA

3.1 Introduction

This study was conducted within the White Volta Basin, which is a sub-basin of the Volta River Basin (Figure 3.1 and 3.2). However, a general description of the entire Volta Basin is provided in this chapter because data available in most literature is for the whole of the Volta Basin and not specifically for the White Volta Basin. Besides, data on most parameters in the White Volta Basin are not expected to show different patterns to those in the entire Volta Basin. Where data on the White Volta are available, these are provided.

3.2 Location

The Volta River Basin is located in the semi-arid and sub-humid zones of West Africa (Figure 3.1). It lies between 5° 30N -14° 30N and 2° 00E - 5° 30W and occupies about 28 % of the total West Coast (FAO, 1997). The basin is shared by six riparian nations with larger areas (82 %) falling within Burkina Faso and Ghana and smaller areas in Togo, Benin, Mali, and Côte d'Ivoire, in a decreasing order (Table 3.1) (Rodgers et al., 2007). The basin has a total surface area of about 400,000 km². The main channel of the Volta River stretches over a distance of about 140,000 km (Andah et al., 2005).

Table 3.1: Spatial distribution of Volta Basin between riparian nations (Andah and Gichuki, 2003)

Country	Area of Volta Basin (km ²)	Fraction of basin in country (%)	Fraction of country in basin (%)
Burkina Faso	178,000	42.65	63.00
Ghana	167,692	40.18	70.00
Togo	26,700	6.40	47.30
Benin	17,098	4.10	15.20
Mali	15,392	3.69	1.20
Côte d'Ivoire	12,500	2.99	3.90

The Volta River basin is drained by three main tributaries. They are the Black Volta River, White Volta and Oti River (Figure 3.1). The Black and White Volta Rivers join in northern Ghana to form the Lower Volta River, which is fed by the Oti River

further downstream in the southeast of Ghana. The tributaries drain various portions of the basin in Mali, Burkina Faso, Ghana, Côte d'Ivoire, Togo and Benin (Table 3.2). A feature of hydrological importance in the Volta basin worth mentioning is the Volta Lake (Figure 3.1), which is one of the largest man-made lakes in the world. Construction of the Lake started in 1961 and was completed in 1964. With a surface area of 8,500 km², the Volta lake covers about 4 % of the total land area of Ghana and has a storage capacity of 148 km³ (FAO, 1997). The lake is used mainly for generating electric power with a total of about 1,060 MW of hydropower generated at two sites (Akosombo and Kpong). About 95 % of the generated power in Ghana comes from plants at these two sites.

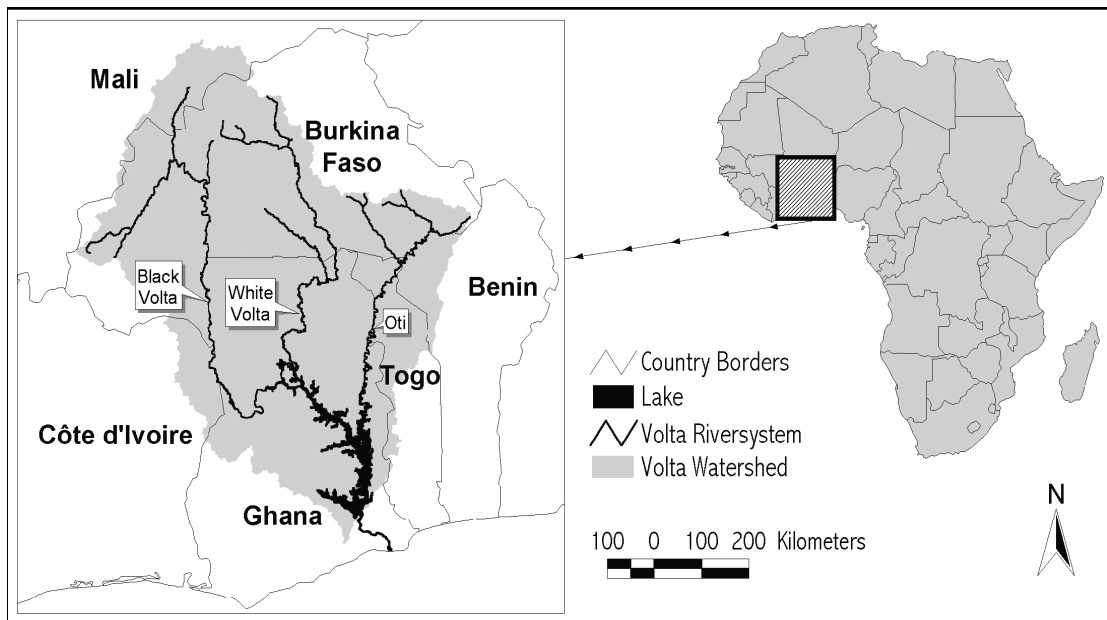


Figure 3.1 Map of the Volta Basin (van de Giesen et al., 2001)

Table 3.2: Main tributaries of the Volta River basin and characteristics (modified from Rodgers et al., 2007)

Main tributaries of the Volta River	Source of River	Drainage coverage	Drainage area (km ²)
Black Volta	Mali	western Burkina Faso and small areas in Mali and Côte d'Ivoire	147, 000
White Volta	Burkina Faso	northern and central Burkina Faso and Ghana	106, 000
Oti	Burkina Faso	North-western Benin and Togo, south-eastern Burkina Faso and Ghana	72, 000
Lower Volta	Ghana	Middle to southern parts of Ghana	73, 000

3.3 Topography

Generally, the Volta Basin has a predominantly flat topography with a mean elevation of 257 m. More than half of the basin lies in the elevation range of 200-300 m. The lowest point is in the Lower Volta Basin at about 1 m and the highest is in the Oti Basin at about 920 m (Barry et al., 2005). In the White Volta Basin, the maximum and mean elevations are 600 m (Andah et al., 2003) and 270 m (Barry et al., 2005), respectively.

3.4 Climate

The climate of the Volta Basin is controlled by the movement of the Inter-tropical Convergence Zone (ITCZ) that dominates the climate of the entire West African region. The ITCZ is the inter-phase of the hot, dry and dusty northeast trade wind that blows from the Sahara in the north of the region and the cool and moist southwest trade wind that blows over the sea from the south Atlantic. The ITCZ moves across the Volta Basin in a complex manner resulting in a mono-modal rainfall pattern in areas that it crosses once and a bi-modal rainfall pattern in areas that it crosses twice. The movement of the ITCZ is associated with vigorous frontal activities, which influence the amount and duration of rainfall over the basin (Amisigo, 2005; Andah et al., 2003).

At least two major climatic zones can be identified in the Volta Basin: the humid south with two distinct seasons of rainfall that peaks in June and September (Figure 3.2), and the tropic north with one rainfall season that peaks in August/September (Figure 3.3). Most areas of the basin fall within the tropic north zone. The rainfall in the tropic north zone is poorly distributed and very much skewed towards the month of June to September during which over 70 % of the total annual rainfall occurs (Amisigo, 2005). In the humid south zone, rainfall is evenly distributed over the year. Average monthly temperatures in both zones are always above 25 °C.

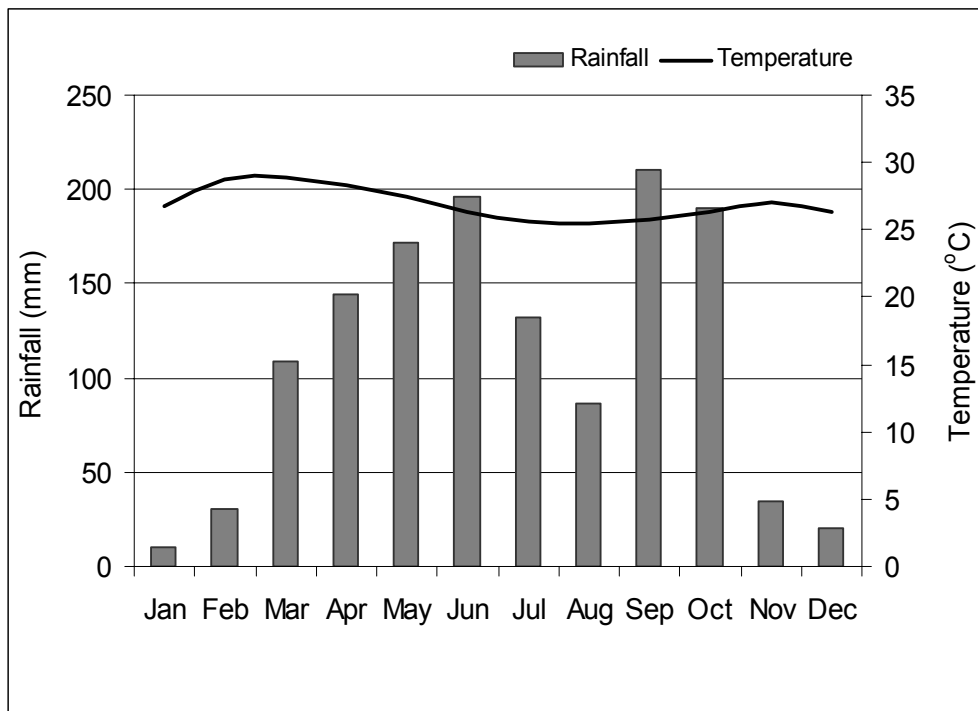


Figure 3.2 Mean monthly rainfall and temperature at Ejura, Ghana (representing the humid south climatic zone) (Data source: Ghana Meteorological Services Department)

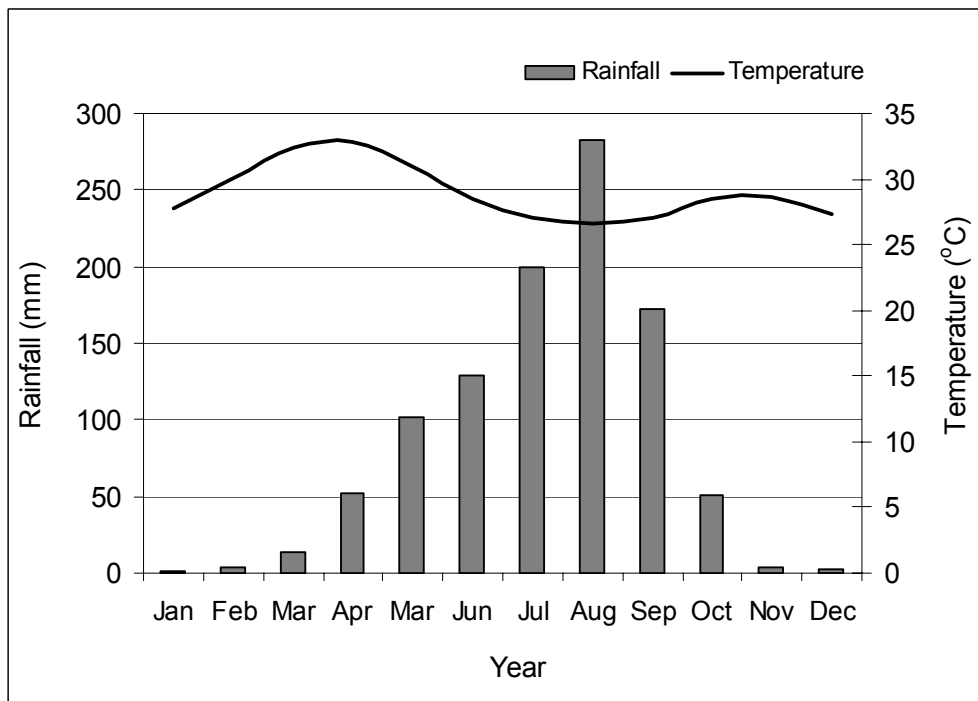


Figure 3.3 Mean monthly rainfall and temperature at Navrongo, Ghana (representing the tropic north climatic zone) (Data source: Ghana Meteorological Services Department)

3.4.1 Rainfall

Annual mean rainfall in the Volta Basin ranges from 600 mm in the extreme north in Mali and Burkina Faso to about 1,600 mm in the humid south in Ghana (VBRP, 2002). The annual mean rainfall in the White Volta Basin varies from 1,200 mm in the south to 600 mm in the north (VBRP, 2002). Similar to other areas in the West African region, rainfall in the Volta Basin is characterized by high spatial and temporal variability. However, compared to runoff, the annual mean rainfall over the entire basin suggests a fairly even temporal distribution with lower coefficient of variation (Figure 3.4) (Andreini et al., 2000). The low temporal variability at the basin scale is attributed mainly to integration over space and time (van de Giesen et al., 2001).

The periods of the rainfall seasons in the Volta Basin are pretty well known, but the onset of the rainy season is unpredictable, making rainfed agriculture a highly risky source of livelihood.

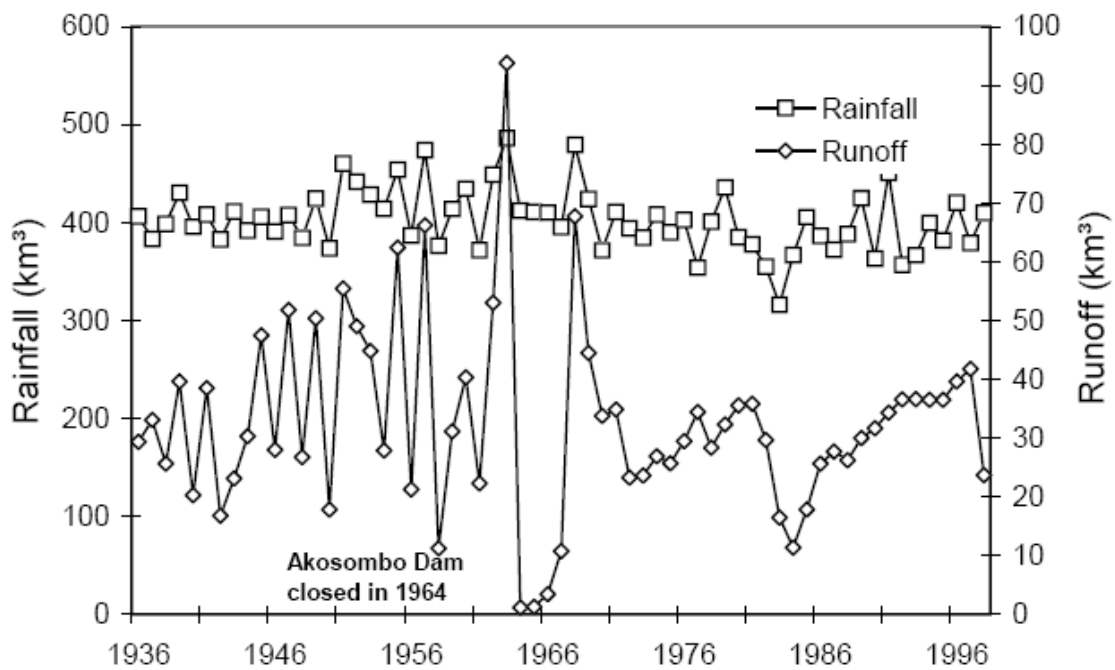


Figure 3.4 Annual rainfall and runoff in the Volta Basin (Andreini et al., 2000)

3.4.2 Temperature

Temperatures increase in a south-north direction in the Volta Basin, although the variation is not high. Mean monthly temperatures vary from 36 °C in March to 27 °C in August in the northern parts of the basin, and from 30 °C in March to 24 °C in August in

the south (Oguntunde, 2004). Daily maximum temperatures vary from 32 to 44 °C, usually recorded in March to April; while daily minimum temperatures are recorded in December to February and can be as low as about 14 °C in January (FAO, 1997).

3.4.3 Evapotranspiration

Evapotranspiration is the most significant component of the water balance in the Volta Basin. The annual mean potential evapotranspiration varies from 2500 mm in the north to 1800 mm in the coastal zone (Amisigo, 2005). Potential evapotranspiration exceeds rainfall for most part of the year, usually from 6 to 9 months (Figure 3.7).

Andreini et al. (2000) and Martin (2005) estimated the actual evapotranspiration rates, as percentage of the total rainfall, for the Volta basin and the Atankwidi catchments within the White Volta basin to be 91 % and 70-87 %, respectively.

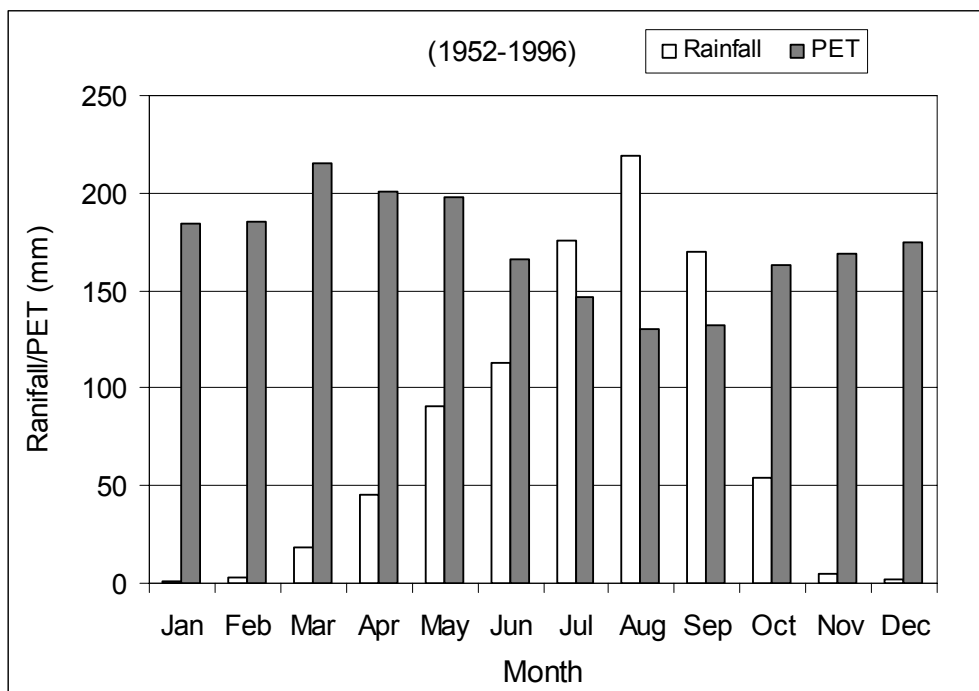


Figure 3.5 Mean monthly rainfall and potential evapotranspiration at Nawuni in the White Volta Basin in Ghana. PET is based on the Penman-Montheith method (Data source: Ghana Meteorological Services Department)

3.5 River runoff

A water balance developed by Andreini et al. (2000) for the Volta Basin shows that about 9 % of the rain falling in the basin ends up in the Volta Lake as total runoff. The

temporal variability of the annual runoff is higher than that of the rainfall in the basin as a whole (Figure 3.4) as well as in each of the sub-basins (Table 3.3). This has been attributed to a non-linear response of runoff to rainfall and to threshold effects in the basin (Andreini, et al., 2000; Amisigo, 2005).

Table 3.3: Rainfall and runoff of the Volta sub-basins (Andreini et al., 2000)

Sub-basin	Black Volta	White Volta	Oti
Period of management	1955-1975	1954-1980	1960-1973
Mean annual rainfall (mm)	952.4	952.8	1166.7
Coefficient of variation, rainfall	0.09	0.07	0.07
Mean annual runoff (mm)	47.6	66.0	152.8
Coefficient of variation	0.52	0.33	0.38
Runoff as % of rainfall in sub-basin	5	7	13

Notwithstanding the relatively high temporal variability of annual runoff in the Volta Basin, Andreini et al. (2000) found a strong correlation between the annual rainfall (P) and runoff (Q) (Equation 3.1), with a regression coefficient of 0.89. Equation 3.1 implies that runoff can occur only after a threshold of 343 km³ of annual rainfall is exceeded in the basin, when about half of the additional rainfall becomes available as runoff in river channels. van de Giesen et al. (2001) noted that runoff in the Volta Basin is very sensitive to variations in rainfall and to changes in land use and cover.

$$Q = 0.529(P - 343) \quad (km^3 year^{-1}) \quad (3.1)$$

The annual stream hydrograph at Nawuni on the White Volta basin, between 1984 and 2000, shows no clear pattern regarding periods of dry and wet years as there are nearly equal number of dry and wet years (Figure 3.6). The monthly stream discharge in the basin has a mono-modal pattern with the peak occurring in September (Figure 3. 7).

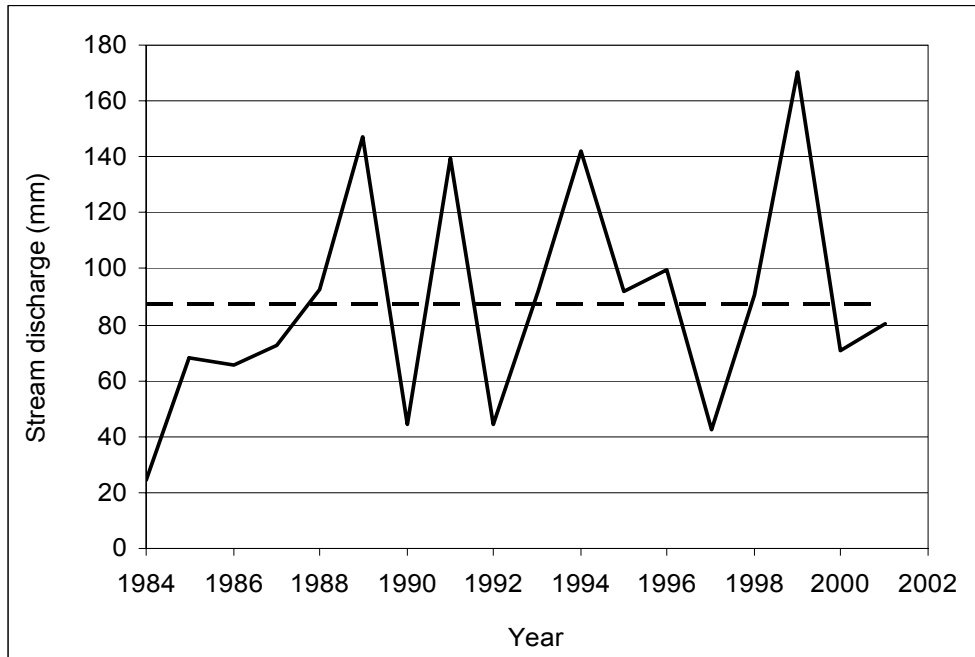


Figure 3.6 Annual stream hydrograph for Nawuni on the White Volta River (Data source: Ghana Hydrological Services Department)

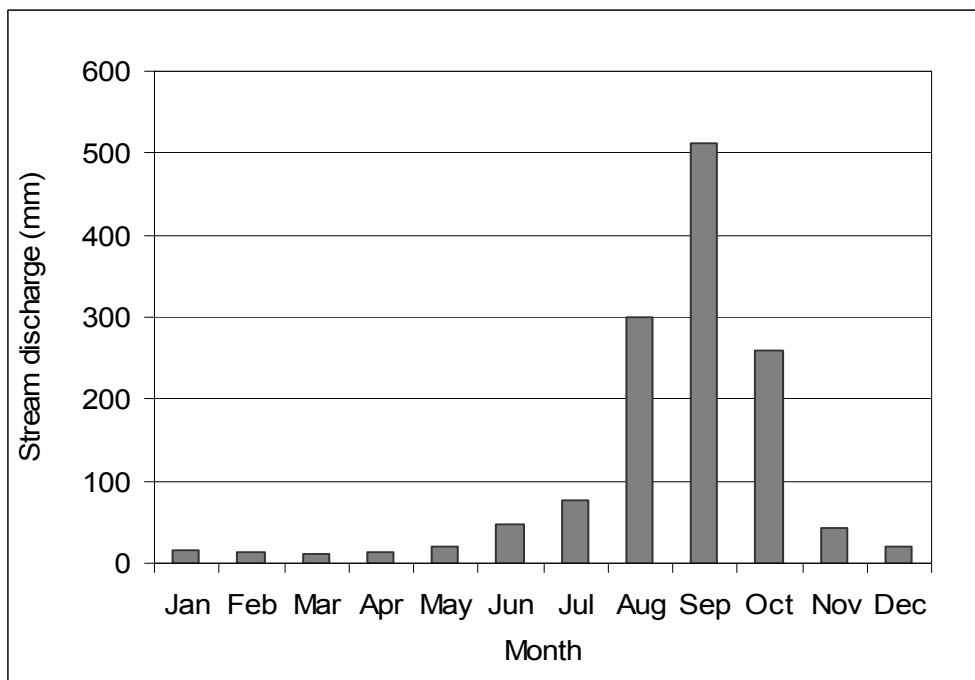


Figure 3.7 Mean monthly stream discharge for Nawuni on the White Volta River (1984-2001) (Data source: Ghana Hydrological Services Department)

3.6 Geology

The geology of the Volta Basin is dominated by basement crystalline rocks associated with the West African Craton. These rocks are of Precambrian age and consist of

granite-gneiss-greenstone rocks, strongly deformed metamorphic rocks, and anorogenic intrusions (Key, 1992). The Precambrian formation is commonly categorized into the Birimian super group (with associated granitoid intrusion), Tarkwan group, Dahomeyan formation, Togo formation and the Buem formation (Figure 3.8).

The dominant geological formation in the southern part of the basin is the Palaeozoic consolidated sedimentary formation, which was formed in a depression of the West African Craton. This formation is commonly called the Voltaian system and consists mainly of sandstones, shales, arkose, mudstones, sandy and pebbly beds, and limestones (MWH, 1998). On the basis of lithology and field relationships, the Voltaian system can be grouped into the upper, middle and lower Voltaian. The upper Voltaian consists of massive and thin-bedded quartzite sandstones, which are interbedded with shale and mudstones in some areas. The middle Voltain (Obusum and Oti Beds) mostly consists of shales, sandstones, arkose, mudstones, and siltstones. The lower Voltaian consists of massive quartzite sandstone and grit (MWH, 1998). Geological formations in the northwestern part of the basin consist of thick layers of sandstones, schist and carbonates of the zone de Sédimentaire and sandstones of the tertiary continental terminal (Martin, 2005).

The White Volta sub-basin is mostly underlain by the Birimian system of the Precambrian age with the associated granitic intrusives and isolated patches of the Tarkwaian formation, and the Voltain sedimentary system. The Birimian system consists of gneiss, phyllite, schist, migmatite, granite-gneiss and quartzite (Gyau-Boakye and Tumbulto, 2006).

Most geological formations in the basin are overlain by the so-called regolith, which is a weathered layer that varies in thickness and lithology (Martin, 2005; HAP, 2006). Regolith thickness in the Precambrian formation varies widely with an average ranging from 10 to 40 m (can be up to 140 m) in the southern part of the basin (Smedley, 1996), and ranging from 15 to 40 m (can be up to 100 m) in the north (Palacky et al., 1981; Groen et al., 1988). In the Voltain system, the regolith thickness is less than the Precambrian formation and generally ranges from 4 to 20 m (Acheampong, 1996).

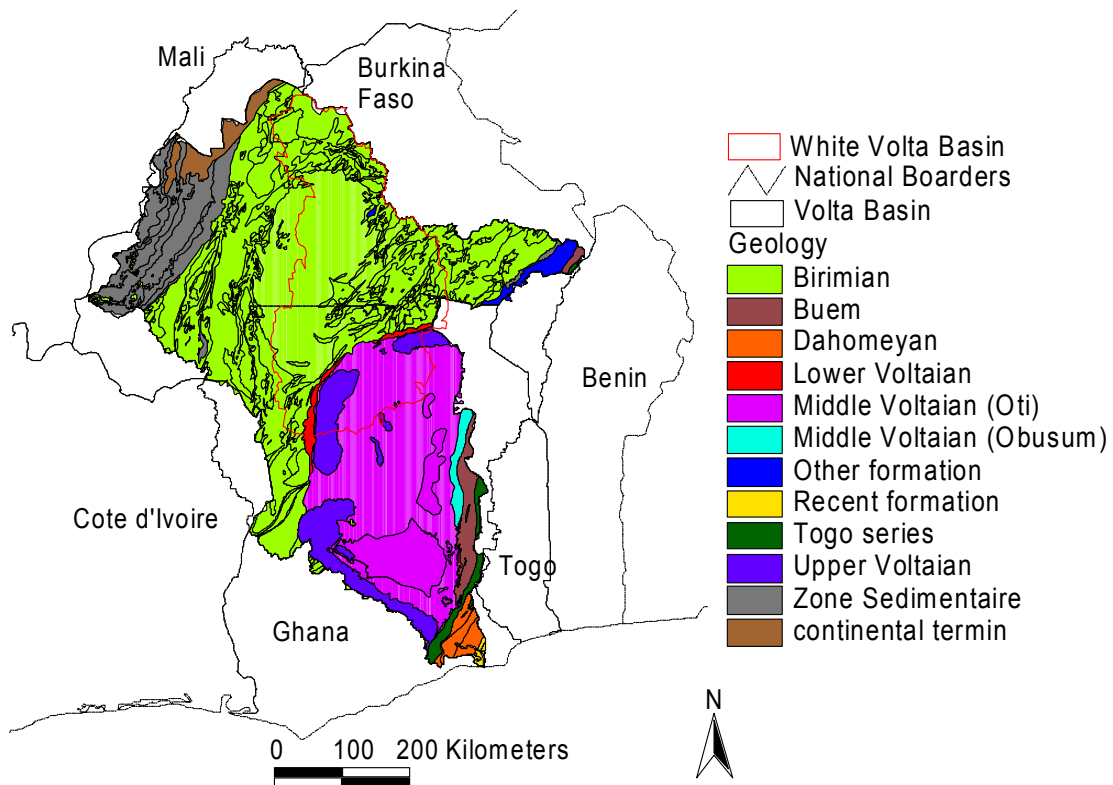


Figure 3.8 Geology of the Volta River Basin (Source: GLOWA Volta Project)

3.7 Soils

Soils in the Volta Basin have been formed from weathered parent materials of the mid Palaeozoic age or older (Andah et al., 2005) and have been leached over a long period (Benneh et al., 1990). The parent materials consist of sandstone, shale, igneous and granite among others. Based on the FAO-UNESCO (1974) soil classifications legend, 12 major soil types can be identified in the Volta basin (Figure 3.9). By far, Luvisols are the dominant soil type in the basin and occur everywhere in the basin except for the areas in the extreme north where Regosols and Arenosols dominate. Luvisols are soils which have an argic B horizon that has a cation exchange capacity equal to or more than 24 cmol (+) kg⁻¹ clay and a base saturation of 50 % or more throughout the B horizon to a depth of 125 cm (FAO-UNESCO, 1994). The Luvisols found in the basin particularly those in the north have low nutrient content and unstable soil structure, thereby making them prone to slaking and erosion on sloping land.

Besides the Luvisols, Regosols and Arenosols are the other dominant soils found in the north of the basin. Regosols are soils from unconsolidated materials that are coarse-texture. They are sensitive to erosion due to low coherence of the soil matrix material (Mando, 2001). Regosols in the basin have high permeability and low water holding capacity which makes them sensitive to drought. Arenosols are found in the upland areas and have high clay activity. They have low fertility and low water holding capacity which limits their ability to produce high yields of crops.

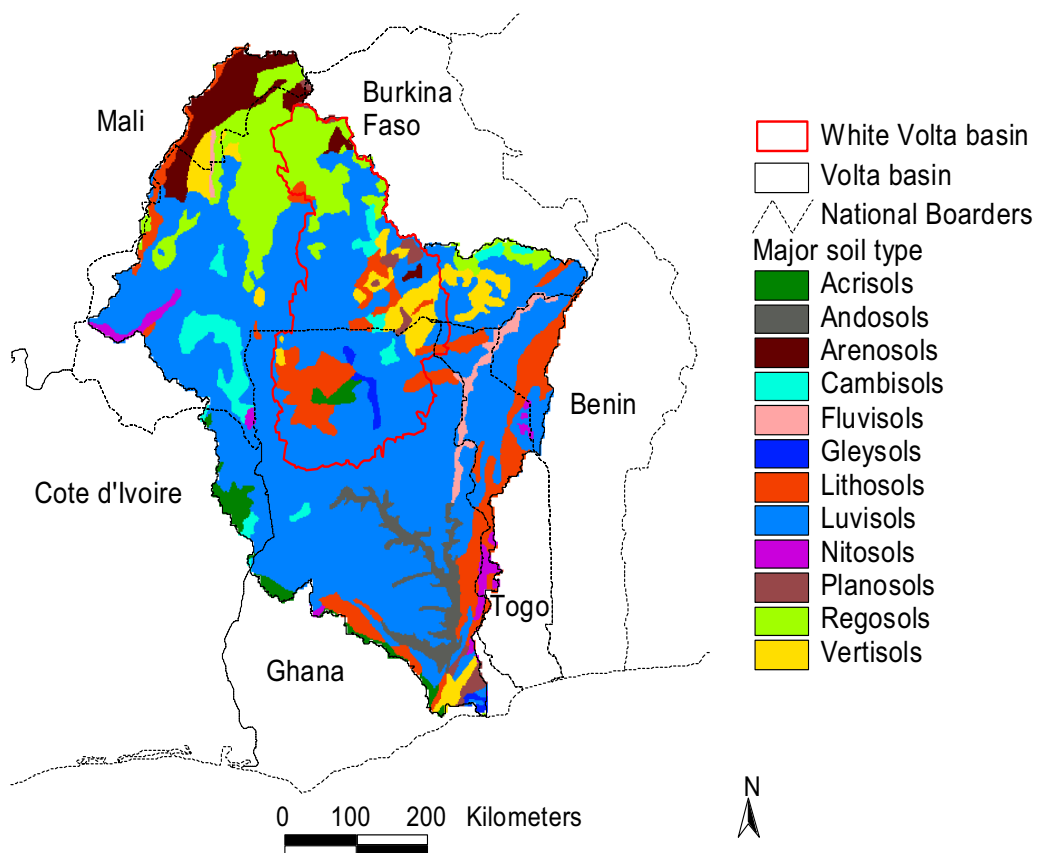


Figure 3.9 Soil map of the Volta River Basin (FAO, 1995)

In the southern parts of the basin in Ghana, Lithosols are the most important soils after Luvisols. These soils are mostly well to moderately well drained, gravely with a light-textured matrix which in some areas in northern Ghana overlies an iron pan developed *in situ* at shallow depth. Generally, Lithosols found in the north of Ghana have low cation exchange capacity, low aggregate stability, low organic content and fertility compared with those found in more humid climatic conditions in the southeast

which are rich in organic matter and have high fertility. Additionally, the Lithosols in the north of Ghana have root-zone limitation due to surface layers of plinthite, ferruginous concretion or ironpan, and surface sealing under the effect of rains resulting in increased runoff.

In the study area, the White Volta basin, the dominant soil types are Luvisols, Regosols found mostly in the extreme north and Lithosols found mostly in the south-eastern parts. Other soils in the study area include Vertisols, Planosols, Cambisols, Gleysols and Arenosols.

3.8 Land-cover and -use

The predominant land cover type in the Volta Basin is savannah (Figure 3.10). The savannah consists of grassland interspersed with shrubs and trees. Together with grassland and shrubs, the savannah covers about 86 % of the entire basin. Other land cover types include croplands and natural vegetation (10.4 %), wetland (4.6 %), forest cover (0.7 %) and urban/industrial coverage (0.5 %) (WRI, 2003).

The density of trees and the vigorousness of grassland associated with the savannah in the Volta Basin decreases in a south-north direction. This follows a pattern similar to that of rainfall. Two distinct types of savannah can be found in the basin: woodland savannah and grassy savannah. Woodland savannah is densely wooded with tall to medium tall grasses such as *Andropogon* and *Pennisetum* spp. It is found mostly in the southern parts of the basin. Main tree species associated with woodland savannah include *Adansonia digitata*, *Vitex paradoxa*, *Daniella oliveri*, *Mitragyna inermis*, *Butyrospermum parkii*, *Khaya senegalensis*, *Parkia biglobosa*, *Tamarindus indica*, *Terminalia macroptera* and *Faidherbia albida* (FAO, 2000; Siaw, 2001).

Grass savannah is found mostly in the northern areas of the basin and is mainly grassland interspersed with trees and shrub in some areas. Tree species found in this type of savannah include *Acacia* spp, *Balanites aegytiaca*, *Leptadenia pyrotecnia*, *Aristida* spp, *Schoenfeldia gracillis*, *Cenchrus biflorus* and *Anogeissus leicarpus*. The basin has a small forest cover located mainly in the south-western fringes. The vegetation in this area is green all year round, although some species do shed their leaves in the dry season (FAO, 2000). Common trees associated the forest are *Cynometra ananta*, *lophira alata*, *Tarrietia utilis*, *Antiaris Africana* and *Chlorophora excelsa*.

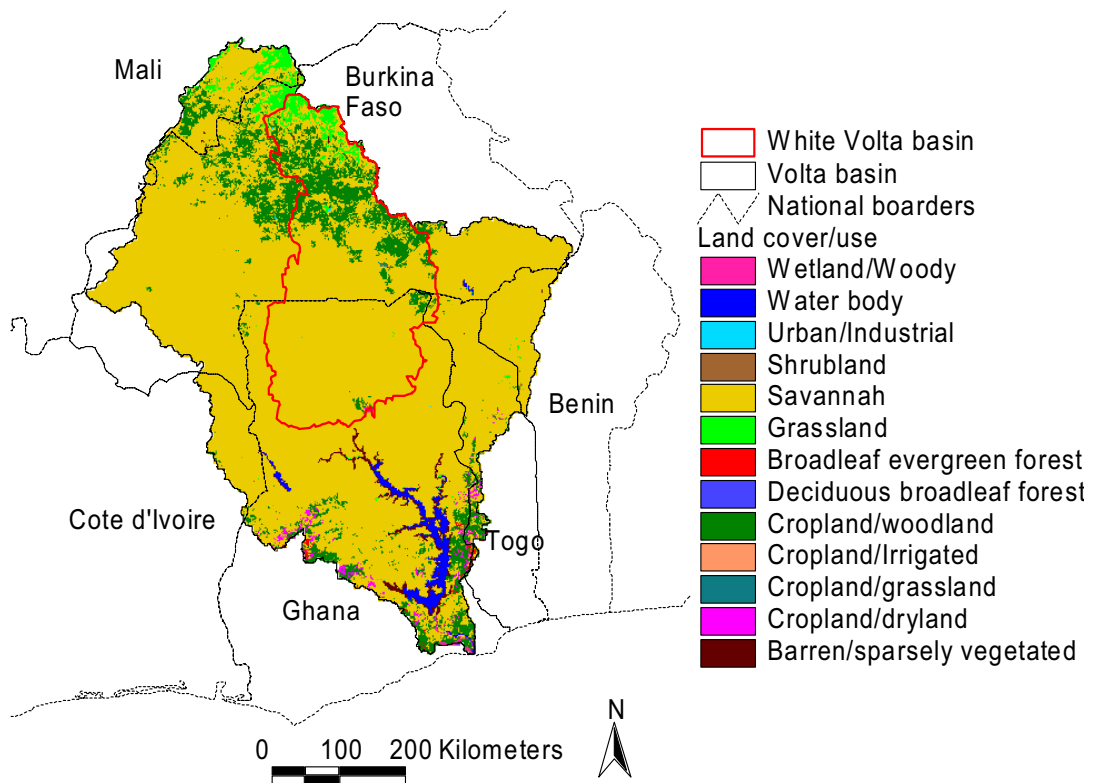


Figure 3.10 Land cover distribution in the Volta River Basin (USGS-GLCC, 2007)

The dominant land use in the basin is agriculture, which includes the cultivation of annual crops, tree crops, bush fallow and unimproved pasture (FAO, 2000). Agriculture in the basin is largely rain fed and essentially manual with the use of very few external inputs like tractors and fertilizers. Major crops cultivated include cereals (millet, maize, and sorghum), root crops, pulses, nuts and vegetables (FAO, 2000). A large part of the land in the basin is degraded and less suitable for crop production.

Landmann et al. (2007) analyzed land cover change within the Volta Basin, between 1990 and 2000/2001, using 26 Landsat tiles each for 1990 and 2000/2001 and augmented with daily and well corrected 250-meter MODIS time-series observations for the year 2000 onwards. The resulting land cover map indicates that 37 % of the total land cover were transformed (change from one class to another) from woodland with additional shrubs to managed herbaceous vegetation; 6 % were modified (change in tree cover density) from closed woodland (40-95 % tree cover density, TC) to open woody

vegetation (15-40 % TC); and 3 % were transformed from closed woodland (40-95 % TC) to herbaceous vegetation (Figure 3.11). Pressure from increasing population was one of the important factors explaining the expansion of cropland areas and thinning of the tree cover.

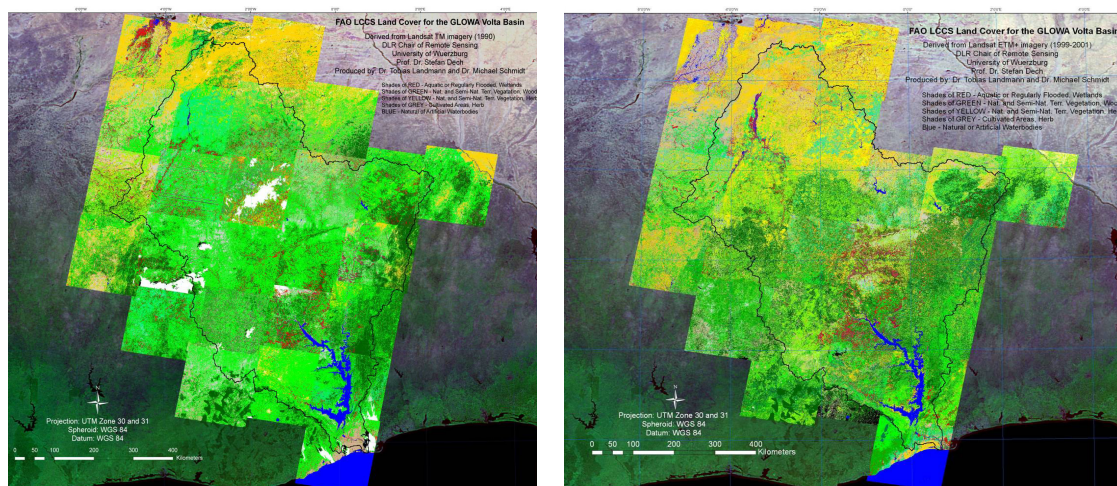


Figure 3.11 LCCS coded land cover for 1990 (left) and 2000/2001 (right). The black solid line depicts the border of the Volta basin. A 1-km SPOT composite image is used as a back drop. The green colors represent woody including shrubs, yellow is herbaceous vegetation, red is wetland areas and blue represents water bodies. The grey colored areas are managed herbaceous vegetation (Landmann et al, 2007)

3.9 Hydrogeology

The geological formations that underlie most parts of the Volta Basin (Birimian rocks and Voltaian formation) have little or no primary porosity. The occurrence of groundwater in these formations is as a result of the development of secondary porosity from weathering, fracturing, jointing and shearing (MWH, 1998). Two main aquifer systems have been identified in the basin, namely the weathered zone and the fractured zone aquifer systems. The weathered zone is usually located at the base of the weathered mantle of the Birimian system. It has a low permeability and high porosity due to high clay content. The fractured zone has developed in fractured bedrock, particularly in the sedimentary formations. The bedrock has high permeability and low porosity.

Groundwater is abstracted from all the geological formations within the basin. Aquifer yields vary from one geological formation to another and across the basin, but yields are generally low. In Ghana, the mean yield of boreholes rarely exceeds 6 m³/h

and ranges from 2.1 m³/h in the White Volta Basin to 5.7 m³/h in the Lower Volta Basin (MWH, 1998). In Burkina Faso, the mean yield is 0.2 - 2 m³/h (Larsson, 1984). A summary of some characteristics of the aquifer systems located in the Precambrian basement rocks in the basin's riparian Nations is presented in Table 3.4 and a summary of average values of some characteristics of aquifer systems in the basin in Ghana is presented in Table 3.5.

Table 3.4: Characteristics of aquifer systems in Precambrian basement rocks in the Volta Basin

Country	Borehole depth (m)	Water table depth (m)	Borehole yield (m ³ /h)	Transmissivity (m ² /d)	Storability
Burkina Faso	-	5 - 15	up to 20	0.5 - 25 (0.9)	0.00001-0.001
Ghana	34	-	0.4 - 24	7.5 - 30	0.003 - 0.008
Côte d'Ivoire	10 - 15	-	2 - 5	-	-
Togo	up to 20	-	0.2 - 175	-	-

Source: HAP (2006), obtained from many sources

Table 3.5: Characteristics of aquifer systems in the Volta Basin of Ghana

Volta Sub-basin	Borehole Yield (m ³ /h)	Specific capacity (m ³ /h/m)	Depth to aquifer (m)	Depth of Borehole (m)
White Volta	0.03-24.0 (2.1)	0.01-21.1	3.7-51.5 (18.4)	7.4-123.4 (24.7)
Black Volta	0.1-36.0 (2.2)	0.02-5.28	4.3-82.5 (20.6)	-
Oti	0.6-36.0 (5.2)	0.06-20.45	6.0-39.0 (20.6)	25.0-82.0 (32.9)
Lower Volta	0.02-36.0 (5.7)	0.05-2.99	3.0-55.0 (22.7)	21.0-129.0 (44.5)

Source: (MWH, 1998); Figures in bracket are mean values

3.10 Demography

The Volta basin is densely populated by African standards, with Ghana having a population density of 90 persons km², which is about three times that of sub-Saharan Africa (Rodgers et al., 2006). The basin population was estimated to be at 18.6 million inhabitants in 2000 with an annual growth rate of 2.54 % (CPWF, 2007). Based on this growth rate, the population is expected to grow to about 35 million inhabitants by 2025, which is an increase of nearly 90 % over a period of 25 years. Burkina Faso and Ghana have the greater share of the basin's population (Table 3.6).

Settlement in the basin is largely rural, with 64-88 % of the total population living in scattered homesteads in the rural areas. Agriculture is by far the most important

economic activity in the area, and the people often exploit the natural resources for their livelihoods. Between 70 and 90 % of the population in the basin depends on subsistence farming (Rodgers et al., 2006). There are only a few cities in the basin and few have more than a thousand inhabitants. Such cities include Ouagadougou in the White Volta basin and Tamale in the Lower Volta basin.

Population density in the basin varies from 104 persons per km² in the White Volta Basin in Ghana to 8 persons per km² in the Black Volta Basin in Côte d'Ivoire. The mean population density is estimated to be 42 persons per km² (WRI 2003).

Table 3.6: Demographic characteristics of the Volta Basin (Barry et al., 2005)

Basin country	Basin population in country			Growth rate (%) (2000)	Pop. density (pers./km ²) (2000)	Rural (%)
	1990	2000	2025			
Burkina Faso	7,014,156	887,4148	1,599,7351	2.4	41.53	77.4
Ghana	5,198,000	667,4376	1,169,6054	2.5	26-104	84.0
Togo	1,189,900	1,594,446	3,385,266	2.8	66	70.0
Mali	380,000	625,000	1,260,000	2.8	45-75	87.8
Benin	382,328	476,775	820,000	2.3	43.4	64.0
Côte d'Ivoire	no data	397,853	717,672	2.5	8-22	77.0

3.11 Groundwater resource utilization and problems

Various sources of water in the Volta Basin are used for the domestic water supply as well as for agriculture and livestock watering. These sources include streams and rivers, lakes, ponds, dug-outs, impoundment reservoirs, springs, rainwater harvesting, boreholes and hand-dug wells. However, groundwater sources are very important for the domestic water supply in both urban and rural areas within the basin's riparian countries. Many smaller cities and rural areas depend solely on groundwater, particularly in the dry season when most streams and rivers dry up.

In Burkina Faso, groundwater abstracted via boreholes and wells accounts for about 60 % of the total drinking water supply in rural areas (DGH, 2001). A similar situation exists in Ghana where, in 1998, about 52 % of the rural population depended on groundwater abstracted by boreholes and wells with or without hand pumps (Gyau-Boakye, 2001). Martin and van de Giesen (2005) reported that 19 of the 23 towns on the Burkinabe side of the basin and 11 of the 20 towns on the Ghanaian side, each with

population of over 10,000 inhabitants, depend exclusively on groundwater for domestic water supply. The importance of groundwater for domestic water supply is not limited to small towns and rural areas. Major basin cities like Ouagadougou in Burkina Faso and Tamale in Ghana also depend on groundwater sources for significant portions of their domestic water supply (HAP, 2006). Based on available data and reasonable assumptions, Martin and van de Giesen (2005) estimated that about 44 % of the total population in the Volta basin depends on groundwater for their water needs (Table 3.7). This reiterates the importance of groundwater in the basin.

Table 3.7: Population coverage by modern groundwater supply in 2001(Martin and van de Giesen, 2005)

	Burkina Faso	Ghana	Total
Population (Million)	9.96	6.91	15.97
Percent of population served by piped systems using groundwater	9.50	9.10	9.3
Percent of population served by boreholes with hand pumps and modern hand dug wells	38.90	28.50	37.6
Percentage of population supplied with groundwater	48.40	37.60	43.7

Two main types of groundwater abstracting structures can be identified in the Volta basin. They are boreholes and hand-dug wells, totaling 10,390 in 2001 (Martin and van de Giesen, 2005). Fifty nine of the boreholes have been mechanized to supply tap water to homes in small towns and urban areas, but the large majority of them (18,676) are equipped with hand pumps of the Afridev, Ghana-modified India mark II and Nira type and counted for over two-thirds of groundwater produced in the Volta basin in 2001 (Table 3.8). The rest of the abstracting structures are modern hand-dug wells, with a total number of 10,390 and accounting for 13 % of the groundwater produced in the basin. The estimated volume of groundwater produced in the Volta basin in 2001 was 88.3 MCM/year.

Table 3.8: Groundwater production in 2001 in the Volta basin in Ghana and Burkina Faso (Martin and van de Giesen, 2005)

Source	Ghana (MCM/y) ^a	Burkina Faso (MCM/y)	Total production (MCM/y)	Share of source in production (%)
Borehole with hand pump	21.5	39.7	61.2 (1.5)	69
Modern hand-dug well ^b	5.0	6.7	1.7 (-)	13
Piped system	2.9	12.5	15.4 (0.6)	18
Total	29.4	58.9	88.3 (2.1)	100
Share of country in production (%)	33	67	100	

NB: Figures in brackets are estimates for 1971; ^aMillion cubic meters per year; ^bWell with improved design and constructed with support from NGO.

In addition to the domestic water supply, groundwater sources are relied on for dry season irrigation of vegetables as well as for watering of cattle and other livestock in the basin particularly on the Ghanaian side. Groundwater-based irrigation is a prominent practice in many areas in the upper east and west regions of Ghana (located in the middle of the basin), where hand-dug wells are used to extract groundwater from alluvial channels along the courses of ephemeral streams for irrigation of vegetables (cabbage, onions, carrots, tomatoes, okra, and pepper) during the dry season. Most of the groundwater irrigators are small-scale farmers who produce for the market as well as for home consumption. The farmers use watering cans and buckets tied with ropes to collect water from dug wells to irrigate between 0.04 and 0.1 hectare vegetable farms (Kortatsi, 1994).

Watering of livestock with groundwater is commonly done in the upper east, upper west and northern regions of Ghana. In these regions, animals are not restricted but are allowed to range in search of food and water. Nearly all the boreholes equipped with hand pumps have troughs constructed between 5 and 10 m from the boreholes to provide water for the animals. Spillways are constructed from the drainage aprons of the boreholes to the watering troughs so that spilled water from the boreholes collects in these troughs for use by livestock, mainly goats, sheep, cattle and pigs. About 70 % of Ghana's 1.34 Million Heads (MH) cattle (2003 estimated figure) and 40 % of other livestock/poultry (sheep-3.02 MH; goats-3.56 MH; pigs-3.03 MH; and poultry-2.64 MH) are produced in these three basin regions and are watered exclusively using groundwater (Obuobie and Barry, 2004; LPIU-MOFA, 2004; Kortatsi, 1994).

Analyses of water samples in several studies (e.g., Amuzu, 1975; Andah, 1993; Kortatsi, 1994; Ministry of Works and Housing, 1998; Darko et al., 2003) indicate that the chemical and biological quality of the groundwater in the basin is generally good for multi-purpose use (Table 3.9) except for waters with low pH (3.5-6.0), high level of iron, manganese, nitrate and fluoride in certain localities. Boreholes or wells in the affected localities have either been abandoned by the inhabitants of the localities or have been capped by authorities.

Beside the problems of poor quality groundwater in some localities, there are signs that groundwater reserves in a significant number of localities in the basin are being over exploited as mentioned already in Chapter 1. Signs of over exploitation reported include diminishing yields from boreholes within a relatively short time, lowering of the water table and depletion of rivers in catchments of high borehole concentration. A typical case is the savannah areas of northern Ghana where inadequate recharge resulting from inappropriate land use, deforestation and scanty rainfall has compounded the problem of over-exploitation of groundwater (Water Research Institute, 2002). Other groundwater problems identified in the basin include the degradation of groundwater resources as a result of high population density, deforestation, inadequate sanitation facilities, deficient water management practices and global changes (HAP, 2006; Amisigo, 2005).

The extent of groundwater use in the Volta basin is rapidly increasing and will continue to do so, particularly in small cities and rural areas, as long as the governments of the riparian nations view groundwater sources as the most cost-effective option for expanding water supply coverage. However, the development of groundwater in the basin should be done in a manner that ensures sustainable use of the resource.

The study area

Table 3.9: Chemical analysis of water samples in the geologic formations of Ghana (all values are in mg/l, except the pH) (Kortatsi, 1994)

Chemical parameter	Gneiss	Granite	Phyllites	Sandstone	Mudstone	Sand and shale	Limestone and gravel	Quartzite
pH	7.5	7.0	6.8	7.0	7.6	7.5	7.7	6.4
Total dissolved salts	4888	387.4	211.2	533.5	424.7	632.0	932.0	398.3
Calcium	595	49.4	32.1	25.1	26.1	68.7	58.1	42.1
Magnesium	207	19.1	15.7	7.6	9.1	33.5	36.1	23.4
Sodium	720	48.0	11.7	262.6	125.4	134.5	296.8	24.5
Chloride	1790	73.5	9.9	70.4	42.0	173.6	196.9	103.6
Sulphate	1800	10.6	7.2	65.2	11.2	101.2	77.3	60.1
Bicarbonate	34	81.2	104.1	97.5	189.3	154.6	149.7	67.1
Total iron	0.1	1.0	2.2	2.0	0.6	1.8	0.5	2.9
Manganese	0.05	0.4	0.4	0.2	0.1	0.2	0.2	0.5
Fluoride	0.25	0.3	0.3	0.8	0.6	0.6	1.8	0.2
Nitrate	0.5	1.6	0.6	0.8	0.1	2.2	1.8	2.3
Total hardness	2340	172.5	123.7	70.8	222.8	239.4	229.9	179.6

4 WATER TABLE FLUCTUATION METHOD FOR ESTIMATING GROUNDWATER RECHARGE

4.1 Overview

The water table fluctuation method (WTF) is one of the most widely used techniques for estimating groundwater recharge over a wide variety of climatic conditions (Scanlon et al., 2002; Hall and Risser, 1993; Healy and Cook, 2002). The use of the method requires knowledge of specific yield and changes in water levels over time. Healy and Cook (2002) have suggested that the wide use of this method could be attributed to the abundance of available water level data and the simplicity of estimating recharge rates from temporal fluctuations or spatial patterns of water levels. The WTF is best suited for estimating recharge rates over short time periods in areas with shallow unconfined aquifers that display sharp rise and fall in water levels (Scanlon et al., 2002). There are no assumptions underlying this method regarding movement of water through the unsaturated zone and, therefore, the presence of preferential flow paths in an area does not restrict its use. The WTF method can be used in studies covering a few square meters as well as in those covering hundreds or thousands of square meters. The recharge estimate given by this method is actual recharge, which is more reliable compared to the potential recharge given by other methods.

The WTF method is based on the assertion that rises in water levels in unconfined aquifers are due to recharge water arriving at the water table, and that all other components of the groundwater budget, including lateral flow, are zero during the recharge period (Scanlon et al., 2002; Healy and Cook, 2002). The groundwater recharge rate can be estimated as the product of the water level rise and the specific yield of the groundwater aquifer material. The recharge can be expressed as:

$$R = S_y \, dh/dt = S_y \, \Delta h/\Delta t \quad (4.1)$$

where: R is groundwater recharge (mm/time); S_y is specific yield (dimensionless); Δh is peak rise in water level attributed to the recharge period (mm); and Δt is the time of the recharge period.

Three main assumptions are inherent in the WTF technique: (i) rise and decline in levels of the water table in shallow unconfined aquifers are solely due to recharge and discharge of groundwater; (ii) the specific yield of aquifer is known and constant over the time period of the water table fluctuation; and (iii) the pre-recharge water level recession can be extrapolated to determine water level rise (Healy and Cook, 2007). These inherent assumptions are not always the case and could be drawbacks of this method in some situations. Changes in water table level may not always be as a result of recharge or discharge. It could be caused by other factors such as evapotranspiration, changes in atmospheric pressure, presence of entrapped air and earth tides, or as a response to changes in stream stage in the case where the well is close enough to a stream (Delin et al., 2007). Studies have shown that obtaining a specific yield that is representative of a large area can be difficult, and besides, specific yield varies with time (Delin et al., 2007; Loheide II et al., 2005; Sophocleous, 1985) and depth to the water table as opposed to the assumption of a known and constant specific yield.

There are no strict limits as to the range of recharge that can be estimated with the WTF method. Scanlon et al. (2002) gives annual recharge rates estimated using the WTF technique as ranging from 5 mm in the Tabalah Basin of Saudi Arabia to 247 mm in a small basin in eastern United States. Martin (2005) and Sandwidi (2007) used the WTF method to estimate the annual groundwater recharge to the Atankwidi and Kompienga dam basins in West Africa. The recharge ranged from 13-143 mm for the Atankwidi basin and 44 - 244 mm for the Kompienga dam basin.

4.2 Method

4.2.1 Description of study area

The water table fluctuation method was applied in the south of the White Volta Basin (Figure 4.1). In many studies, this part of the basin is referred to as the White Volta Basin of Ghana because it lies solely within Ghana. The White Volta basin of Ghana covers an area of about 45,804 km² (UNESCO, 2007) and had a population of about 1.6 million inhabitants in 2000 with an annual growth rate of 1.5 % (Codjoe, 2004). The topography is generally flat to gently rolling with few undulating hills. The dominant soils types based on the FAO-UNESCO (1974) soil classification legends are Luvisols

and Lithosols, which together constitute more than 85 % of the soil resources in the area. Other soils are Acrisols, Vertisols, Gleysols and Cambisols (section 3.6). The vegetation of the area is predominantly Savannah which is made up of grasses, shrubs and trees (section 3.7).

The annual mean rainfall across the area ranges from 800 mm in the north to 1140 mm in the south (Shahin, 2002; Gyau-Boakye and Tumbulto, 2006). The mean monthly temperature is about 27 °C; mean relative humidity varies from 80 % at the peak of the rainy season in September to about 20 % in January (peak of the harmattan period). The water table depth varies from ground level in the rainy season to about 15 m in the dry season. Previous monitoring of water levels in the study area revealed a sharp rise and decline in the water table during the wet and dry seasons, respectively (Martin, 2005).

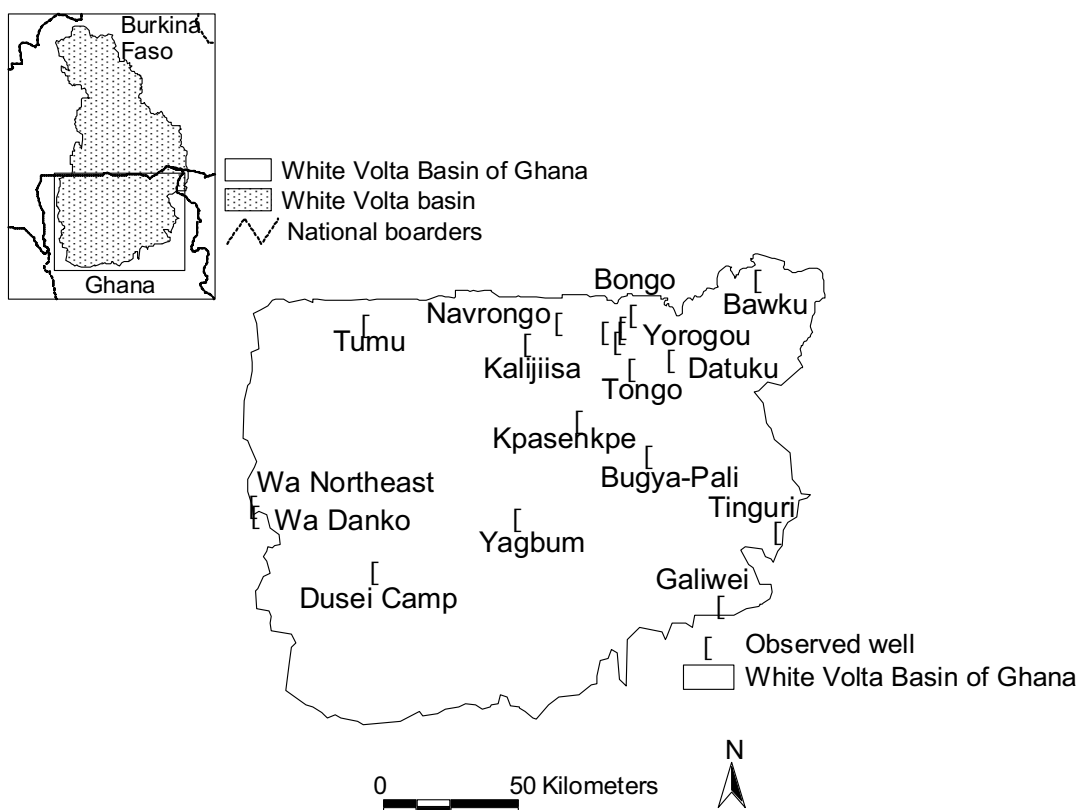


Figure 4.1 Map of the Lower White Volta basin showing the location of selected monitoring wells

4.2.2 Water level measurement

Groundwater levels were monitored in 19 observation wells equipped with automatic water level recorders (data-logger divers) spread across the study area (Figure 4.1; Table 4.1). Six of the 19 wells were installed and monitored specifically for this study; the other 13 were installed and monitored by the Water Research Institute of Ghana (WRI). The monitoring of the 13 boreholes is part of a Danish government-funded water resource information services project being undertaken by the WRI in the White Volta Basin of Ghana. The project aims at providing decision support for integrated water resources management in the White Volta Basin. For purposes of identification, wells monitored by the WRI are labeled WVB1-WRI to WVB13-WRI; and those monitored as part of this study are labeled WVB14-GVP to WVB19-GVP.

Table 4.1: Characteristics of wells monitored in the Lower White Volta Basin (Agyekum et al, 2006; CWSA^a database)

Well location	Well ID	Elevation (m)	Geology	Well Depth (m)	Well yield (m ³ /hr)
Wa Danko	WVB1-WRI	308	Granite	104.0	1.2
Wa Northeast	WVB2-WRI	313	Granite	37.5	2.4
Tumu	WVB3-WRI	312	Granite	105.0	30.0
Navrongo	WVB4-WRI	179	Granite	72.0	10.2
Gowrie-Tingre	WVB5-WRI	181	Granite	90.0	12.0
Bongo	WVB6-WRI	224	Granite	35.0	2.7
Datuku	WVB7-WRI	194	Birimian	90.0	1.2
Bawku	WVB8-WRI	224	Granite	100.0	18.0
Ducie Camp	WVB9-WRI	276	Basal sandstone	78.0	0.7
Yagbum	WVB10-WRI	242	Mainly sandstone	100.0	27.0
Bugya-Pali	WVB11-WRI	143	Mudstone & shale	56.0	0.5
Tinguri	WVB12-WRI	185	Mudstone & shale	51.0	7.2
Galiwei	WVB13-WRI	211	Mudstone & shale	100.0	0.3
Yorougu	WVB14-GVP	179	Granite	60.0	4.7
Tongo	WVB15-GVP	280	Granite	60.0	1.5
Kalijiisa	WVB16-GVP	198	Birimian	54.0	1.7
Sumbrungu	WVB17-GVP	194	Granite	60.0	1.2
Sokabiisi	WVB18-GVP	124	Granite	43.0	1.0
Kpasenkpe	WVB19-GVP	130	Shale & sandstone	56.0	5.4

^a Community Water and Sanitation Agency (CWSA)

Three of the wells monitored by the WRI (Wa Danko, Wa Northeast and Tumu-WVB3-WRI) are located within a distance of about 300 m from existing mechanized boreholes, and an additional 2 (Navrongo, Gowrie) are within 500 m downstream of irrigation dams (Agyekum et al., 2005). The groundwater hydrographs of these 5 wells may be influenced by the mechanized wells and dams.

Installation of the divers and the monitoring of water levels in 7 of the 13 WRI- wells started in 2005. The monitoring of the remaining WRI-wells and the study-wells started in 2006. The installed data loggers were programmed to record and store water level data at daily and sub-daily intervals. Data recorded were retrieved in 3 month intervals. In addition to monitoring water levels, atmospheric pressure was monitored in 7 of the 13 WRI-wells using barometric data logger (baro diver). The atmospheric pressure data were used for correcting the water level data. A well with no baro diver had the water level data corrected with pressure data from the nearest well with baro diver.

4.2.3 Estimation of water level rise (Δh)

The water level rise (Δh) in the observed wells was estimated using the recorded water level data. The water level rise is generally computed as the difference between the peak of a water level rise and the value of the extrapolated antecedent recession curve at the time of the peak. The recession curve is the trace that the well hydrograph would have followed had there not been any recharge (Delin et al., 2007). There are various approaches for estimating the water level rise. They include the master recession curve (MRC) and the graphical extrapolation approach.

The MRC is an automated or semi-automated technique for estimating the water level rise at a site. The MRC for a given site is a characteristic water table recession hydrograph, which represents the average behavior for a declining water table for the site and can be used to predict what the water table decline should be in the absence of recharge (Christopher et al., 2005). Once the master recession curve is determined, the water level rise is calculated as the difference between the predicted and the measured elevations. The MRC approach provides a mean for overcoming the difficulty associated with accurately determining the water level rise due to the transient state of decline of water levels between recharge events. Different MRC approaches

have been developed in separate studies and used along side the water table fluctuation method, to estimate the recharge (Delin et al., 2007; Crosbie et al., 2005; Heppner and Nimmo, 2005). The MRC approach can be time consuming and though it has less subjectivity, there is the possibility of mistakenly including water level rises that did not happen as a result of recharge. In practice, the MRC is applied to every data point in the water level record, which can be difficult to do if a computer code is not used.

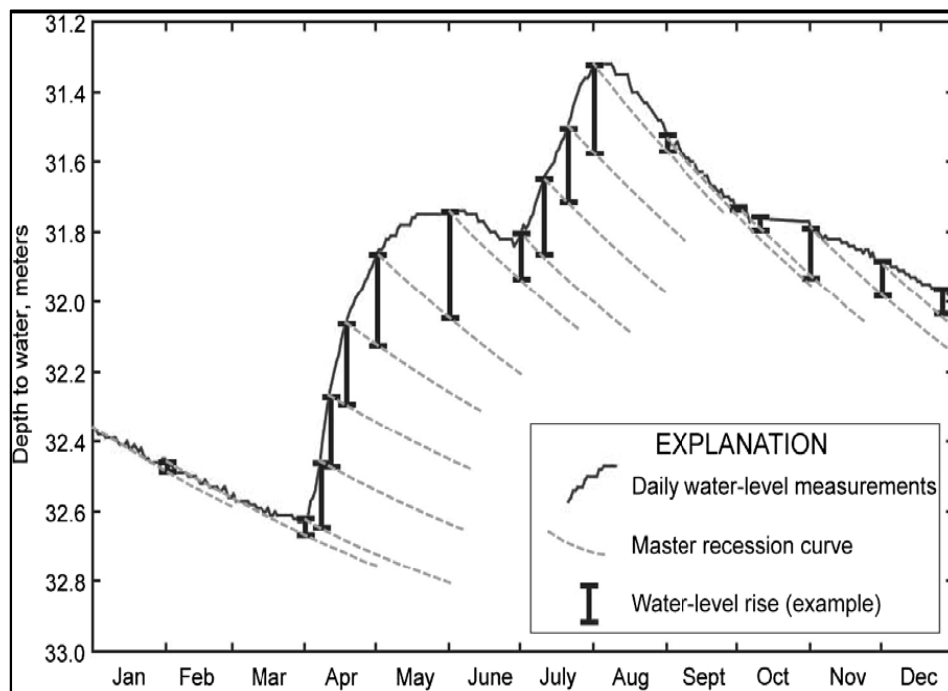


Figure 4.2 Recharge estimated using the master recession curve (MRC) approach to the WTF method (Delin et al., 2007)

The graphical extrapolation method is the simplest of the available methods and less time consuming. This approach was used in this study to estimate the groundwater level rise in each of the observed wells. This was done by visually examining the entire water level data for each well and manually extrapolating the antecedent recession curves. The rise in water level during the recharge period was obtained as the difference between the peak of the rise and the low point of the extrapolated antecedent recession curve at the time of the peak (Figure 4.2). The graphical interpolation approach has more subjectivity compared to the MRC, since different persons could obtain slightly different recession curves and subsequently different values for the water level rise.

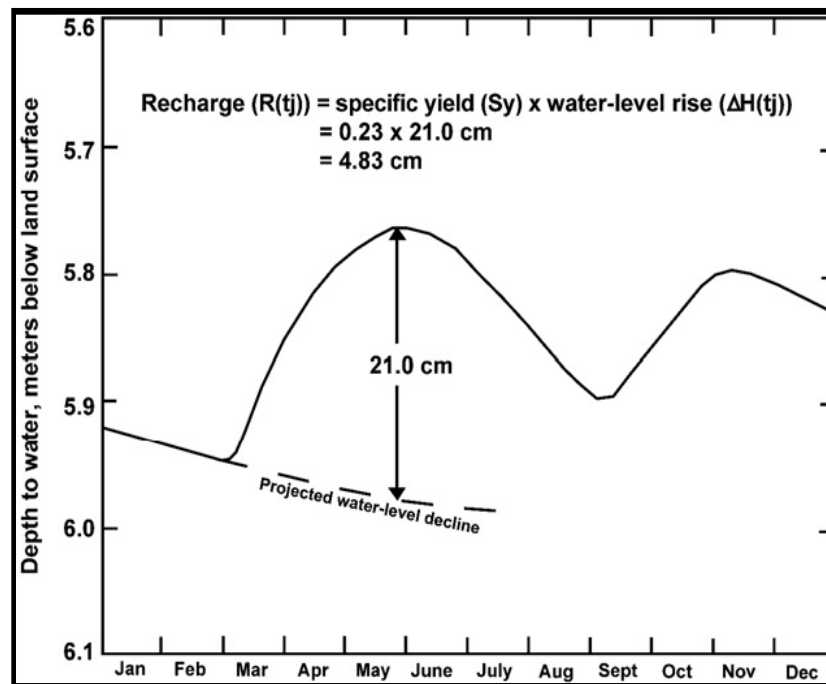


Figure 4.3 Recharge estimated using the graphical approach to the WTF method, illustrated with hypothetical data (Delin et al., 2007)

4.2.4 Specific yield

The specific yield of a rock or soil is defined as the ratio of the volume of water, which after being saturated, will yield by gravity to its own volume (Meinzer, 1923 cited in Healy and Cook, 2002). In simple terms, the specific yield is a fraction of the porosity of an aquifer that can be drained by gravity. The value depends on the grain size, shape and distribution of pores and compaction of the strata (Gupta and Gupta, 1999). The specific yield value can be calculated from the porosity and specific retention as below (Healy and Cook, 2002):

$$S_y = \phi - S_r \quad (4.2)$$

where: ϕ is porosity and S_r is specific retention (the volume of water retained by the rock per unit volume of rock).

In theory, specific yield is treated as a storage term that does not depend on time, accounting for instantaneous release of water from storage. In practice, however, the release of water is often not instantaneous but time dependent (Healy and Cook, 2002; Lerner, 1990; Nachabe, 2002). This is more evident in situations of relatively fast

lowering of the water table, in which case the drainage from the unsaturated zone may lag behind depending on the soil properties (Storm, 1988). Specific yield is affected by lithology, temperature (Meizer, 1923 cited in Healy and cook, 2002) and depth to water table. Determination of the specific yield value is complicated by two major issues. First, there is always some water remaining in the aquifer material even after drainage, clinging to the sand and clay particles in the aquifer material. Secondly, due to the complications of unsaturated flows, the specific yield value may not be fully realized until after a long time (Johnson, 1967; Morris and Johnson, 1967).

Several methods exist for estimating the specific yield value. They include laboratory- and field- methods such as aquifer pumping test, volume-balance methods, water-budget methods, geophysical methods, and field capacity tests (Healy and Cook, 2002; Lerner, 1990). The complexity of determining the specific yield value has resulted in a wide range of values for the same textural class as reported in various literature (Tables 4.2; 4.3). Such variation has been attributed to natural heterogeneity in geologic material, differences in determination methods and largely to the amount of time spent in determining the value (Prill et al., 1965 cited in Healy and Cook, 2002). Lerner (1990) suggested the use of specific yield values determined from laboratory measurement of drainable porosity over a reasonable sample size instead of values determined from pumping tests which are often very different because they are derived for short times. In situations where laboratory measurements of specific yield values are not available, Lerner (1990) recommended the use of standard values in literature.

In this study, the exact specific yield values for the aquifer material in the study area were not determined. Specific yield values were selected from literature, based on the values used in India (Table 4.3) and the range of specific yield value (0.01-0.05) reported in Shahin, (2002), for the weathered zone material in neighboring Burkina Faso. Burkina Faso and the study area in Ghana, largely, share the same geology.

Table 4.2: Statistics on specific yield (S_y) from 17 studies (Johnson, 1967 cited in Healy and Cook, 2002)

Texture	S_y	Coefficient of variation (%)	Minimum specific yield	Maximum specific yield	Number of determinations
Clay	0.02	59	0.00	0.05	15
Silt	0.08	60	0.03	0.19	16
Sandy clay	0.07	44	0.03	0.12	12
Fine sand	0.21	32	0.10	0.28	17
Medium sand	0.26	18	0.15	0.32	17
Coarse sand	0.27	18	0.20	0.35	17
Gravelly sand	0.25	21	0.20	0.35	15
Fine gravel	0.25	18	0.21	0.35	17
Medium gravel	0.23	14	0.13	0.26	14
Coarse gravel	0.22	20	0.12	0.26	13

NB: The values were determined with different methods

Table 4.3: Values of specific yield as used in recharge calculations in India (Sinha and Sharma, 1988; cited in Lerner, 1990)

Material	Range of specific yield
Sandy alluvium	0.12-0.18
Valley fills	0.10-0.14
Silt/clay rich alluvium	0.05-0.12
Sandstone	0.01-0.08
Limestone	0.03
Highly karstified limestone	0.07
Granite	0.02-0.04
Basalt	0.01-0.03
Laterite	0.02-0.04
Weathered phyllites, shales, Schists and associated rocks	0.01-0.03

4.3 Results and discussions

4.3.1 Water level rise

The highest monthly rainfall for the study area in 2006 and 2007 were measured in August and water levels were highest in September/October (Figures 4.4a to 4.4d). Although the rainfall season in the study area starts in April/May, water level in all wells started to rise in June/July when about 40 % of the annual rainfall had occurred.

The 2- to 4- month lag between the start of the rainfall season and water level rise can be described as a period of refilling of the soil due to moisture deficit inherited from the past dry season. The lag suggests that there are threshold effects and a non-linear relationship between rainfall and recharge in the study area. Additionally, the lag suggests that most wells in the study area recharge slowly. Similar observations were made in the Kompienga dam basin (Sandwidi, 2006) and the Atankwidi catchment (Martin, 2005), both in the Volta River Basin.

Critical examination of the groundwater hydrographs and water level data of the observed wells for the two study years suggests that recharge to groundwater in the study area is almost entirely from the seasonal rainfall, since water level rise occurred mostly in the rainfall period. Though there was some accumulation of recharge in the dry season possibly due to regional flow of groundwater, this is very small. Therefore, it can be reasonably concluded that, the contributions from aquifers outside the study area to groundwater recharge in the White Volta basin of Ghana is insignificant.

The annual and spatial variations in water level were quite high as depicted in the groundwater hydrographs. The estimated annual water level rise ranged from 1240 to 5000 mm for a mean annual rainfall of 870 mm in 2006 and from 1600 to 6800 mm for a mean annual rainfall of 1294 mm in 2007 (Table 4.4). The highest and lowest water level rises in 2006 were recorded at Tumu and Bongo respectively (Figure 4.4a; 4.4d). In 2007, the highest water level rise was recorded in Bongo and the lowest at Bugya-Pali. The water level rise measured at Kpasenkpe (Table 4.4) was rather high and may have been influenced by lateral flow due to its close proximity (within 100 m) to the main channel of the White Volta River. The overall mean annual water level rise and coefficient of variation were 2652 mm and 0.42 for 2006, and 3577 mm and 0.39 for 2007.

A comparison of the mean annual water level rise shows an increase of 35 % in 2007 over that of 2006. The mean annual rainfall in 2007 shows an increase of 50 % over that of 2006. In most of the observed wells, there were no short-term water level fluctuations in response to daily rainfall events. This is most likely due to attenuation of water table fluctuation as a result of the large storage capacity of the observed wells.

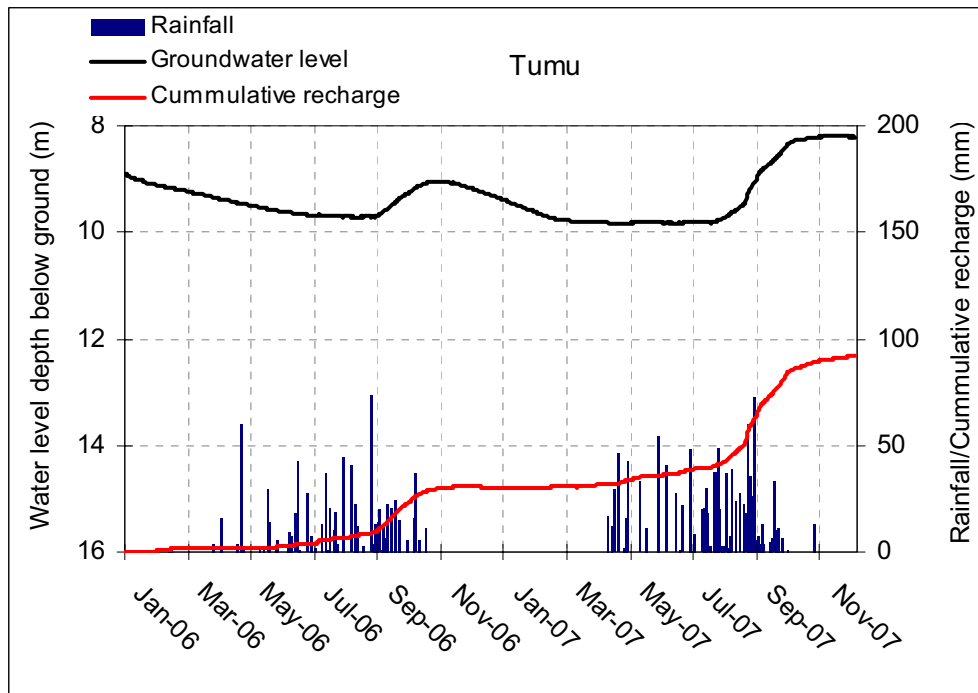


Figure 4.4a Groundwater hydrograph and bar graphs of daily rainfall at Tumu in the White Volta Basin of Ghana

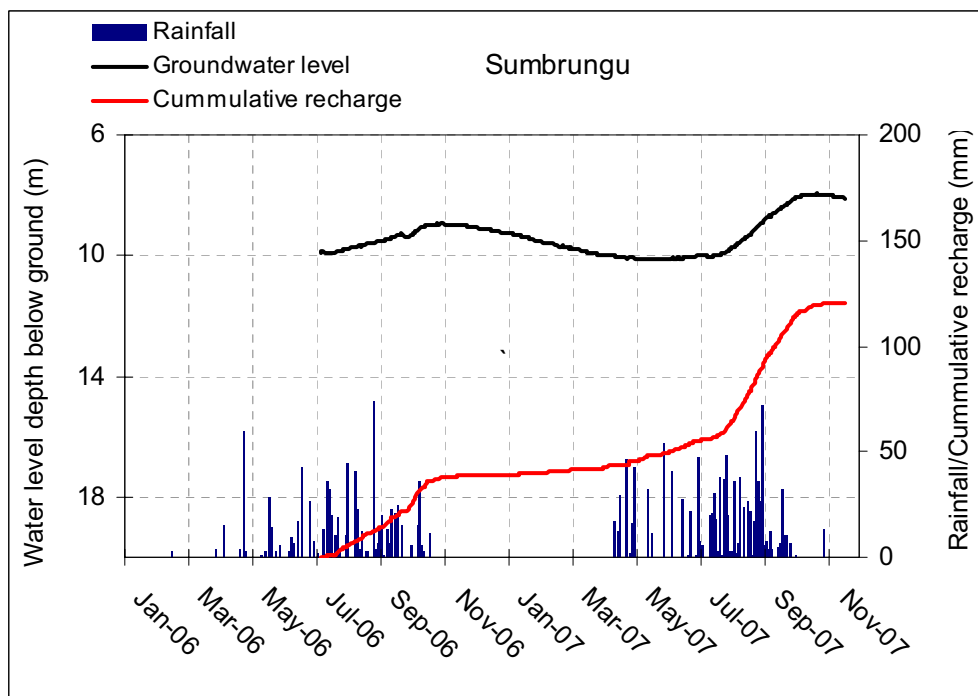


Figure 4.4b Groundwater hydrograph and bar graphs of daily rainfall at Sumbrungu in the White Volta Basin of Ghana

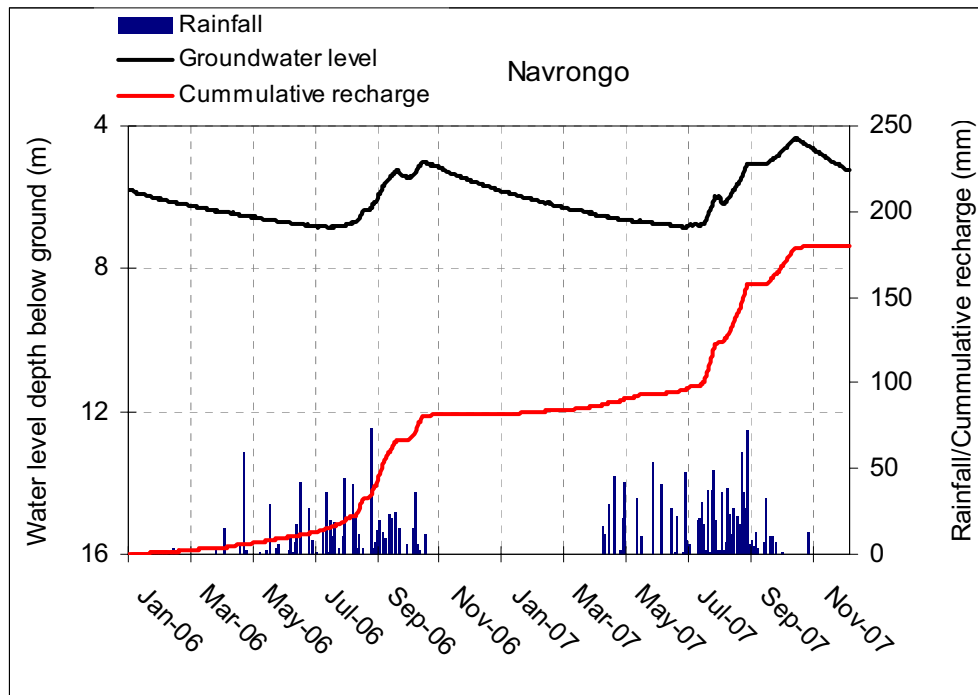


Figure 4.4c Groundwater hydrograph and bar graphs of daily rainfall at Navrongo in the White Volta Basin of Ghana

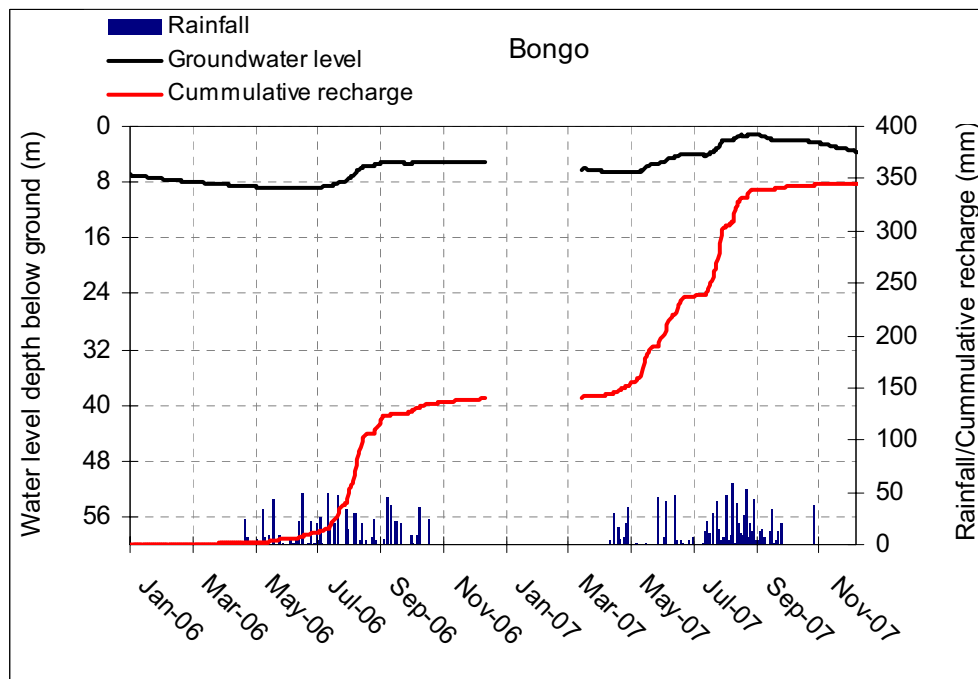


Figure 4.4d Groundwater hydrograph and bar graphs of daily rainfall at Bongo in the White Volta Basin of Ghana

4.3.2 Recharge estimates

The groundwater recharge for each of the observed wells was calculated by multiplying the water level rise with the specific yield values of the aquifer material in which the wells are situated. The calculated mean recharge for the study area ranged from 28.0 to 150.0 mm in 2006, representing 3.5 to 16.5 % of the mean annual rainfall, and from 32.0 to 204.0 mm in 2007, representing 2.5 to 16.0 % of the mean annual rainfall (Table 4.4). Spatial interpolation of the recharge for 2006 and 2007 shows that with the exception of a few areas like Bongo, Datuku, Tongo, Kpasenkpe, Yorogou and Sokabiisi, groundwater recharge in the study area ranged from 28 to 88 mm (Figure 4.5 and 4.6). The highest and lowest recharge values in 2006 were estimated at Bongo and Galiwei, respectively. In 2007, the highest recharge was estimated at Bongo and the lowest at Bugya-Pali.

The overall recharge to the study area was estimated using the area weights of the observed wells determined with the Thiessen polygon method. The overall mean groundwater recharge in the White Volta basin of Ghana was estimated to be 70.0 mm in 2006, representing 8.0 % of the mean annual rainfall for that year and 92.0 mm in 2007, representing 7.0 % of the mean annual rainfall. The difference in the recharge values for the two study years could be attributed to differences in the annual rainfall distribution and intensity.

The recharge estimate obtained in this study is similar to estimates from groundwater studies done elsewhere in the Volta Basin and in West Africa, using the water table fluctuation method. Sandwidi (2007) applied this method to the Kompienga Dam Basin, Burkuna Faso, in 2005 and estimated the recharge to be from 5.3 to 29.4 % of the annual rainfall. Similarly, Martin (2005) applied the method in the Atankwidi catchment and estimated the recharge to vary from 1.8 to 12.5 % of the annual rainfall in 2003 and from 1.4 to 10.3 % of the annual rainfall in 2004. van der Sommen and Geirnaert (1988), used multiple recharge estimation methods, including the WTF to estimate the recharge to the groundwater in the West African region to be between 2.0 and 16.0 % of the annual rainfall.

Table 4.4: Recharge values estimated in the White Volta Basin of Ghana, in 2006/2007

Well	Aquifer material (topsoil texture)	Specific yield	Year	Δh (mm)	Recharge (mm)	% of Rainfall
WVB7-WRI	Birimian (sandy clay loam)	0.020-0.050	2006	4200	84-210 (147)	10-24 (17.0)
WVB13-WRI	Mudstone & shale (Clay sandy loam)	0.010-0.030	2006	1380	14-41 (28)	2-5 (3.5)
WVB3-WRI	Granite (Sandy loam)	0.020-0.040	2006 2007	1240 3199	25-50 (38) 64-128 (96)	3-6 (4.5) 5-10 (7.5)
WVB4-WRI	Granite (Sandy clay loam)	0.020-0.040	2006 2007	2606 3533	52-104 (78) 71-141 (106)	6-12 (9.0) 5-11 (8.0)
WVB5-WRI	Granite (Sandy loam)	0.020-0.040	2006 2007	2320 2310	46-93 (70) 46-92 (69)	5-11 (8.0) 4-7 (5.5)
WVB6-WRI	Granite (Sandy loam)	0.020-0.040	2006 2007	5000 6800	100-200 (150) 136-272 (204)	11-22 (16.5) 11-21 (16.0)
WVB9-WRI	Basal sandstone (Clay sand loam)	0.010-0.050	2006	2800	28-140 (84)	3-16 (9.5)
WVB11-WRI	Mudstone & shale (Sandy clay loam)	0.010-0.030	2006 2007	2109 1600	21-63 (42) 16-48 (32)	2-7 (4.5) 1-4 (2.5)
WVB14-GVP	Granite (Sandy loam)	0.020-0.040	2006 2007	2691 3522	54-108 (81) 70-141 (106)	6-12 (9.0) 5-11 (8.0)
WVB10-WRI	Sandstone (Sandy clay loam)	0.010-0.050	2006 2007	2181 3500	22-109 (66) 35-175 (105)	3-13 (8.0) 3-14 (8.5)
WVB1-WRI	Granite (Sandy loam)	0.020-0.040	2007	2920	58-117 (88)	4-9 (6.5)
WVB8-WRI	Granite (Sandy clay loam)	0.020-0.040	2007	2875	58-115 (87)	4-9 (6.5)
WVB2-WRI	Granite (Sandy clay loam)	0.020-0.040	2007	2080	42-83 (63)	3-6 (4.5)
WVB12-WRI	Mudstone & shale (Clay sand loam)	0.010-0.030	2007	3778	38-113 (76)	3-9 (6.0)
WVB15-GVP	Granite (Sandy loam)	0.020-0.040	2007	4148	83-166 (125)	6-13 (8.5)
WVB16-GVP	Birimian (Sandy clay loam)	0.020-0.050	2007	2268	45-91 (68)	3-7 (5.0)
WVB17-GVP	Granite (Sandy clay loam)	0.020-0.040	2007	3435	69-137 (103)	5-11 (8.0)
WVB18-GVP	Granite (Sandy clay loam)	0.020-0.040	2007	4605	92-184 (138)	7-14 (10.5)
WVB19-GVP	Shale & sandstone (Sandy clay loam)	0.010-0.050	2007	6659	67-333 (200)	5-26 (16)

NB: Figures in brackets are approximate mean values of the range

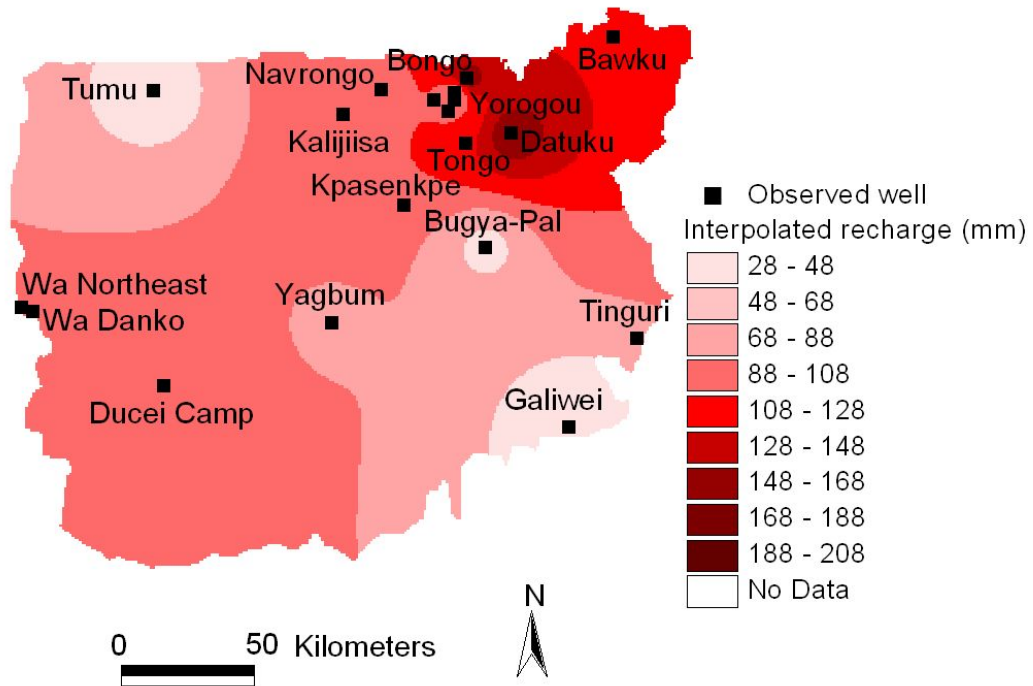


Figure 4.5 Spatially interpolated groundwater recharge in the White Volta basin of Ghana, in 2006

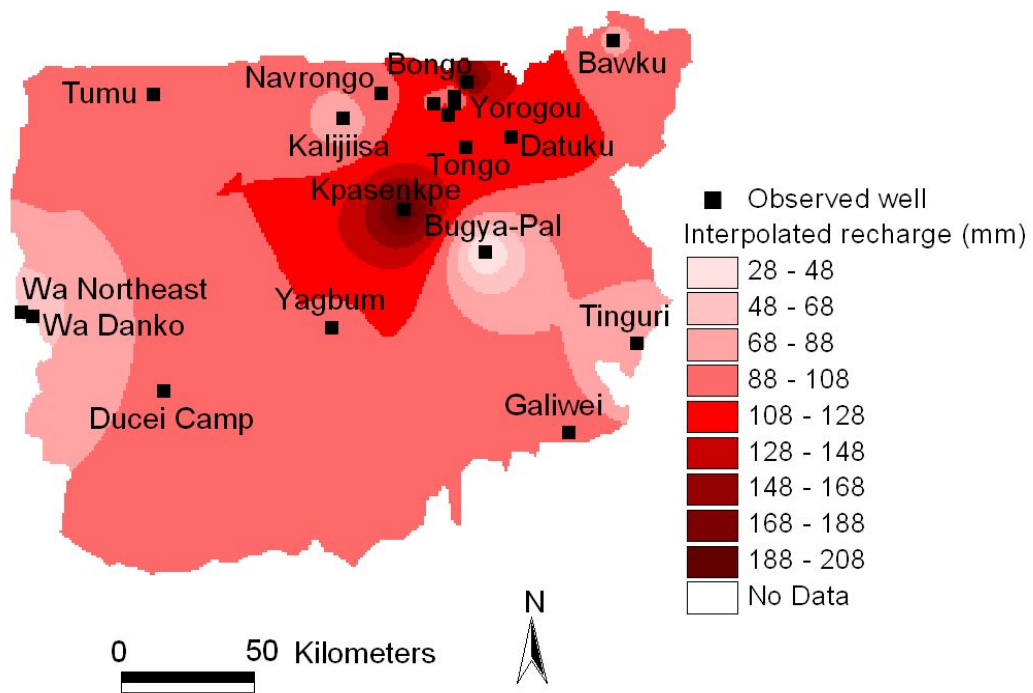


Figure 4.6 Spatially interpolated groundwater recharge in the White Volta basin of Ghana, in 2006

5 THE CHLORIDE MASS BALANCE METHOD FOR ESTIMATING GROUNDWATER RECHARGE

5.1 Introduction

The chloride mass balance (CMB) method has been used extensively for estimating groundwater recharge in arid and semi-arid areas worldwide (Gee et al., 2004; Scanlon et al., 2002; Tindall and Kunkel, 1999). The method originates from Eriksson and Khunakasem (1969), who applied it in the saturated zone to estimate the groundwater recharge on the coastal plain of Israel (Scanlon et al., 2002).

In the Volta Basin, the CMB method was used by Martin (2005) and Sandwidi (2007) to estimate the groundwater recharge in the Atankwidi river Basin (275 km²) in Ghana and the Kompienga Dam Basin (5911 km²) in Burkina Faso, respectively. The CMB method provides long-term mean recharge estimates that integrate large areas. The method can be used to estimate groundwater recharge over wide time and spatial scales. The time scale ranges from a year to thousands of years and the spatial scale ranges from few meters to several kilometers.

Recharge estimation using the CMB method is based on the premise that a known fraction of chloride in precipitation and dry-atmospheric deposition is transported to the water table by the downward flow of water (Sumioka and Bauer, 2004). Recharge estimates are obtained from measurement of the concentration of chloride directly associated with the recharging waters. The CMB method has several assumptions including (i) no storage of chloride in the unsaturated zone; (ii) precipitation and dry atmospheric deposition are the only sources of chloride in groundwater and in surface runoff; (iii) measured chloride concentrations are at depths high enough such that, seasonal variations in concentration are small; and (iv) the concentration of chloride in surface runoff is the same as that in precipitation (McNamara, 2005; Sumioka and Bauer, 2004). A detailed description of the chloride mass balance method is found in Sumioka and Bauer (2004), Stone (1992), and Johnston (1987).

Assuming a steady-state condition with advection strongly dominating diffusion; and neglecting the mass of chloride from dry atmospheric deposition, a mass balance of chloride in precipitation, surface runoff and groundwater is obtained. The balance can be represented mathematically as (McNamara, 2005; Sumioka and Bauer, 2004):

$$PC_p = RC_{gw} + QC_r \quad (5.1)$$

where: P is annual precipitation (mm); C_p is concentration of chloride in precipitation (mg/l); R is annual groundwater recharge (mm); C_{gw} is concentration of chloride in groundwater (mg/l); Q is annual surface runoff (mm); and C_r is concentration of chloride in surface runoff (mg/l).

Neglecting surface runoff due to the lack of data for the area studied, the terms in equation 5.1 can be re-arranged to calculate the groundwater recharge as:

$$R = \frac{PC_p}{C_{gw}} \quad (5.2)$$

However, neglecting surface runoff in the recharge estimation leads to an overestimation of the recharge rates. Martin (2005) reported that, neglecting surface runoff in the estimation of groundwater recharge in the Atankwidi catchment resulted in an overestimation of the recharge by less than 10 %, since surface runoff as in equation 5.1 accounted for about 7 % of the annual rainfall in 2003.

5.2 Study area

The CMB was applied to the northeastern part of Ghana within the White Volta Basin (mainly the Upper East Region of Ghana) (Figure 4.1), to estimate the long-term groundwater recharge in the region. With a population density of 104 persons per km², the Upper East Region is one of the most densely populated areas in the White Volta Basin. It has a population of about 920,000 people with an annual growth rate of 3 % (Ghana Statistical Service, 2002). The region has a total land area of about 8,842 km² and a slope of less than 2 %. The climate is semi-arid with a long-term mean annual rainfall of 990 mm (Ghana Meteorological Services Department). The economy of the region depends heavily on groundwater.

Over 80 % of the urban population in the Region is served with tapwater from groundwater sources (Martin and van de Giesen, 2005). In 1994, the Upper East Region had about 1680 boreholes that provided potable water for small towns and rural

communities (Kortatsi, 1994). Small-scale farmers in the region depend mostly on groundwater abstracted from alluvial channels along the courses of ephemeral streams for irrigation of vegetables during the dry season. This is a major source of income for such farmers. Cattle and livestock in the region are mostly watered from groundwater sources, particularly in the dry season.

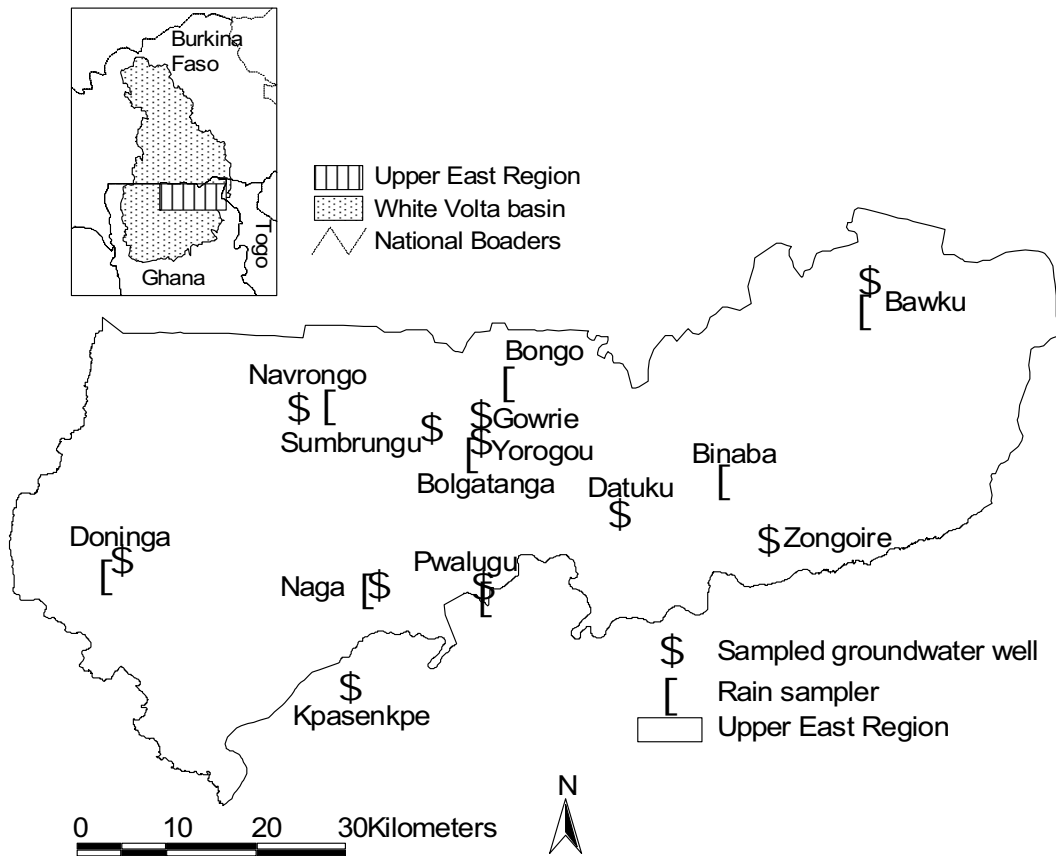


Figure 5.1 Location of the Upper East Region, Ghana, and water sampling sites

5.3 Data

The use of the CMB method for estimating groundwater recharge requires data of chloride concentrations in rainfall and groundwater as well as data on rainfall amount. To obtain a long-term mean recharge for the study area, long-term values of the terms in equation 5.2 are required. The values of chloride concentrations measured in groundwater can be said to be long-term because of mixing and generally multi-year residence time of water in most aquifers (Sumioka and Bauer, 2004). Long-term rainfall

series data were available for determining the long-term mean annual rainfall. The long-term mean concentrations of chloride in rainfall could not be determined because such data does not exist. The data used were mean values for the year 2006.

5.3.1 Water sampling and chloride analysis

Samples of rainfall and groundwater were collected from selected locations and wells in the study area (Figure 5.1) in 2006 and taken to the laboratory for the analysis of chloride content. Rainwater samplers (two-liter container equipped with a large funnel) were mounted on wooded structures erected at few centimeters above ground level to collect composite samples of rainwater at two-week intervals at 8 locations spread across the region, from May to October, 2006.

Groundwater samples were taken from 7 wells that are equipped with hand pumps in March, June, August and December of 2006. In addition to the 7 wells, chloride concentration data from 4 other groundwater wells (Gowrie, Bawku, Datuku and Bongo) studied by the Water Research Institute (WRI), Ghana, in 2006 were obtained and used in this study.

All water samples were collected according to standard procedures and were transported in appropriate containers, and under conditions specified by the chemistry laboratory of the Ghana Atomic Energy Commission, where analyses of chloride concentrations were done.

5.3.2 Rainfall measurements

Long-term rainfall data for the study area, including rainfall for 2006, were obtained from the Ghana Meteorological Services Department (GMSD), Accra. As part of this study, 6 automatic rain gages (HOBO event data loggers) were installed at 6 of the 8 sites where the rainwater samplers were mounted, to improve the rainfall data collection coverage in the study area (Figure 5.1)

5.4 Results and discussions

5.4.1 Chloride concentrations in rainfall

Chloride concentrations in rainwater in the study area in 2006 ranged from 0.2 to 6.8 mg/l (Tables 5.1). Chloride concentration measured at Doninga in September was

exceptionally high (6.8 mg/l). This was taken to be an outlier and was not considered in the estimation of the overall recharge. Eliminating the outlier, chloride concentration in rainfall ranged from 0.2 to 2.1 mg/l, with area-weighted mean and standard deviation of 0.8 mg/l and 0.43 mg/l, respectively.

Table 5.1: Chloride concentrations in rainwater samples collected in the Upper East Region, Ghana, in 2006

Sampling site	Site coordinates		Monthly chloride concentrations (mg/l)					
	Easting	Northing	May	Jun	Jul	Aug	Sept	Oct
Manga	798780	1219124	0.9	0.7	0.7	0.2	0.5	1.1
Pwalugu	735581	1171153	1.2	0.5	0.6	0.4	0.6	0.9
Naga	715778	1172466	1.9	0.7	0.6	0.4	0.7	1.8
Binaba	775263	1190695	1.3	0.8	0.4	0.5	0.9	2.3
Bongo	739369	1207109	1.2	0.9	0.7	0.4	0.5	2.1
Bolgatanga	733256	1195202	0.8	1.0	0.8	0.3	0.8	1.5
Navrongo	709506	1203188	1.4	0.9	0.6	0.4	0.5	1.1
Doninga	672294	1174830	0.9	0.4	0.3	0.2	0.7	6.8 ^a

NB: ^a treated as outlier and not used in the estimation of the recharge.

High chloride concentrations were measured in May and October, which were respectively, the beginning and end of the rainfall season. At all the rainwater sampling locations, the lowest concentrations were measured in August. Generally, monthly chloride concentrations in rainfall decreased with increasing rainfall amounts (Figure 5.2). This gives credence to the inverse relationship between rainfall amount and chloride concentration in rainfall as depicted in equation 5.2. With the exception of the month of August, significant spatial variations were observed throughout the rainfall season.

Compared to measurements obtained in areas with similar climate, chloride depositions in the study area are reasonable and acceptable. In the Atankwidi catchment, Martin (2005) obtained chloride deposition between 0.1 and 3.7 mg/l for 2004, with a mean of 0.2 mg/l. Similarly, Sandwidi (2007) measured chloride deposition of 0.87 and 0.88 mg/l, for 2005 and 2006, respectively, in the Kompienga Dam Basin. In other places in Africa, Nkotagu (1996) reported chloride deposition of 2.0-2.8 mg/l for Tanzania; Larsen et al. (2001) and Edmunds et al. (2002) used the values 0.5 and 0.65

mg/l, respectively, to estimate the recharge to groundwater in western Zimbabwe and Maiduguri in Nigeria.

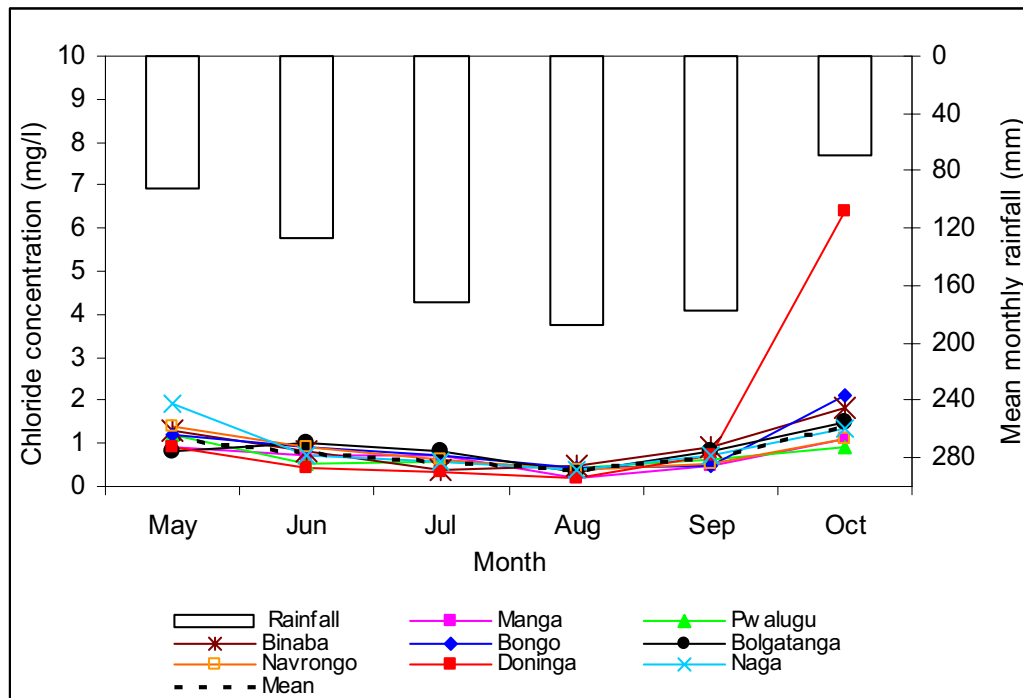


Figure 5.2 Monthly rainfall amount and chloride concentration in rainwater in the Upper East Region, in 2006

5.4.2 Chloride concentrations in groundwater

Monthly chloride concentrations measured in groundwater for the 12 selected wells used in this study ranged from 4.0 to 39.7 mg/l (Table 5.2). Concentrations at Bongo were found to be too high and were therefore treated as outliers. Excluding the Bongo well, monthly chloride concentrations lie in the range 4.0-23.8 mg/l. The mean chloride concentration for the study area was 13.2 mg/l and the standard deviation 9.0 mg/l. There seem to be no correlation between chloride concentration and location of well. Compared to other areas in West Africa with similar geology and climatic condition (Table 5.3), the chloride concentrations measured in the groundwater in the study area are reliable.

The lowest chloride concentrations were measured in water samples taken from wells located at Datuku, Doninga, Gowrie and Kpasenkpe with Datuku having the lowest values. This suggests that the highest rates of recharge to groundwater in the study area in 2006 occurred at these four locations, as depicted in the inverse

relationship of recharge rate and chloride concentration in groundwater in equation 5.2. The low chloride concentrations and potentially high recharge rates at Datuku, Doninga, Gowrie and Kpasenkpe can be explained by the soil texture. The soil textures in the four locations are Sandy clay loam (Datuku), Loamy sand (Doninga), Sandy loam (Gowrie) and Loam (Kpasenkpe). These soils have high hydraulic conductivity, which allows relatively easy infiltration of the rainfall through the soil to the groundwater table.

Soil texture alone was not sufficient to explain the variation in chloride content in some locations in the study area. The value measured at Bongo was the highest obtained in this study. This was not expected, since the soils in the Bongo area are sandy loam, which has a very high hydraulic conductivity compared to the soils at most of the other locations in the study area. Martin (2005) obtained similarly high value from a well in a neighbouring area with the same geological formation and concluded, based on a hydrochemical analysis, that the high chloride concentrations measured were a result of mineral dissolution. This could also be the reason for the high chloride concentrations measured in the groundwater at Bongo and not the low recharge from rainfall. This is very well supported by records of groundwater level and recharge estimated with the water table fluctuation method (chapter 4). The recharge estimate at Bongo was the highest obtained for the White Volta Basin of Ghana in 2006 and 2007 (Table 4.1).

Table 5.2: Summary of chloride concentrations in groundwater samples taken from selected wells in the Upper East Region, Ghana, in 2006

Well location	UTM Coordinates		Altitude of land surface (m)	Monthly chloride concentration (mg/l)			
	Northing	Easting		Mar	Jun	Aug	Dec
Kpasenkpe	712994	1155700	122	6.3	6.8	7.0	6.7
Sumbrungu	726544	1199243	114	11.2	10.9	10.9	11.0
Yorougu	734764	1196872	191	10.1	9.8	10.3	9.6
Zongoire	782889	1180367	230	18.5	18.0	18.6	18.6
Pwalugu	735237	1172564	221	22.1	23.8	23.7	23.5
Doninga	674960	1177106	164	5.9	5.7	5.8	6.2
Naga	717775	1172774	159	11.4	11.0	10.9	12.1
Navrongo	704408	1202456	179	13.9	-	12.9	12.9
Gowrie	734709	1201218	181	6.0	-	6.0	7.0
Bawku	799594	1223879	224	9.9	-	11.9	11.9
Datuku	757915	1184680	194	4.0	-	4.0	5.0
Bongo	739687	1207007	224	39.7	-	28.8	39.7

Table 5.3: Chloride concentrations (Cl_{gw}) measured in groundwater and CMB recharge from previous studies in (semi-)arid West Africa

Author(s)	Country	Cl_{gw} (mg/l)	Recharge	
			(mm)	(% rainfall)
Sandwidi (2007)	Burkina Faso	(16.5)	(43.9)	(5.3)
Martin (2005)	Ghana	0.8-39 (6.2)	30-61	3.0-6.2 (5.9)
Bromley et al. (1987)	Niger	5-150 (36.4)	10-19	1.8-3.4
Houston (1988)	Zimbabwe			2.0-5.0
Nyagwambo	Zimbabwe	4.3-25.5 (9.2)	62-117 (90)	4.0-25.0 (12)

NB: Figures in brackets are mean values

5.4.3 Recharge estimates

The overall groundwater recharge for the study area was calculated based on the recharge values of the individual wells and the area weight of the wells. The recharge value of each of the 11 wells sampled for chloride analysis was estimated using the area-weighted mean chloride concentration in rainwater (0.80 mg/l), the long-term mean annual rainfall in the study area (990 mm) and the mean chloride concentrations in

groundwater (Table 5.4). The recharge rate for Bongo was excluded from the calculation of the overall recharge due to reasons already discussed in section 5.4.2.

The results show that the groundwater recharge in the Upper East Region ranged from 34.0 to 182.8 mm, representing 3.4 to 18.5 % of the mean annual rainfall. The overall mean groundwater recharge was estimated to be 82.0 mm, representing 8.3 % of the long-term mean annual rainfall. The highest and lowest values were obtained at Datuku and Pwalugu, respectively (Table 5.4). Figure 5.3 is a plot of the spatial interpolation of recharge in the study area, based on the CMB recharge estimates. High recharge areas are mostly located in the middle parts of the study area, around Datuku, Bongo, Gowrie and Yorogou.

The recharge values obtained for the Upper East Region are reliable compared to recharge values estimated with the CMB method in other parts of the Volta basin and West Africa (Table 5.3). The reliability of the values can be improved if long-term data on chloride deposition are used instead of the one-year mean values used in this study. This is because chloride deposition is influenced by the amount and distribution of rainfall, so that in a year where rainfall amount and distribution are very different from the long-term mean, chloride deposition may vary much from the long-term mean and therefore will not represent the average situation. Data on long-term mean chloride deposition in the study area do not exist. The mean annual rainfall in 2006 (870 mm) when chloride deposition measurements were taken for recharge estimates was about 12 % below the long-term mean (990 mm), and therefore the mean chloride deposition was not expected to change that much.

The recharge value calculated for the Upper East Region with the CMB method is very much close to what was obtained with the water table fluctuation method for the White Volta Basin of Ghana (chapter 4). A comparison of spatial interpolated recharge obtained with the CMB and the WTF methods for the Upper East Region, show that the two methods are generally in agreement regarding potentially high and low recharge areas (Figures 5.3 and 5.4) although there are disagreements regarding the recharge values for some locations, particularly Navrongo, Bawku, Zongoire and Pwalugu. The spatially interpolated recharge could be used as first hand information on the groundwater recharge for water resources planning. Detail studies may be required for a more reliable recharge values in places that are far from any of the wells sampled.

Table 5.4: Mean chloride concentrations in groundwater in selected wells and long-term recharge estimated in the Upper East Region, Ghana, in 2006

Well location	Mean chloride concentration (mg/l)	Recharge (mm)	Recharge (%)
Kpasenkpe	6.7	117.8	11.90
Sumbrungu	11.0	72.0	7.30
Yorougu	10.0	79.6	8.00
Zongoire	18.4	43.0	4.30
Pwalugu	23.3	34.0	3.40
Doninga	5.9	134.2	13.60
Naga	11.4	69.8	7.00
Navrongo	13.2	59.9	6.00
Gowrie	6.3	125.1	12.60
Bawku	11.2	70.5	7.10
Datuku	4.3	182.8	18.50
Bongo ^a	36.1	22.0	2.20

NB: ^a excluded from overall recharge estimation

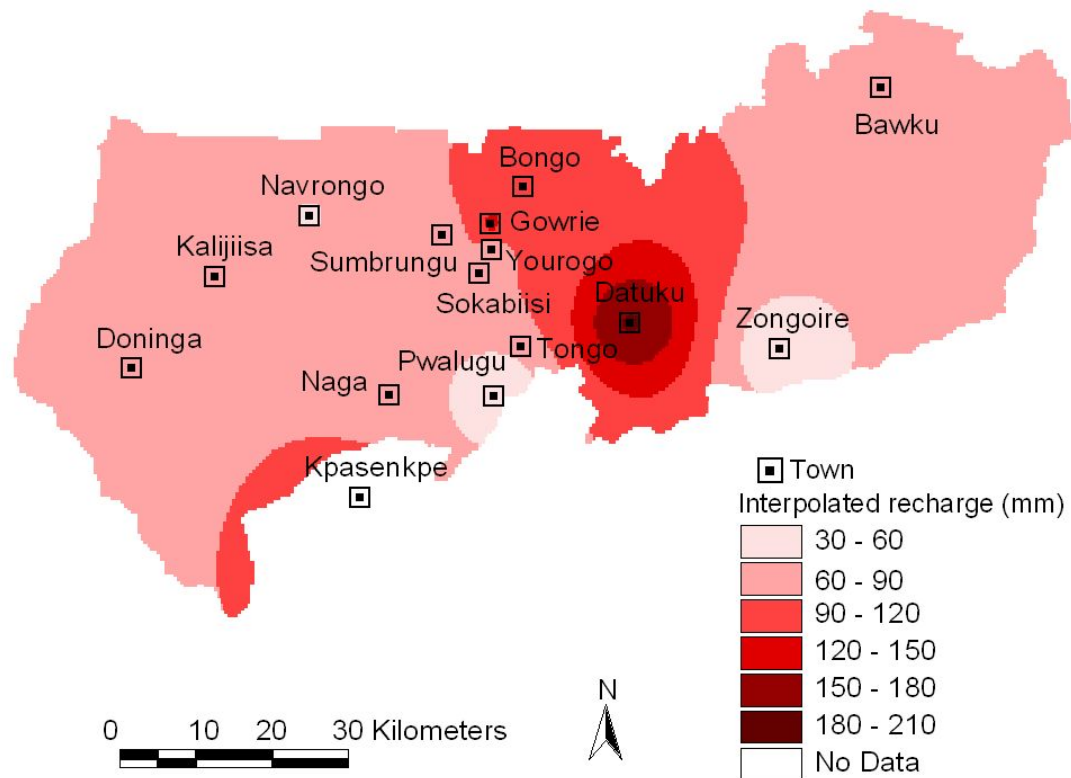


Figure 5.3 Spatially interpolated long-term recharge estimated with the chloride mass balance method in the Upper East Region, Ghana, in 2006

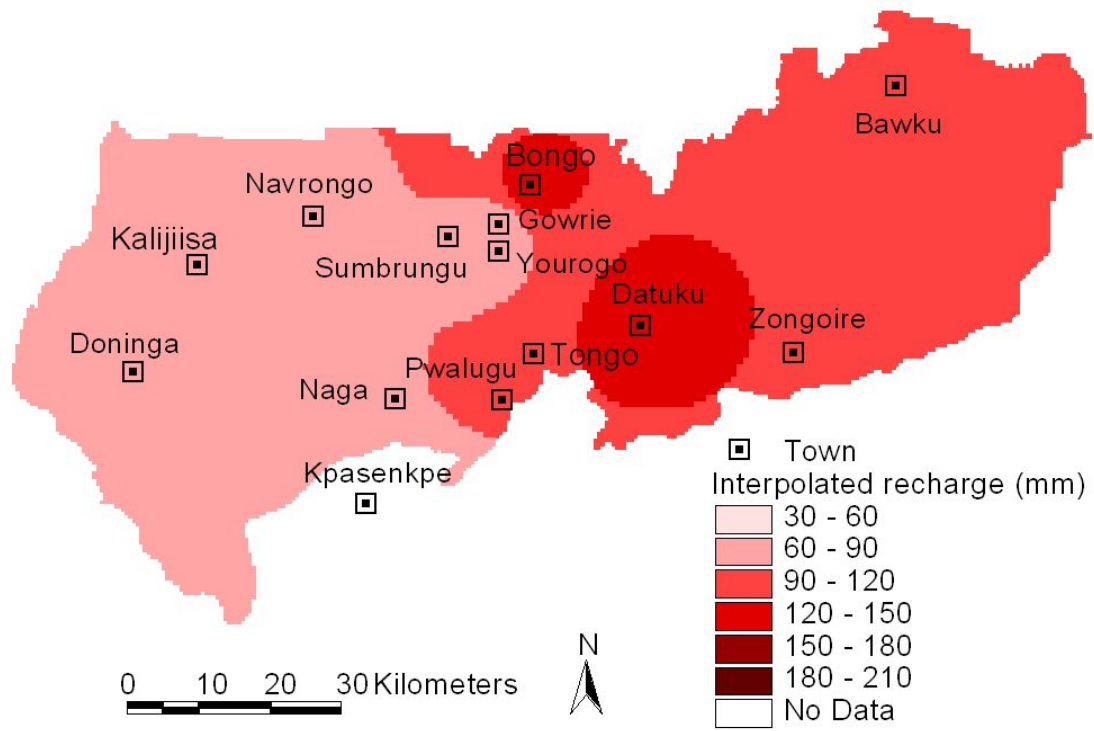


Figure 5.4 Spatially interpolated recharge estimated with the water table fluctuation method in the Upper East Region, Ghana, in 2006

6 RECHARGE ESTIMATION USING THE SOIL AND WATER ASSESSMENT TOOL (SWAT)

6.1 Introduction

The Soil and Water Assessment Tool (SWAT) model is a medium- to large-scale river basin model that was developed to predict the impact of land management practices such as land-use and -cover changes, reservoir management, groundwater withdrawals, and water transfers on sediment, water, and agricultural chemical yields in complex watersheds with varying soils, landuse and management conditions over long periods of time (Neitsch et al., 2005). SWAT is a physically based, spatially semi-distributed and computationally efficient model that can be used to simulate a single basin or a system of multiple basins that are hydrologically connected (Luzio et al., 2002). It is a continuous time series model with a GIS interface and that uses readily available input data.

SWAT has proven to be an effective model for river basin studies under different environmental and climatic conditions. It has been used extensively to assess the impact of various land management practices and potential climate change on water quantities and sediment yields in many river basins in the United States (Arnold and Allen, 1996; Srinivasan and Arnold, 1994; Rosenthal et al., 1995; Arnold et al., 1999; Saleh et al., 2000; Arnold et al., 2000; Afinowicz et al., 2005; Arabi et al., 2006; Jha, et al., 2006; Santhi et al., 2001). The model has been adapted by major institutions including the United States Environmental Protection Agency for research that aids policy implementation. Outside of the United States, the SWAT model has been used in basin studies in many countries worldwide, including previous studies in Europe e.g., Lenhardt et al., 2002; El-Nasr et al., 2005; Grizetti et al., 2005; Bouraoui et al., 2004; Conan et al., 2003; Gikas et al., 2005; Asia e.g., Hao et al., 2004; Gosian et al., 2005; Kang et al., 2006; Huisman et al., 2004; Tripathi et al., 2003; and Africa e.g., Bouraoui et al., 2005; Lijalem, 2006; Chekol, 2006; Schuol and Abbaspour, 2006; Sintondji, 2005; Busche et al, 2005; Hiepe and Diekkrueger, 2007; Govender and Everson, 2005; Ndomba et al., 2005; and Githui, 2007.

The main components of the SWAT model are weather, hydrology, plant growth, nutrients, pesticides, bacteria and pathogens, and land management. Basic input information required for modeling a river basin in SWAT include a digital elevation

model, soil, landuse and climate data. SWAT uses the topographic data to divide a river basin into multiple sub-basins, which are further subdivided into hydrologic response units (HRUs) that consist of homogeneous landuse, management, and soil characteristics (Gassman et al., 2007). Through the subdivision of a basin, the model can reflect the differences in evapotranspiration for different crops and soils. Further subdivision of sub-basins into HRUs makes it possible to account for the impact of very different landuse types, soil properties and management practices on the hydrology of a basin.

Much of the SWAT input data are provided at the sub-basin level and grouped into climate, HRUs, ponds/wetlands, groundwater, and the main channel draining the sub-basin, among others. Input climate variables required by SWAT are precipitation, maximum and minimum air temperature, solar radiation, wind speed and relative humidity.

6.2 SWAT hydrology

Similar to most river basin models, SWAT is driven by the water balance of a river basin. The simulation of a basin's hydrology can be separated into (i) the land phase of the hydrologic cycle that controls the amount of water, sediment, nutrient and pesticide loadings to the main channel in each sub-basin, and (ii) the routing phase of the hydrologic cycle, which is the movement of water, sediments, etc., through the channel network of the basin to the outlet (Neitsch et al., 2005). Irrespective of the problem studied in a river basin, predictions made with SWAT can only be accurate if the model is able to mimic the hydrologic cycle in the basin. The hydrologic cycle that takes place in a basin is explained by the water balance in the basin.

The water balance equation that represents the hydrologic cycle simulated in SWAT (Figure 4.6) can be expressed mathematically as (Neitsch et al., 2005):

$$SW_t = SW_0 + \sum_{i=1}^t (R_{day} - Q_{surf} - E_a - W_{seep} - Q_{gw}) \quad (6.1)$$

where: SW_t is the soil water content at time t (mm); SW_0 is the initial soil water content on day i (mm); t is time (days); R_{day} is the amount of precipitation on day i (mm);

Q_{surf} is the amount of surface runoff on day i (mm); E_a is the amount of evapotranspiration on day i (mm); W_{seep} is the amount of water entering the vadose zone from the soil profile on day i (mm); and Q_{gw} is the amount of return flow on day i (mm).

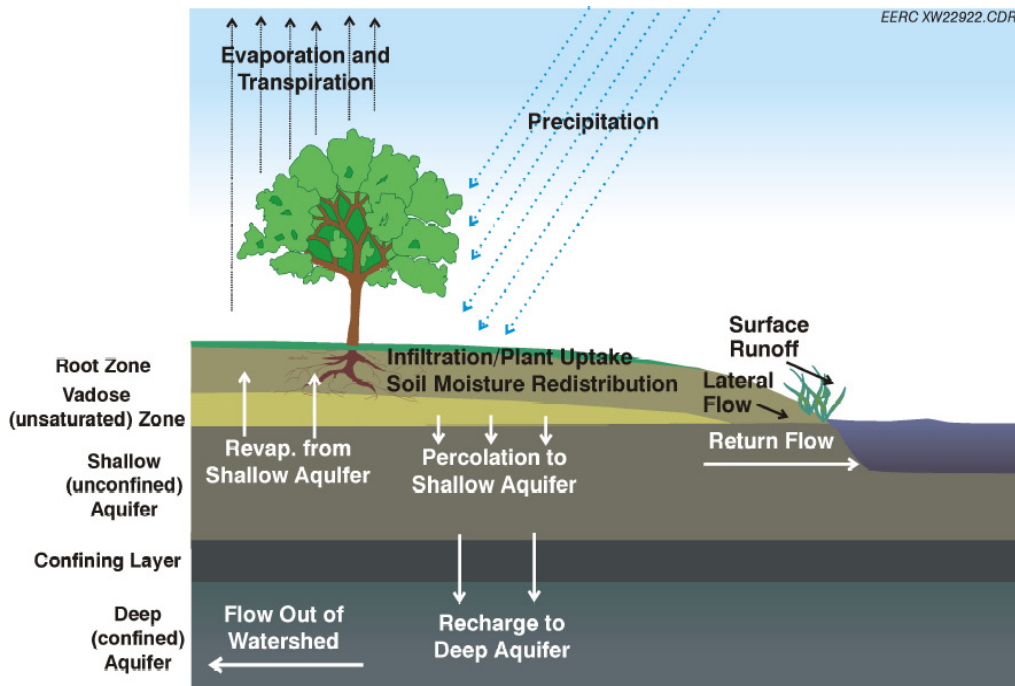


Figure 6.1 Schematic representation of the hydrologic cycle (EERC-University of North Dakota, 2008, modified from Neitsch et al., 2005)

In SWAT, most of the hydrologic processes take place at the HRU level, and the water balance is simulated at this level before runoff is routed to the reaches of sub-basins and then to the basin channel. The major hydrologic components modeled in SWAT as depicted in the water balance equation are precipitation, surface runoff, evapotranspiration, infiltration, groundwater flow and soil water content.

6.2.1 Precipitation

Precipitation controls the water balance in a basin because it is the mechanism by which water enters the land phase of the hydrologic cycle (Neitsch et al., 2005). In SWAT, precipitation is one of the very important and basic input data types required for modeling a basin's hydrology. Precipitation is obtained from records of observed data or generated by SWAT during the simulation. Neitsch et al. (2005) recommend the use of observed precipitation data any time such data are available, as the ability of SWAT

to reproduce observed stream hydrographs is very much improved by the use of observed precipitation data. The time frequency of precipitation data required for use with SWAT can be daily or sub-daily. For various reasons, sufficient observed precipitation data are not available in many areas of the world, particularly in developing countries. Even in areas where long-term precipitation data is available, there may be missing gaps that need filling. SWAT uses a precipitation generator to either generate daily precipitation for simulations in areas where observed data are not available or to fill in gaps in areas where records are available but with missing data.

The SWAT precipitation generator uses a first-order Markov-chain model to define a day as wet or dry by comparing a random number (0.0-1.0) generated by the model to monthly wet-dry probabilities input by the model user. If a day is classified as wet, SWAT uses either a skewed distribution model proposed by Nick (1974) or an exponential model proposed by Williams (1995) to generate the precipitation amount (Neitsch et al., 2005). The equation used for computing the amount of precipitation on a wet day with the skewed distribution model is given as (Neitsch et al., 2005):

$$R_{day} = \mu_{month} + 2 \cdot \sigma_{month} \cdot \left[\frac{\left[\left(\left(SND_{day} - \frac{g_{month}}{6} \right) \left(\frac{g_{month}}{6} \right) + 1 \right)^3 - 1 \right]}{g_{month}} \right] \quad (6.2)$$

where: R_{day} is the amount of precipitation on a given day (mm); μ_{month} is the mean daily precipitation (mm) for the month; σ_{month} is the standard deviation of daily precipitation (mm) for the month; SND_{day} is the standard normal deviate calculated for the day; and g_{month} is the skew coefficient for daily precipitation in the month.

The standard normal deviate for the day is calculated as:

$$SND_{day} = \cos(6.283 \cdot rnd_2) \cdot \sqrt{-2 \ln(rnd_1)} \quad (6.3)$$

where: rnd_1 and rnd_2 are random numbers between 0.0 and 1.0.

The exponential distribution requires fewer inputs and is often used in areas where data on precipitation events are limited. With this distribution, daily precipitation is calculated using the equation (Neitsch et al., 2005):

$$R_{day} = \mu_{month} \cdot (-\ln(rnd_1))^{r_{exp}} \quad (6.4)$$

where: R_{day} is the amount of precipitation on a given day (mm); μ_{month} is the mean daily precipitation (mm) for the month; rnd_1 is a random number between 0.0 and 1.0; and r_{exp} is an exponent that should be set between 1.0 and 2.0.

In this study, daily observed precipitation data were available for the simulation. However, records from some measuring stations had missing data that were filled by the SWAT precipitation generator using the option of skewed distribution for calculating the amount of precipitation on a wet day.

6.2.2 Surface runoff

Surface runoff occurs when the rate of water falling on the ground exceeds the infiltration rate of the soil and all surface depressions are filled to capacity. It can be defined as the water leaving an area of drainage and flowing across the land surface to points of lower elevation.

There are two methods available for estimating the surface runoff in SWAT: a modification of the SCS curve number procedure (SCS, 1972) and the Green and Ampt infiltration method (1911). The SCS curve number is a function of landuse, soil permeability and antecedent soil water conditions (Neitsch et al., 2005). Curve numbers decrease as soil moisture approaches wilting point and increases to near 100 as soil moisture approaches saturation. The Green Ampt method calculates infiltration as a function of the wetting front matrix potential and effective hydraulic conductivity, and water that does not infiltrate becomes surface runoff (Neitsch et al., 2005). The Green Ampt method is data intensive; it requires sub-daily precipitation data that is not available in the study area. Therefore, the SCS curve number option was used for estimating the runoff in this study.

The SCS curve number method uses an empirical model with an established relationship between rainfall and runoff that provides a consistent basis for estimating the amount of runoff under varying landuse and soil types. The equation underlying the SCS curve number is mathematically expressed as (SCS, 1972):

$$Q_{surf} = \frac{(R_{day} - I_a)^2}{(R_{day} - I_a + S)} \quad (6.5)$$

where: Q_{surf} is the accumulated runoff or rainfall excess (mm); R_{day} is the amount of precipitation on a given day (mm); I_a is the initial abstractions which includes surface storage, interception and infiltration prior to runoff (mm); and S is the retention parameter (mm).

The retention parameter (S) varies spatially due to changes in soils, landuse, management and slope and temporally due to changes in soil water content. In SWAT, the retention parameter relates to the curve number for the day (CN) and is defined as (Neitsch et al., 2005):

$$S = 25.4 \left(\frac{1000}{CN} - 10 \right) \quad (6.6)$$

The initial abstraction, I_a , in (6.5) is commonly approximated as $0.2S$ and equation (6.6) becomes (all parameters defined as in 6.5):

$$Q_{surf} = \frac{(R_{day} - 0.2S)^2}{(R_{day} + 0.8S)} \quad (6.7)$$

It can be deduced from (6.7) that runoff will only occur when $R_{day} > I_a$. Tables of typical curve numbers for various soil types and land covers that are appropriate for a land slope of 5 % can be obtain from the SCS Engineering Division (1986).

In SWAT, the runoff is calculated separately for the individual HRUs and routed to obtain the total runoff for each sub-basin. The sub-basin runoff is then routed to obtain the total runoff for the entire basin.

6.2.3 Peak runoff rate

The peak runoff rate is the maximum runoff flow rate that occurs with a given rainfall event. The peak runoff rate is an indicator of the erosive power of a storm and is used to predict sediment loss. SWAT calculates the peak runoff rate with a modified rational method (Neitsch et al., 2005).

The rational method is based on the assumption that if a rainfall of intensity i begins at time $t = 0$ and continues infinitely, the rate of runoff will increase until the time of concentration, $t = t_{conc}$, when the entire sub-basin area is contributing to flow at the outlet. The modified rational formula is (Neitsch et al., 2005):

$$q_{peak} = \frac{\alpha_{tc} \cdot Q_{surf} \cdot A}{3.6 \cdot t_{conc}} \quad (6.8)$$

where: q_{peak} is the peak runoff rate ($m^3 s^{-1}$); Q_{surf} is the surface runoff (mm); A is the sub-basin area (km^2); t_{conc} is the time of concentration for a sub-basin (h); α_{tc} is the fraction of daily rainfall that occurs during the time of concentration; and 3.6 is a unit conversion factor.

The time of concentration (t_{conc}) in equation 6.8 is a summation of overland flow time and channel flow time. Overland flow time is defined as the time it takes for water to travel from the furthest point in the sub-basin to reach the stream channel, and channel flow time is the time it takes for flow in the upstream channel to reach the outlet. The overland and channel flow time are calculated using Manning's formula.

$$t_{conc} = t_{ov} + t_{ch} \quad (6.9)$$

where: t_{conc} is the time of concentration; t_{ov} is the overland flow time; and t_{ch} is the channel flow time. The overland flow time is:

$$t_{ov} = \frac{L_{slp}^{0.6} \cdot n^{0.6}}{18 \cdot slp^{0.3}} \quad (6.10)$$

where: L_{slp} is the average sub-basin slope length (m); Slp is the average sub-basin slope (m/m); and n is the Manning's roughness coefficient.

The channel flow time is:

$$t_{ch} = \frac{0.62 \cdot L \cdot n^{0.75}}{Area^{0.125} \cdot slp_{ch}^{0.375}} \quad (6.11)$$

where: t_{ch} is the time of concentration for channel flow (hr); L is the channel length from the most distant point to the sub-basin outlet (km); n is the Manning's roughness coefficient for the channel; $Area$ is the sub-basin area (km²); and slp_{ch} is the channel slope (m m⁻¹).

6.2.4 Surface runoff lag

In large sub-basins with a time of concentration greater than 1 day, only a portion of the surface runoff will reach the main channel on the day it is generated. SWAT incorporates a surface runoff storage feature to lag a portion of the surface runoff release to the main channel (Neitsch et al., 2005). After surface runoff is computed, the amount released to the main channel is (Neitsch et al., 2005):

$$Q_{surf} = (Q'_{surf} + Q_{stor,i-1}) \cdot \left(1 - \exp\left[\frac{-surlag}{t_{conc}} \right] \right) \quad (6.12)$$

where: Q_{surf} is the amount of surface runoff discharged to the main channel on a given day (mm); Q'_{surf} is the amount of surface runoff generated in the sub-basin on a given day (mm); $Q_{stor,i-1}$ is the surface runoff stored or lagged from the previous day (mm); $Surlag$ is the surface runoff lag coefficient; and t_{conc} is the time of concentration for the sub-basin (hrs).

It can be deduced from (6.12) that, for a given time of concentration, more water is held in storage as the surface runoff lag coefficient decreases. A delay in the release of surface runoff smoothes the streamflow hydrograph simulated in the channel (Neitsch et al., 2005)

6.2.5 Transmission losses

In many arid- and semi-arid-basins, rivers are ephemeral in nature and flow only in response to specific heavy rainfall events. Since recharge from rainfall to the groundwater aquifer in arid- and semi-arid-areas is low, groundwater heads are usually low and river beds are above the aquifer saturated zone except downstream or at the aquifer boundary, or at specific sites where aquifer thickness is reduced. As a result, streams in arid- and semi-arid-areas lose water recharging the aquifers. Water losses along ephemeral rivers are commonly known as transmission losses.

Generally, transmission losses in a river channel include two important processes, namely, seepage or aquifer recharge and evapotranspiration. The rate of seepage depends on factors such as the type and hydraulic properties of the channel material, channel geometry, wetted perimeter, and depth of groundwater. Evaporation losses depend on meteorological conditions and the rate of transpiration of vegetation. Transmission losses reduce runoff volume as the flood wave travels downstream. In SWAT, transmission losses from runoff are assumed to percolate to the shallow aquifer. The model uses a procedure described by Lane (1983) to estimate the transmission losses of ephemeral rivers.

6.2.6 Evapotranspiration

Evapotranspiration is a term used to describe the sum of evaporation and plant transpiration from the earth's land surface to the atmosphere. Evaporation accounts for the movement of water to the atmosphere from sources such as the soil, canopy interception, and water bodies. Transpiration accounts for the movement of water within a plant and the subsequent loss of water as vapour through stomata in its leaves. Evapotranspiration is an important part of the water cycle and the primary mechanism by which water is removed from a basin. In SWAT, evaporation from soils is computed separately from transpiration from plants (Neitsch et al., 2005). Potential soil water

evaporation is estimated as a function of potential evapotranspiration and leaf area index, and the actual soil water evaporation is estimated using exponential functions of soil depth and water content. Plant transpiration is estimated as a linear function of potential evapotranspiration and leaf area index. Evapotranspiration can be categorized into potential and actual evapotranspiration.

Potential evapotranspiration (PET) is defined as the rate at which evapotranspiration would occur from a large area completely and uniformly covered with growing vegetation, which has access to an unlimited supply of soil water (Neitsch et al., 2005). PET is usually measured indirectly from other climatic factors. SWAT provides three options for estimating the PET, namely, the Hargreaves method (Hargreaves et al., 1985), Priestly-Taylor method (Priestly and Taylor, 1972) and the Penman-Monteith method (Monteith, 1965; Allen et al., 1989). The Hargreaves method requires only air temperature as input data, the Priestly-Taylor method requires solar radiation, air temperature and relative humidity, and the Penman-Monteith method requires solar radiation, air temperature, relative humidity and wind speed. SWAT provides an additional option for the user to input data of PET that has been determined outside of SWAT. The Penman-Monteith method was chosen for estimating the PET in the study area.

The actual evapotranspiration (AET) is the amount of water that is actually removed from a surface through the processes of evaporation and transpiration. The AET is equal to the PET when there is enough water. SWAT calculates the AET once the total PET is determined. SWAT first evaporates any rainfall intercepted by plant canopies and then calculates the maximum amount of transpiration and sublimation or soil evaporation using an approach similar to that of Richtie (1972). If snow is present in the HRU, sublimation will occur. It is only when no snow is present that evaporation from the soil takes place.

6.2.7 Soil water

When water enters the soil, it may move in any of the three major pathways. It can be removed from the soil through the process of evapotranspiration or percolate through the bottom of the soil profile and ultimately becomes groundwater recharge, or may move laterally in the soil profile and contribute to streamflow (Neitsch et al., 2005).

Percolation is simply the movement of water downward through the subsurface to the zone of saturation. In SWAT, percolation is calculated for each soil layer in the profile. Water is allowed to percolate only if the water content exceeds the field-capacity water content for that layer, and if the layer below is not saturated. When the soil is frozen, no water flow out of the layer is calculated. SWAT uses a storage routing methodology to compute the amount of water that moves from one layer to the underlying layer. The equation used to calculate the amount of water that percolates to the next layer is (Neitsch et al., 2005):

$$w_{perc,ly} = SW_{ly,excess} \cdot \left(1 - \exp \left[\frac{-\Delta t}{TT_{perc}} \right] \right) \quad (6.13)$$

Where: $w_{perc,ly}$ is the amount of water percolating to the underlying soil layer on a given day (mm of water); $SW_{ly,excess}$ is the drainable volume of water in the soil layer on a given day (mm of water); Δt is the length of the time step (hrs); and TT_{perc} is the travel time for percolation (hrs).

If the HRU has a seasonal high water table, percolation is not allowed when:

$$SW_{ly+1} \leq FC_{ly+1} + 0.5 \cdot (SAT_{ly+1} - FC_{ly+1}) \quad (6.14)$$

where: SW_{ly+1} is the water content of the underlying soil layer (mm); FC_{ly+1} is the water content of the underlying soil layer at field capacity (mm); and SAT_{ly+1} is the amount of water in the underlying soil layer when completely saturated (mm). The water will instead stay ponded in the upper layer.

The travel time for percolation TT_{perc} in (6.13) is unique for each layer and it is calculated using the equation:

$$TT_{perc} = \frac{SAT_{ly} - FC_{ly}}{K_{sat}} \quad (6.15)$$

where: TT_{perc} is the travel time for percolation (hr); SAT_{ly} is the amount of water in the soil layer when completely saturated (mm); FC_{ly} is the water content of the soil at field-capacity (mm); and K_{sat} is the saturated hydraulic conductivity for the layer (mmh^{-1}).

Lateral flow of water in the soil refers to the lateral movement of water in the soil profile. When rainfall is received in an area that has soils with high hydraulic conductivities in the surface layers and an impermeable or semi-permeable layer at a shallow depth, the water percolates vertically until it reaches the impermeable layer and cannot percolate any further. The water then pond above the impermeable layer forming a saturated zone of water that leads to lateral subsurface flow (Neitsch et al., 2005). In SWAT, a kinematic storage model developed by Sloan et al. (1983) is used for simulating the subsurface flow in a two-dimensional cross section along a flow path down a steep hillslope.

The kinematic storage model is based on the mass continuity equation, with the entire hill slope segment used as the control volume (Figure 6.2). The kinematic storage model calculates the lateral flow as (Neitsch et al., 2005):

$$Q_{lat} = 0.024 \cdot \left[\frac{2 \cdot SW_{ly,excess} \cdot K_{sat} \cdot slp}{\phi_d \cdot L_{hill}} \right] \quad (6.16)$$

where: Q_{lat} is lateral flow (mmd^{-1}); $SW_{ly,excess}$ is the drainable volume of soil water (mm); K_{sat} is the saturated hydraulic conductivity (mmh^{-1}); slp is slope (m/m); ϕ_d is the drainable porosity (mm/mm); and L_{hill} is the hillslope length (m).

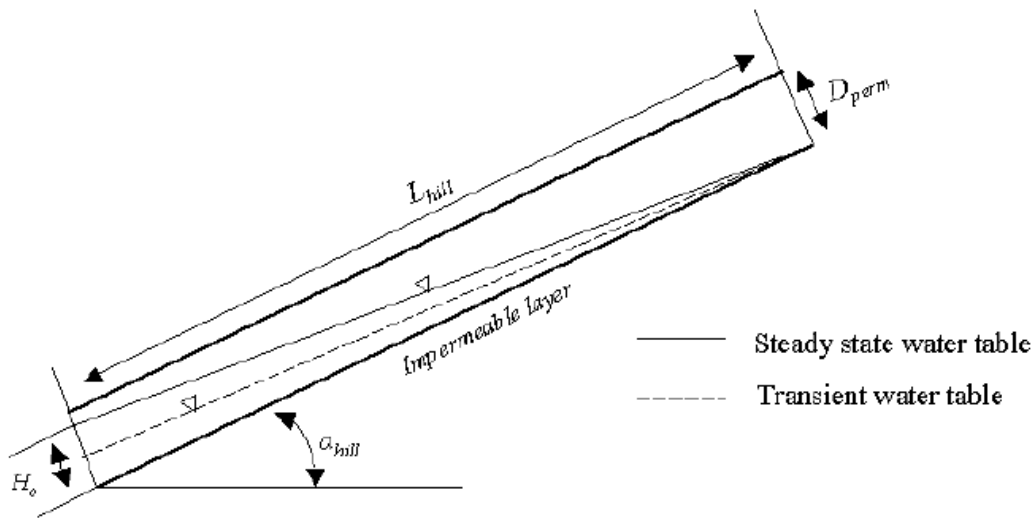


Figure 6.2 Behavior of the water table as assumed in the kinematic storage model (Neitsch et al., 2005).

In large sub-basins with a time of concentration greater than 1 day, only a portion of the lateral flow will reach the main channel on the day it is generated. A lateral flow storage feature has been built into the SWAT model to lag a portion of lateral flow released to the main channel. The amount of lateral flow released to the main channel is calculated as (Neitsche et al., 2005):

$$Q_{lat} = (Q'_{lat} + Q_{latstor,i-1}) \cdot \left(1 - \exp\left[\frac{-1}{TT_{lat}} \right] \right) \quad (6.17)$$

where: Q_{lat} is the amount of lateral flow discharged to the main channel on a given day (mm); Q'_{lat} is the amount of lateral flow generated in the sub-basin on a given day (mm); $Q_{latstor,i-1}$ is the lateral flow stored or lagged from the previous day (mm); and TT_{lag} is the lateral flow travel time (days).

The lateral flow travel time can be calculated by the SWAT model or defined by the model user. Neitsche et al. (2005) recommend that the user allows SWAT to calculate the travel time. If drainage tiles are present in the HRU, lateral flow travel time is calculated as:

$$TT_{lag} = \frac{tile_{lag}}{24} \quad (6.18)$$

where: TT_{lag} is the lateral flow travel time (days); and $tile_{lag}$ is the drain tile lag time (hr). In HRUs without drainage tiles, lateral flow travel time is calculated as:

$$TT_{lag} = 10.4 \cdot \frac{L_{hill}}{K_{sat, mx}} \quad (6.19).$$

where: TT_{lag} is the lateral flow travel time (days); L_{hill} is the hillslope length (m), and $K_{sat, mx}$ is the highest layer saturated hydraulic conductivity in the soil profile (mmhr^{-1}).

6.2.8 Groundwater

Two types of groundwater aquifers are simulated in each sub-basin in the SWAT model. They are the shallow unconfined aquifer that contributes to flow in the main channel or reach of the sub-basin and the deep confined aquifer that is assumed to contribute to streamflow outside of the basin (Arnold et al., 1993). In a groundwater storage system, water enters primarily by infiltration and percolation and possibly by seepage from water bodies. Water leaves the groundwater storage system by discharge into rivers or lakes and possibly by capillary rise. In SWAT, recharge to unconfined aquifers occurs by percolation to the water table from a significant area of the land surface. In contrast, recharge to the confined aquifers by percolation from the surface occurs only at the upstream end of the confined aquifer, where the geologic formation containing the aquifer is exposed at the earth's surface, flow is not confined, and a water table is present (Neitsch et al., 2005).

The water balance of the shallow aquifer as simulated in SWAT is:

$$aq_{sh,i} = aq_{sh,i-1} + w_{rchrg,sh} - Q_{gw} - w_{revap} - w_{pump,sh} \quad (6.20)$$

where: $aq_{sh,i}$ is the amount of water stored in the shallow aquifer on day i (mm); $aq_{sh,i-1}$ is the amount of water stored in the shallow aquifer on day $i-1$ (mm); $w_{rchrg,sh}$ is the amount of recharge entering the shallow aquifer on day i (mm); Q_{gw} is the groundwater flow, or baseflow, into the main channel on day i (mm); w_{revap} is the amount of water moving into the soil zone in response to water deficiencies on day i (mm); and $w_{pump,sh}$ is the amount of water removed from the shallow aquifer by pumping on day i (mm).

The water balance for the deep aquifer is:

$$aq_{dp,i} = aq_{dp,i-1} + w_{deep} - Q_{gw} - w_{pump,dp} \quad (6.21)$$

where: $aq_{dp,i}$ is the amount of water stored in the deep aquifer on day i (mm); $aq_{dp,i-1}$ is the amount of water stored in the deep aquifer on day $i-1$ (mm); w_{deep} is the amount of recharge percolating from the shallow aquifer into the deep aquifer on day i (mm); Q_{gw} is the groundwater flow, or baseflow, into the main channel on day i (mm); and $w_{pump,dp}$ is the amount of water removed from the deep aquifer by pumping on day i (mm).

Recharge to the groundwater aquifers

Recharge to the shallow and deep aquifers occurs via percolation and bypass flow of water from the soil surface through the vadose zone. The time taken for water to exit the soil profile and enter the shallow aquifer as recharge depends on the hydraulic properties of the geologic materials in the vadose and the groundwater zones, and the depth to the water table. SWAT uses an exponential decay weighting function used by Sangrey et al. (1984) to account for the time delay in aquifer recharge once the water exits the soil profile (Neitsch et al., 2005). Recharge to both the shallow and deep aquifers is calculated in SWAT to be:

$$w_{rchrg,i} = (1 - \exp[-1/\delta_{gw}]) \cdot w_{seep} + \exp[-1/\delta_{gw}] \cdot w_{rchrg,i-1} \quad (6.22)$$

where: $w_{rchrg,i}$ is the amount of recharge entering the aquifer on day i (mm); δ_{gw} is the delay time or drainage time of the overlying geologic formations (days); w_{seep} is the total amount of water exiting the bottom of the soil profile on day i (mm); and $w_{rchrg,i-1}$ is the amount of recharge entering the aquifer on day $i-1$ (mm).

The total amount of water exiting the bottom of the soil profile on day i is calculated as:

$$w_{seep} = w_{perc,ly=n} + w_{crk,btm} \quad (6.23)$$

where: w_{seep} is the total amount of water exiting the bottom of the soil profile on day i (mm); $w_{perc,ly=n}$ is the amount of water percolating out of the lowest layer; n in the soil profile on day i (mm); and $w_{crk,btm}$ is the amount of water flow past the lower boundary of the soil profile due to bypass flow on day i (mm).

The delay time, δ_{gw} , cannot be directly measured. It can be estimated by simulating aquifer recharge using different values for δ_{gw} and comparing the simulated variations in water table level with observed values.

Once the total daily recharge is calculated, SWAT partitions this between the shallow and deep aquifer. The amount of water diverted from the shallow aquifer to the deep aquifer via percolation on a given day is:

$$w_{deep} = \beta_{deep} \cdot w_{rchrg} \quad (6.24)$$

where: w_{deep} is the amount of water moving into the deep aquifer on day i (mm); β_{deep} is the aquifer percolation coefficient; and w_{rchrg} is the amount of recharge entering both aquifer on day i (mm).

The amount of recharge to the shallow aquifer is:

$$w_{rchrg,sh} = w_{rchrg} - w_{deep} \quad (6.25)$$

where: $w_{rchrg,sh}$ is the amount of recharge entering the shallow aquifer on day i (mm).

Groundwater/baseflow

In the SWAT model, stream baseflow is sustained mostly by recharge entering the shallow aquifer. SWAT simulates the shallow aquifer contribution to the main stream channel or to the reach within the sub-basin. Baseflow is allowed to enter the channel only if the amount of water stored in the shallow aquifer exceeds a threshold value specified by the user. The baseflow into the main channel on a given day as simulated in SWAT is (Neitsch et al., 2005):

$$Q_{gw,i} = Q_{gw,i-1} \cdot \exp[-\alpha_{gw} \cdot \Delta t] + w_{rchrg} \cdot (1 - \exp[-\alpha_{gw} \cdot \Delta t]) \quad (6.26)$$

if $aq_{sh} > aq_{shthr,q}$

$$Q_{gw,i} = 0 \quad \text{if } aq_{sh} \leq aq_{shthr,q} \quad (6.27)$$

where: $Q_{gw,i}$ is the groundwater or baseflow into the main channel on day i (mm); $Q_{gw,i-1}$ is the groundwater flow into the main channel on day $i-1$ (mm); α_{gw} is the baseflow recession constant; Δt is the time step (1 day) $w_{rchrg,sh}$ is the amount of recharge entering the shallow aquifer on day i (mm); aq_{sh} is the amount of water stored in the shallow aquifer at the beginning of day i (mm) and $aq_{shthr,q}$ is the threshold water level in the shallow aquifer for groundwater contribution to the main channel to occur (mm).

The baseflow values vary from 0.1-0.3 for land with slow response to recharge to 0.9-1.0 for land with a rapid response.

The baseflow recession constant may be calculated but the best estimates are obtained by analyzing measured streamflow during periods of no recharge in the

watershed (Neitsch et al., 2005). The baseflow constant is estimated as a function of the number of baseflow days:

$$\alpha_{gw} = \frac{2.3}{BFD} \quad (6.28)$$

where: α_{gw} is the baseflow recession constant and BFD is the number of baseflow days for the watershed. The number of baseflow days is the number of days for baseflow recession to decline through one log cycle.

“Revap”

“Revap” is a term used to describe the combined processes of evaporation of water from the shallow aquifer storage through the overlying unsaturated zone and direct water uptake from the shallow aquifer storage by deep-rooted plants. SWAT allows for the movement of water from the shallow aquifer via capillary rise to the overlying unsaturated zone to help meet evapotranspirative demands when the soil profile is dry. Revap is important in basins where the saturated zone is not very far below the soil surface or where deep-rooted plants are growing. Revap is simulated separately from soil evaporation and transpiration. SWAT allows revap to occur only if the amount of water stored in the shallow aquifer exceeds a threshold value specified by the modeler. The amount of revap that will occur on a given day is calculated to be (Neitsch et al., 2005):

$$w_{revap} = 0 \quad \text{if } aq_{sh} \leq aq_{shthr,rvp} \quad (6.29)$$

$$w_{revap} = w_{revap,mx} - aq_{shthr,rvp} \quad \text{if } aq_{shthr,rvp} < aq_{sh} < (aq_{shthr,rvp} + w_{revap,mx}) \quad (6.30)$$

$$w_{revap} = w_{revap,mx} \quad \text{if } aq_{sh} \geq (aq_{shthr,rvp} + w_{revap,mx}) \quad (6.31)$$

where: w_{revap} is the actual amount of water moving into the soil zone in response to water deficiencies (mm); $w_{revap,mx}$ is the maximum amount of water moving into the soil zone in response to water deficiencies (mm); aq_{sh} is the amount of water

stored in the shallow aquifer at the beginning of day i (mm); and $aq_{shthr,rvp}$ is the threshold water level in the shallow aquifer for revap or percolation to deep aquifer to occur (mm).

The maximum amount of water that will be removed from the aquifer through revap on a given day is:

$$w_{revap, mx} = \beta_{rev} \cdot E_o \quad (6.32)$$

where: $w_{revap, mx}$ is the maximum amount of water moving into the soil zone in response to water deficiencies (mm); β_{rev} is the revap coefficient; and E_o is the potential evapotranspiration for the day (mm).

6.2.9 Reservoir

SWAT provides the opportunity to incorporate water ponding structures such as reservoirs, ponds and wetlands in the basin being modeled. SWAT makes no distinction between natural and man-made impoundments and defines a reservoir to be an impoundment situated in the main channel network of a basin. The water balance of a reservoir in SWAT is (Neitsch et al., 2005):

$$V = V_{stored} + V_{flowin} - V_{flowout} + V_{pcp} - V_{evap} - V_{seep} \quad (6.33)$$

where: V is the volume of water in the impoundment at the end of the day (m^3); V_{stored} is the volume of water stored in the water body at the beginning of the day (m^3); V_{flowin} is the volume of water entering the water body during the day (m^3); $V_{flowout}$ is the volume of water flowing out of the water body during the day (m^3); V_{pcp} is the volume of precipitation falling on the water body during the day (m^3); V_{evap} is the volume of water removed from the water body by evaporation during the day (m^3); and V_{seep} is the volume of water lost from the water body by seepage (m^3).

6.2.10 Flow routing

SWAT uses a command structure similar to that of HYMO (Williams and Hann, 1973) to route the loadings of water, sediment, nutrients and pesticides to the main channel. The user is offered two options for routing streamflow: the variable storage routing method developed by Williams (1969) and the Muskingum River routing method. In this study, the Muskingum method was selected.

6.3 Sensitivity analysis

Sensitivity analysis is commonly done on a model to determine how sensitive the output of the model is to changes in the input parameter values in order to understand the behavior of the model. If a small change in an input parameter results in relatively large changes in the output, then the outputs are said to be sensitive to that parameter. The implication is that the particular parameter concerned has to be determined more accurately. Models have several parameters, and the user has to calibrate the model by assigning values to each one of them and adjusting the values based on certain criteria to obtain best fit between the model output and measured data. Knowing the input parameters that are sensitive to the model output and focusing attention on those parameters during the calibration process saves much time and leads to reduction in parameter uncertainty. Sensitivity analysis helps the modeler to determine, in order of priority, the parameters that show the highest contribution to the output variability (Lenhart et al., 2002).

SWAT uses the Latin Hypercube One-factor-At-a-Time (LH-OAT) method proposed by Morris (1991) to perform the sensitivity analysis. The LH-OAT method is a combination of the Latin Hypercube (LH) sampling (global sensitivity analysis method) and the One-factor-at-a-Time (OAT) design (local sensitivity analysis method), and uses the LH samples as initial points for an OAT design (van Griensven and Meixner, 2006).

The LH is a sophisticated random sampling technique with a concept based on the Monte Carlo Simulation. However, it uses a stratified sampling approach, which ensures that the full range of all input parameters has been sampled. In the LH procedure, the distribution of each parameter is first subdivided into m ranges, each with a probability of occurrence of $1/m$. Following, random values of the parameters are

produced ensuring that each range is sampled only once (Figure 6.3). The model is then run m times with the random combinations of the parameters (Griensven et al., 2005). The output of the model is analyzed with multivariate linear regression. The main shortcomings of the LH sensitivity analysis are: (i) the assumption of linearity in the multivariate regression analysis and (ii) the changes in the output variables cannot always be unambiguously attributed to a change in a specific input parameter because all parameters are changing simultaneously (Christiaens and Feyen, 2002, cited in van Griensven et al., 2002).

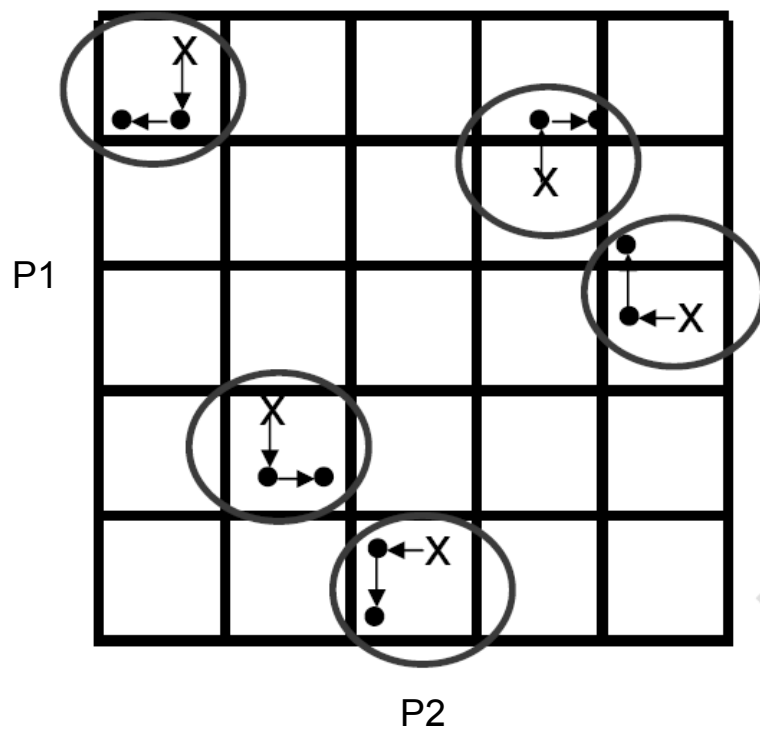


Figure 6.3 Illustration of the LH-OAT sampling for a 2 parameter case. X represents the initial parameters of the Latin Hypercube sampling and • represents the two one-factor-at-a-time points (van Griensven et al., 2002)

In the OAT design, each input parameter is changed in a sequence starting from an initial parameter vector of n , $(X_1 \dots, X_n)$ (Griensven et al., 2002). This provides the assurance that the changes in the output in each run of the model can be unambiguously attributed to variations in a particular input parameter. The main limitation is that the method is only a local measure of sensitivity because the sensitivity of the model towards X_i may depend on the values chosen for the other model

parameters (Griensven et al., 2005). This limitation is overcome in the LH-OAT combination, which results in a robust analysis requiring only few runs while allowing efficient estimation of the output statistics (Saltelli et al., 2000; Holvoet et al., 2005).

6.4 Model calibration and performance evaluation

Generally, a hydrological model needs some form of calibration before it can be used in an area other than where it was originally made. This becomes more important if the model is to be used for forecasting or predicting future scenarios. Model calibration involves modifying values of sensitive input parameters, within an acceptable range, in an attempt to match model output to measured data based on a predefined objective function. In SWAT, the user has the option to calibrate the model manually or automatically.

Manual calibration in SWAT is based on trial and error analysis, and consists of changing one parameter at a time and re-running the model to obtain output that is similar to the measured data. With automatic calibration, SWAT uses a method known as PARASOL (Parameter Solutions method) developed by van Griensven et al. (2002). This method is based on the Shuffled Complex Evolution algorithm developed at the University of Arizona (SCE-UA). The SCE-UA is a global search algorithm that minimizes a single objective function for up to 16 model parameters (Duan et al., 1992 cited in van Griensven et al., 2002). SCE-UA has been widely used in watershed model calibration and other areas of hydrology, and was generally found to be robust

PARASOL uses two predefined objective functions to achieve calibration, namely, the sum of the squares of the residuals (SSQ) and the sum of the squares of the difference of the measured and simulated values after ranking (SSQR) (van Griensven et al., 2002):

$$SSQ = \sum_{i=1,n} [X_{i,measured} - X_{i,simulated}]^2 \quad (6.34)$$

$$SSQR = \sum_{j=1,n} [X_{j,measured} - X_{j,simulated}]^2 \quad (6.35)$$

where: n is the number of pairs of measured ($X_{measured}$) and simulated ($X_{simulated}$) variables; and j represents the rank

Santhi et al. (2001) proposed a procedure for manually calibrating SWAT for river discharge and sediment yield. They recommended that the results of SWAT calibration are acceptable if: (i) the simulated mean flow (monthly or daily) differs from the mean measured flow by a value that is within $\pm 15\%$; (ii) the coefficient of determination is (R^2) greater than 0.60; and (iii) the Nash-Sutcliffe model efficiency (NSE) is greater than 0.50. A modified form of the proposed procedure (Figure 6.4) was used for calibrating streamflow in this study.

The R^2 and NSE are statistics that have been used in many studies for evaluating the predictive performance SWAT (Wu and Xu, 2006; Sintondji, 2005; Chekol, 2006; Abraham, 2007). The R^2 provides information about the goodness of fit of the model output to the measured data, and can range from 1 (perfect fit) to 0. The NSE was proposed by Nash and Sutcliffe (1970). It is commonly used by hydrogeologists as a model performance evaluation criterion (Moussa, 2008). NSE can range from 1 to $-\infty$. NSE of 1 corresponds to a perfect match of modeled output to measured data; NSE of 0 indicates that the model predictions are as accurate as the mean of the measured data; and NSE less than zero indicates that the measured mean is a better predictor than the model. The R^2 and NSE can be calculated as:

$$R^2 = \left[\frac{\sum_{i=1}^N (O_i - \bar{O})(P_i - \bar{P})}{\left[\sum_{i=1}^N (O_i - \bar{O})^2 \right]^{0.5} \left[\sum_{i=1}^N (P_i - \bar{P})^2 \right]^{0.5}} \right]^2 \quad (6.36)$$

$$NSE = 1 - \frac{\sum_{i=1}^N (O_i - P_i)^2}{\sum_{i=1}^N (O_i - \bar{O})^2} \quad (6.37)$$

where: O_i is the measured data; P_i is the simulated data; \bar{O} is the mean of the measured data; \bar{P} is the mean of the simulated data; and N is the number of compared values.

Other studies have used the Index of Agreement (IA) as an additional statistic to evaluate the performance of the SWAT model (Sintondji, 2005; Chekol, 2006; Hiepe and Diekkrüger, 2007). The IA is used to assess the quality of the temporal reproduction of the measured data by the model. Where all the terms are as defined above, the IA is computed to be (Willmott, 1981):

$$IA = 1 - \frac{\sum_{i=1}^N (O_i - P_i)^2}{\sum_{i=1}^N (|P_i - \bar{O}| + |O_i - \bar{O}|)^2} \quad (6.38)$$

All the three statistics defined above were used in this study to evaluate the predictive performance of the SWAT model that was built for the study area.

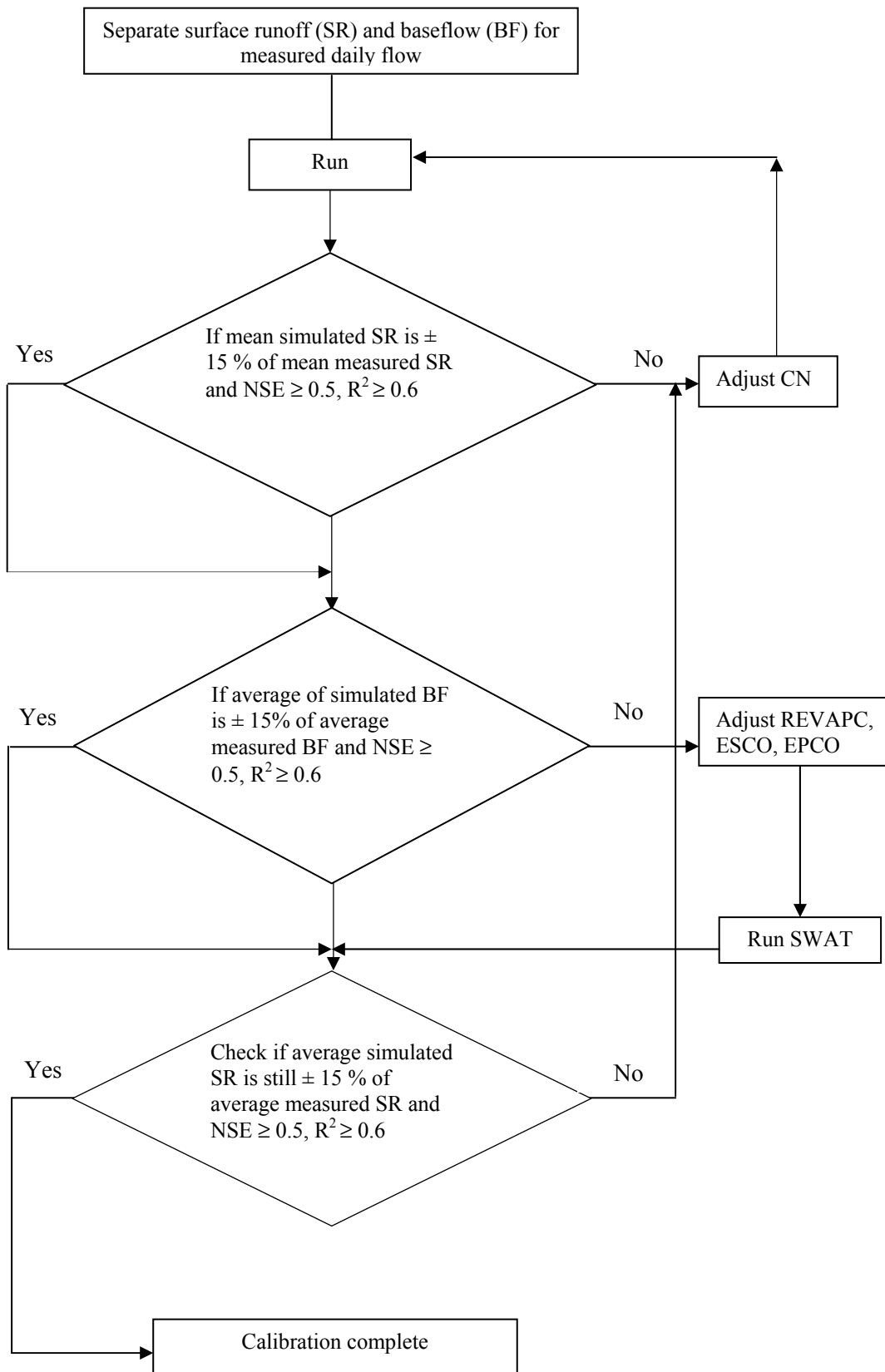


Figure 6.4 Manual calibration procedure for discharge, surface runoff and baseflow in SWAT (modified after Santhi et al., 2001)

6.5 Baseflow separation

The SWAT calibration procedure recommended by Santhi et al. (2001) requires the separation of streamflow into the surface runoff and baseflow components. The process of separating the baseflow from the streamflow is referred to as baseflow separation. The separation can be achieved through graphical methods (e.g., constant discharge method, constant slope method and concave method) and the filtering method (e.g., smooth minima, fixed-interval, sliding-interval and recursive digital filters). In this study, an automated recursive digital filter program developed by Arnolds et al. (1999) was used to separate the streamflow into baseflow and surface runoff. The digital filter generated additional information on the baseflow such as the baseflow recession constant and the baseflow days.

6.6 SWAT input data preparation

Data used for setting up the SWAT model for the White Volta basin included a digital elevation model (DEM), soil and land-use maps, data on soil properties, plant growth, climate, reservoir, and management. Streamflow data were used for calibrating and validating the model.

6.6.1 Digital elevation model (DEM)

Digital elevation models are digital data files that contain terrain elevations over a specified area, usually at regularly spaced horizontal fixed grid intervals, over the earth surface. The intervals between each of the grid points are always referenced to a common datum. The DEM is often a common source of information for developing other models that are dependent on topography. Therefore, the quality of a DEM determines to a large extent the quality of the dependent model. Most DEMs have errors that develop when they are being created. These errors need to be detected and corrected before the DEM is used. Several techniques and software are available for correcting errors in DEM.

The SRTM (Shuttle Radar Topography Mission) 90 m resolution DEM was used in this study (Figure 6.5). SRTM is an international project spearheaded by the United States National Aeronautics and Space Administration (NASA) and the National Geospatial-Intelligence Agency (NGA). The data are made freely available by the

United States Geological Survey (USGS) in agreement with the NASA and can be downloaded from the server of NASA (<ftp://e0srp01u.ecs.nasa.gov>). The SRTM data are already processed to correct the errors with the exception of the error of ‘voids’. These voids were filled, as part of this study, using an open source software SAGA (System for Automated Geo-Scientific Analysis) (Cimmery, 2007).

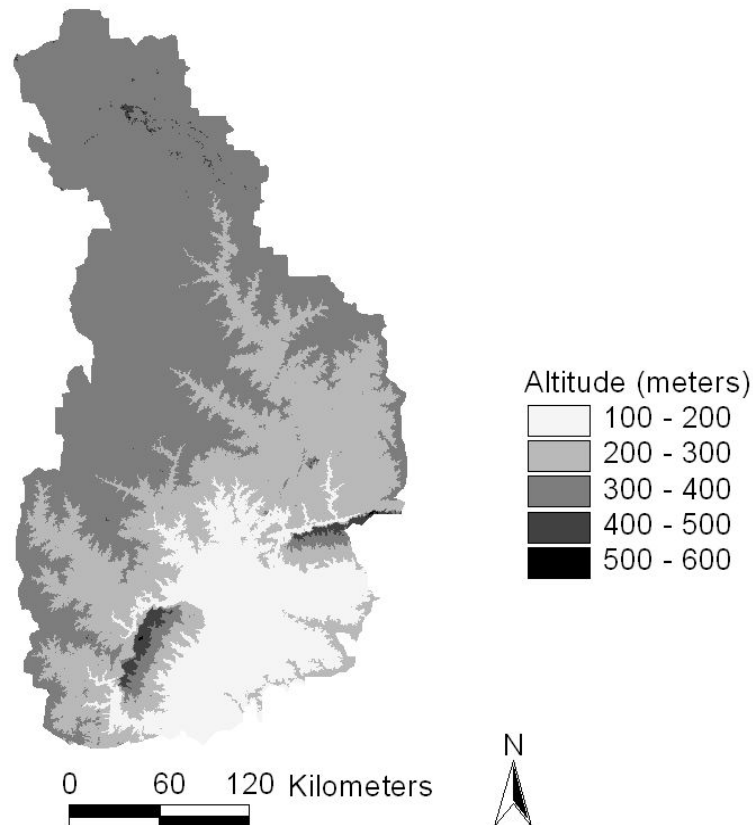


Figure 6.5 Processed SRTM DEM of the White Volta Basin (Source: U.S. NASA server - <ftp://e0srp01u.ecs.nasa.gov>)

6.6.2 Land-use/ -cover data

Together with the soil data, SWAT uses the land-use data to determine the area and the hydrologic parameters of each land-use and soil category simulated within each sub-basin (Di Luzio et al., 2002). The land-use/-cover map used in this study has a resolution of 250 m and was obtained from the GLOWA Volta project of the Center for Development Research (ZEF), Germany. The map was originally made from 30-m Landsat ETM+ data from 1990 that were EarthSAT ortho-rectified to achieve geodetic accuracy and calibrated to surface reflectance using the atmospheric correction tool

ATCOR2 (Landmann et al., 2007). The legend of the map is based on the Food and Agriculture Organization (FAO) Land Cover Classification System (LCCSS) legend. Some modification of the original legend was necessary for using the map for modeling in SWAT.

Based on the modified legends, 10 land-use/-cover classes can be identified in the study area (Figure 6.6), but three are dominant. These are cropland/woodland, savannah, and mixed forest in a decreasing order of dominance (Table 6.1). The sharp boundaries in the land-use/-cover classes in Figure 6.6 are due to the use of Landsat images from different years to fill in patches (mainly from cloud cover and bush fires) in the 1990 Landsat images, and difficulty in differentiating certain land-use categories as a result of mixed cropping.

Table 6.1: Distribution of land-use/-cover types in the White Volta Basin

No	Land-use/-cover type	Code	Area covered (km ²)	% coverage in the basin
1	Savannah	SAVA	23,278	21.96
2	Cropland/Woodland	CRWO	37,513	35.39
3	Grassland	GRAS	3,180	3.00
4	Barren/Sparsely vegetated	BSVG	6,275	5.92
5	Evergreen broadleaf forest	FOEB	10,314	9.73
6	Mixed forest	FOMI	17,903	16.89
7	Herbaceous wetland	WEHB	5,183	4.89
8	Wooded wetland	WEWO	1,897	1.79
9	Urban medium density	URMD	297	0.28
10	Water body	WATB	159	0.15

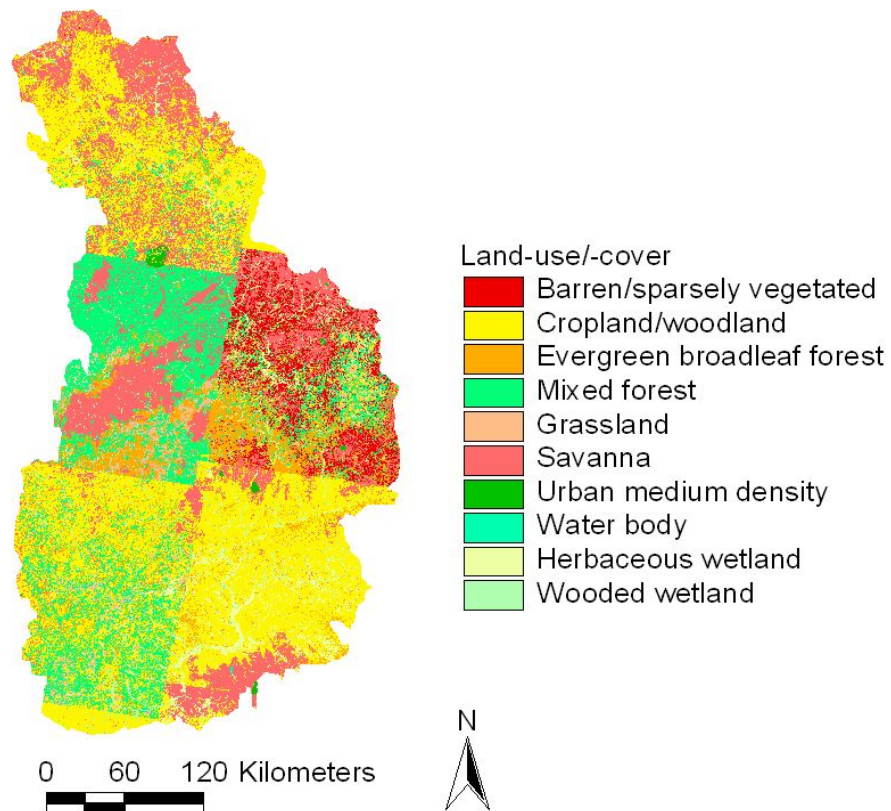


Figure 6.6 Land-use/-cover types in the White Volta Basin (Landmann et al., 2007)

6.6.3 Soil data

The soil map for the study area was obtained from the FAO digital soil map of the world and derived soil properties (FAO, 1995). The soil map has a spatial resolution of 10 km and almost 5000 soil types can be differentiated with some soil properties for two layers (0-30 cm and 30-100 cm depth) (Schuol et al., 2008). Seven different soil textures can be identified in the study area; the dominant ones are clay loam, sandy clay loam and loam (Table 6.2; and Figure 6.7).

Table 6.2: Soil textures in the White Volta Basin

Soil texture	Area covered (km ²)	% coverage in the basin
Clay loam	31,100	29.34
Sandy clay loam	26,595	25.09
Loam	23,935	22.58
Sandy loam	15,868	14.97
Loamy sand	5,258	4.96
Clay	2,820	2.66
Silt loam	424	0.40

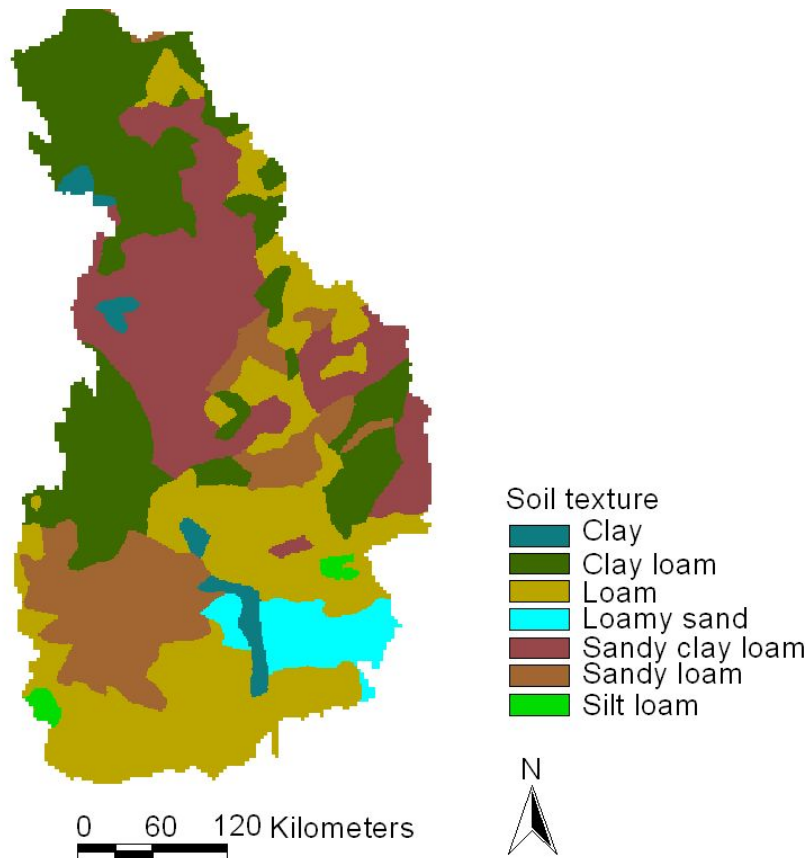


Figure 6.7 Texture of soils in the White Volta Basin (Schuol et al., 2008, modified after FAO, 1995)

In addition to a digital soil map, SWAT requires information on some physical properties of soils (Table 6.3) for each layer of the soil modeled. These data were obtained from different sources including the FAO-derived soil properties, Ghana soil data obtained from the Soil Research Institute (SRI), Ghana, and field research soil analysis carried out as part of this study. The soil analysis was done mainly to complement the data from FAO and SRI.

During field research in 2006/2007, 70 soil samples were taken from 6 major soil groups in the study area and were analyzed for texture, bulk density, saturated hydraulic conductivity (SHC), organic carbon content, and available water content (AWC) (Table 6.4 and 6.5). The samples were taken from 5 layers within the soil profile. Each layer had a profile depth of 20 cm. The maximum soil sampling depth was fixed at 100 cm, which was assumed to be the average maximum rooting depth in the study area. Analyses of the soil properties were done at the SRI soil laboratory.

Table 6.3: Soil physical properties required for modeling in SWAT (modified from Neitsch et al., 2002)

Soil parameter	Description	Unit
NLAYERS	Number of layers in the soil (min 1, max 10)	-
HYDGRP	Soil hydrologic group (A, B, C, D)	-
SOL_ZMX	Maximum rooting depth of soil profile	mm
ANION_EXCL	Fraction of porosity from which anions are excluded	-
SOL_CRK	Crack volume potential of soil [optional]	-
TEXTURE	Texture of soil layer [optional]	-
SOL_Z	Depth from soil surface to bottom of layer	mm
SOL_BD	Moist bulk density	g/ cm ³
SOL_AWC	Available water capacity of the soil layer	mm/mm
SOL_K	Saturated hydraulic conductivity	mm/hr
SOL_CBN	Organic carbon content	% by weight
CLAY	Clay content	%
SILT	Silt content	%
SAND	Sand content	%
ROCK	Rock fragment content	-
SOL_ALB	Moist soil albedo	-
USLE_K	Soil erodability factor	-

Table 6.4: Statistics of soil properties in the topsoil and subsoil at selected locations in the White Volta Basin in Ghana

Soil property	Soil layer	Minimum	Maximum	Mean	Standard deviation
Sand (%)	Topsoil	28.30	81.64	61.03	13.83
	Subsoil	22.58	78.68	50.68	13.33
Clay (%)	Topsoil	4.29	26.13	10.03	5.34
	Subsoil	6.02	34.15	18.93	7.58
Silt (%)	Topsoil	12.25	50.74	28.97	11.62
	Subsoil	13.19	48.81	30.40	9.40
Bulk density (g/cm ³)	Topsoil	1.42	1.81	1.62	0.09
	Subsoil	0.68	2.11	1.76	0.23
SHC (mm/hr)	Topsoil	9.00	101.00	54.10	23.20
	Subsoil	5.10	81.10	24.60	21.00
Organic carbon (%)	Topsoil	0.09	0.64	0.32	0.14
	Subsoil	0.01	0.43	0.16	0.08
AWC (mm/mm)	Topsoil	0.06	0.16	0.11	0.03
	Subsoil	0.07	0.16	0.12	0.02

SHC: Saturated hydraulic conductivity; AWC: Available Water Capacity of Soil

Table 6.5: Mean values of soil properties in the topsoil and subsoil at selected locations in the White Volta Basin in Ghana.

Soil texture	Soil layer	Bulk density (g/ cm ³)	SHC (mm/h)	Organic carbon (%)	AWC (mm/mm)
Sandy loam	Topsoil	1.59 (17)	58.70	0.30	0.10
	Subsoil	1.80 (12)	48.60	0.16	0.10
Sandy clay loam	Topsoil	1.70 (1)	11.80	0.48	0.12
	Subsoil	1.66 (10)	11.80	0.17	0.11
Clay loam	Topsoil	-	-	-	-
	Subsoil	1.84 (3)	5.60	0.17	0.15
Loam	Topsoil	1.71 (5)	26.20	0.36	0.15
	Subsoil	1.76 (13)	18.30	0.15	0.14
Silt loam	Topsoil	1.64 (2)	46.50	0.26	0.15
	Subsoil	-	-	-	-
Loamy sand	Topsoil	1.66 (3)	93.20	0.36	0.07
	Subsoil	2.11 (1)	73.50	0.12	0.07

6.6.4 Climate data

Daily climate data from 26 weather stations spread within and around the White Volta Basin were used as the climate input to the SWAT model (Figure 6.8). The data were obtained from the Ghana Meteorological Services Department and the Direction de la Météorologie Nationale, Burkina Faso. The data covered the period 1980-1999 and included rainfall, minimum and maximum air temperature, relative humidity, wind run (converted to wind speed), and sunshine hours (converted to solar radiation) (Table 6.6). Six of the weather stations are synoptic (Ouagadougou, Ouahigouya, Po, Navrongo, Tamale and Yendi), 15 are agro-meteorological stations and the rest are rainfall measuring points.

Some of the weather stations have missing data in their records, which were filled using the WXGEN weather generator model offered in SWAT. The WXGEN model requires long-term statistics of rainfall, minimum and maximum temperature, relative humidity, solar radiation and wind speed to be able to fill in missing data. Long-term climate statistics (30 years) from the 6 synoptic stations were used for generating missing data in all the climate records.

Table 6.6: Weather station and climate data used for SWAT modeling in the White Volta basin

Id ^a	Station	Lat.	Long	Period of data obtained				
	location			Rainfall	Temp.	Relative humidity	Wind run	Sunshine hours
1	Ouagadougou	12.35	-1.52	1980-1999	1980-1999	1980-1999	1980-1999	1980-1999
2	Gaoua	10.33	-3.18		1980-1999	1980-1999	1980-1999	1980-1999
3	Fada N'gourma	12.07	0.35		1980-1999	1980-1999	1980-1999	1980-1999
4	Dori	14.03	-0.03		1980-1999	1980-1999	1980-1999	1980-1999
5	Dedougou	12.47	-3.48		1980-1999	1982-1999	1984-1999	1980-1999
6	Boromo	11.73	-2.92		1980-1999	1980-1999	1980-1999	1980-1999
7	Bousse	12.67	-1.88	1980-1999				
8	Kaya	13.10	-1.08	1980-1999				
9	Kombissiri	12.07	-1.33	1980-1997				
10	Koupela	12.18	-0.35	1980-1997				
11	Niaogho	11.77	-0.77	1980-1999				
12	Ouahigouya	13.58	-2.43	1980-1999	1980-1999	1980-1999	1980-1999	1980-1999
13	Tenkodogo	11.77	-0.38	1980-1999				
14	Zabre	11.17	-0.60	1980-1999				
15	Sandema	10.73	-1.28	1980-1998				
16	Bole	9.03	-0.25	1980-1999		1980-1999	1980-1999	1980-1999
17	Binduri	10.97	-0.32	1980-1999	1980-1999			
18	Zuarungu	10.78	-0.80	1980-1999	1980-1999			
19	Tamale	9.40	-0.85	1980-1999	1980-1999	1980-1999	1980-1999	1980-1999
20	Walewale	10.33	-0.80	1980-1999				
21	Yendi	9.45	-0.02	1980-1999	1980-1999	1980-1999	1980-1999	1980-1999
22	Bogande	12.98	-0.13		1980-1994	1988-1999	1988-1999	
23	Garu	10.85	-0.18		1980-1999			
24	Navrongo	10.90	-1.10	1980-1999	1980-1999	1987-1999	1980-1999	1980-1999
25	Sapouy	11.55	-1.77	1980-1997				
26	Po	11.17	-1.15	1980-1999	1980-1999	1983-1999	1982-1999	1980-1999

^aId is the weather station identification

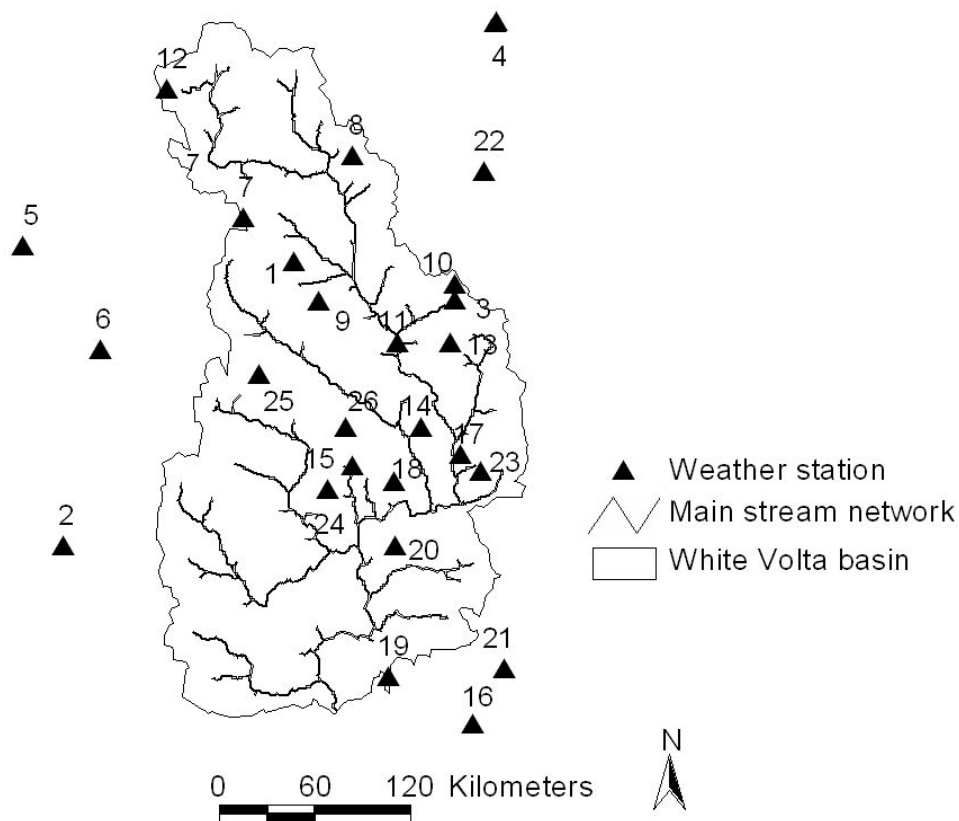


Figure 6.8 Location of weather stations in the White Volta Basin

6.6.5 River discharge data

Daily, monthly and annual discharge data from the streamflow gage at Nawuni on the main course of the White Volta River (Figure 6.9) were used for calibrating and validating the SWAT model. Though Lankatere is the outlet gage on the White Volta River, Nawuni was used as the outlet for the modelling because it has the longest discharge period data in the basin. Nawuni has a drainage area of 90,856 km². The discharge data were obtained from the Ghana Hydrological Services Department and the Water Research Institute (WRI) of Ghana

The White Volta Basin has over 25 discharge measuring gages. However, the accuracy and quality of the discharge data are generally poor. Taylor et al. (2006) assessed the accuracy and quality of discharge data in the Volta basin by considering discharge data from 59 streamflow gages over an average data period of 20 years. The discharge data used were obtained from two sources: the WRI and the L'Institut de Recherche pour le Développement (ORSTOM). The study found that, between the two data sources, 20 % of the discharge data over the Volta basin is missing, and for many

of the gages as much as 50 % of their data is missing. For the White Volta basin, the same study obtained over 15 % missing data for most gages, and a few of them, including Wiasi and Nasia, had more than 50 % of their data missing. The difference between the two data sources and the high percentage of missing data suggests data inaccuracy.

Taylor et al. (2006) evaluated the accuracy of discharge data by using a linear regression of the annual rainfall and runoff, and an arbitrary criterion of coefficient of determination (R^2) of 0.50, below which gages were deemed highly inaccurate. The results show that discharge data from only half of the streamflow gages in the Volta Basin could be used for any watershed management practices since only half of the gages met the criterion. In the White Volta Basin, only 6 of the 24 gages evaluated met the criterion (Table 6.7). The 6 gages are Nawuni, Lankatere, Nasia, Yagaba, Wiasi and Nangodi.

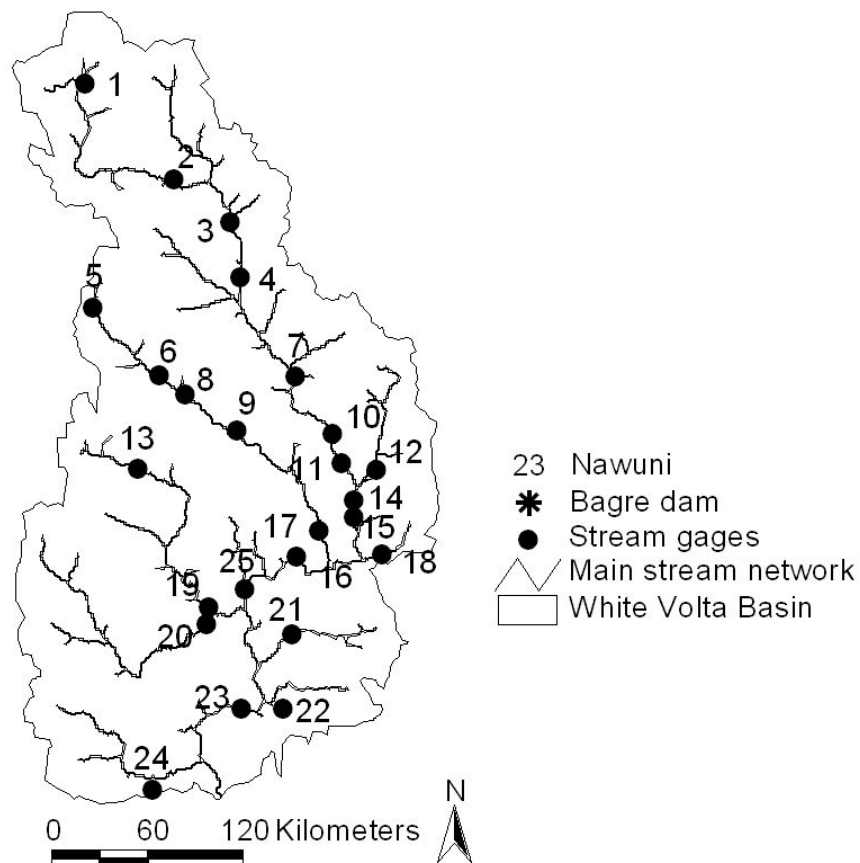


Figure 6.9 Location of stream gages and the Bagre dam in the White Volta Basin

Table 6.7: Results of quality assessment of river discharge data from 24 gages in the White Volta Basin (modified after Taylor et al., 2006)

Gage ID	Gage location	Lat.	Long.	Data period	Regression equation	R ²
1	Rambo ^a	13.60	2.07	9183-1987	0.1*(P-270)	0.80
2	Yilou	13.00	1.55	1973-1983	0.02*(P-30)	0.06
3	Bissiga	12.75	1.15	1974-1983	-	0.00
4	Wayen	12.38	1.08	1965-1987	0.01*(P+4)	-
5	Sakoïnse	12.20	2.02	1979-1985	0.02*(P-400)	0.29
6	Dakaye	11.78	1.60	1975-1986	-0.01*(P-1956)	0.03
7	Niagho	11.77	0.75	1951-1984	0.24*(P-223)	0.15
8	Bagre (Tcherbo)	11.69	1.47	1978-1986	-	0.005
9	Nobere	11.43	1.18	1958-1975	1.13*(P+690)	0.38
10	Yakala	11.35	0.52	1956-1984	0.08*(P-380)	0.28
11	Bagre (Nakambe)	11.20	0.43	1974-1990	0.09*(P-370)	0.16
12	Bittou	11.18	0.28	1974-1985	0.10*(P-430)	0.06
13	Nebbou	11.28	1.93	1974-1985	-0.04(P-1258)	0.15
14	Yarugu	10.98	0.40	1962-1977	0.30*(P-600)	0.29
15	Garu	10.90	0.39	1966-1970	0.04*(P-500)	0.012
16	Nangodi	10.87	0.62	1963-1973	0.25*(P-690)	0.31
17	Pwalugu	10.58	0.85	1952-1973	0.14*(P-320)	0.10
18	Nakpandur	10.65	0.23	1958-1963	0.02*(P-2500)	0.03
19	Wiasi	10.34	1.33	1962-1990	0.31*(P-780)	0.50
20	Yagaba	10.26	1.29	1958-1979	0.52*(P-800)	0.51
21	Nasia	10.15	0.77	1963-1989	0.95*(P-956)	0.67
22	Nabogo	9.77	0.88	1962-1988	0.43*(P-780)	0.35
23	Nawuni	9.70	1.08	1953-1990	0.19*(P-526)	0.50
24	Lankatere	9.29	1.25	1971-1977	1.10*(P-915)	0.54

^a The quality of discharge data from Rambo was rejected for other reasons

6.6.6 Reservoir data

The only reservoir located in the main course of the White Volta River is the Bagre dam (Figure 6.6). This dam was included as reservoir in the SWAT model developed for the basin. Data required for reservoir water balance modeling in SWAT include the year and month in which the reservoir became operational, the surface area and volume of the reservoir when filled to principal and emergency spillways, the initial reservoir volume (Table 6.8), the hydraulic conductivity of the reservoir bottom, minimum and

maximum daily outflow for the month, and monthly reservoir outflow. These data were obtained for the Bagre reservoir from the Société Nationale d'Électricité du Burkina (SONABEL). The Bagre reservoir became operational in February 1995. The data obtained covered the period: 1995-1999.

Table 6.8: Characteristics of the Bagre dam in the White Volta Basin

Parameter	Description	Value	Unit
MORES	Month the reservoir became operational	February	-
IYRES	Year of the simulation the reservoir became operational	1995	-
RES_ESA	Reservoir surface area when the reservoir is filled to the emergency spillway	43900	ha
RES_EVOL	Volume of water needed to fill the reservoir to the emergency spillway	336300*10E4	m ³
RES_PSA	Reservoir surface area when the reservoir is filled to the principal spillway	25200	ha
RES_PVOL	Volume of water needed to fill the reservoir to the principal spillway	168900*10E4	m ³
RES_VOL	Initial reservoir volume	168900*10E4	m ³

6.6.7 Other data

Other data used for building the SWAT model for the study area included leaf area index, potential heat unit, plant-cover and landuse factor, tillage practices, fertilizer types and application rates. These data were obtained from literature, agricultural research institutions and interviews with farmers and experts.

6.7 Results and discussion

6.7.1 White Volta Basin SWAT setup and sensitivity analysis

The SWAT model was set up for the White Volta basin via the AVSWATX and following the step by step procedure outlined in the SWAT user guide (Luzio et al., 2002). The AVSWATX is an Arc View extension and a graphical user interface for the SWAT-2005 model. The basin was divided into 90 sub-basins based on the DEM and stream network of the study area. The minimum and maximum sizes of the sub-basins were 62 km² and 4484 km², respectively. The sub-basin delineation was followed by automatic parameterization of streams and subdivision of the sub-basins into 484 hydrologic response units (HRUs) based on soil and landuse data and a predefined threshold of 10 % soil and 10 % landuse. The maximum HUR size was 2690 km² and the minimum was 1.4 km². The model was simulated for the period: 1980-1999. The

first six years (1980-1985) were used for warming the model. The period: 1986-1991 was used for calibration, and 1992-1999 was used as the validation period.

The sensitivity of SWAT-simulated discharge to model input parameters was analyzed using the automatic sensitivity analysis tool provided in AVSWATX. Twenty selected SWAT hydrology input parameters were analyzed. The purpose of the sensitivity analysis was to determine the most sensitive model parameters that needed to be given high priority during model calibration. Two cases of sensitivity analysis were done. The first analysis (SENSE 1) did not utilize measured streamflow data. The second (SENSE 2) utilized measured streamflow data at Nawuni. The results show that the 10 most sensitive parameters and their ranking were the same for the two cases of sensitivity analysis (Table 6.9). The initial SCS runoff curve number (CN2), soil evaporative compensation factor (ESCO), and the threshold water depth in the shallow aquifer for revap (GWQMN) were the three most sensitive model parameters for the White Volta basin (Table 6.8). The CN2 determines the amount of precipitation that becomes runoff and the amount which infiltrates. The ESCO is used for modifying the depth distribution for meeting soil evaporative demand to account mainly for the effect of capillary action, and the GWQMN is used for regulating the return flow.

Table 6.9: SWAT-sensitivity analysis of the White Volta Basin

Parameter	Description	Sensitivity ranking	
		SENSE 1	SENSE 2
CN2	SCS runoff curve number	1	1
ESCO	Soil evaporation compensation factor	2	2
SOL_Z	Soil depth	3	3
GWQMN	Threshold water depth in the shallow aquifer for 'revap'	4	4
SOL_AWC	Available water capacity of the soil layer	5	5
SOL_ALB	Moist soil albedo	6	6
RECHRG_DP	Deep aquifer percolation fraction	7	7
SOL_K	Saturated hydraulic conductivity	8	8
GW_REVAP	Groundwater 'revap' coefficient	9	9
SURLAG	Surface runoff lag time	10	10

6.7.2 Effects of the number of rainfall stations and land-use on model output

In SWAT, the first level of sub-division is the sub-basin. The number of sub-basins obtained in a watershed is determined by the minimum threshold input value for defining a drainage area. The number of sub-basins modeled in SWAT influences the number of climate stations (more importantly, the number of rainfall stations) that are utilized in the modeling of the output. Since rainfall is the major input to the hydrological system, the modeled output can be affected. Generally, the higher the number of sub-basins modeled in a watershed, the higher the number of rainfall stations utilized by the model. Consequently, the model output is more accurate.

The HRU is the lowest sub-division in SWAT, and the number of them modeled is determined by the landuse and soil threshold defined by the user. Increasing the number of HRUs in a watershed with diverse plant cover increases the accuracy in the prediction of loadings from sub-basins, which in turn results in a more accurate output (Neitsche et al., 2005).

Prior to the calibration of the White Volta basin SWAT, the effects of the number of rainfall stations and landuse on the model output were assessed through 6 scenarios which were developed from 3 sub-basin thresholds and 2 landuse/soil thresholds within each of the sub-basin thresholds (Table 6.10).

Table 6.10: Scenarios of sub-basin and HRUs discretization and model performance for the White Volta River basin at Nawuni for the period 1980-1999

Scenario	Sub-basin threshold (ha)	Number of sub-basin	Number of rain gage used in simulation	Landuse/soil threshold	Number of HRU simulated	Mean annual rainfall (mm)	Mean annual discharge (mm)
1A	150,000	26	12	15/10	148	806.90	161.27
1B	150,000	26	12	10/10	180	806.90	156.96
2A	80,000	52	14	15/10	237	824.05	165.35
2B	80,000	52	14	10/10	296	824.05	165.08
3A	60,000	90	14	15/10	364	824.05	165.77
3B	60,000	90	14	10/10	484	824.05	165.42

The results show that increasing the number of sub-basins from 26 in scenarios 1A and B to 52 in scenarios 2A and B led to an increase in the number of rain gages used in the simulation from 12 to 14 (Table 6.9). This in turn resulted in the increase in

the annual rainfall from 806.90 mm to 824.05 mm and subsequently an increase in the annual discharge. Increasing the number of sub-basins from 52 to 90 resulted in no change in the number of rain gages used in the simulation. This suggests that there is a limit to which an increase in the number of sub-basins can influence the number of rain gages used by the model and for that matter the accuracy of the output.

The results also show that there is a limitation to which an increase in the number of landuse can have on the discharge. Increasing the number of HRUs from 140 in scenario 1A to 180 in scenario 1B led to an increase in the number of landuse types from 6 to 7. This resulted in a decrease in discharge from 161.27 mm to 156.96 mm. An increase in the number of HRUs from 364 in scenario 3A to 484 in scenario 3B led to an increase in the number of landuse types from 7 to 8. However, the resulting discharge showed no significant change. This was because the additional landuse type modeled in scenario 3B covers less than 0.2 % of the study area.

6.7.3 Model calibration

The White Volta SWAT model was calibrated at Nawuni (90,856 km²) for the period 1986-1991. The period 1980-1985 was used for warming the model. The calibration was done manually, using measured daily stream discharge data for Nawuni and following the procedure outlined in Figure 6.2 and the SWAT user manual (Neitsch et al., 2002). Calibrations were done for discharge, surface runoff and baseflow. The calibration for discharge was done at annual, monthly and daily time scales while annual and monthly calibrations were done for the surface runoff and baseflow.

The first step in the calibration process was the calibration for water balance and discharge for mean annual conditions in the calibration period (1986-1991). This was followed by monthly and daily calibrations. The calibration process focused on adjusting model-sensitive input parameters determined from the sensitivity analysis (section 6.7) (Table 6.11 and 6.12) to obtain best fit between simulated and observed data.

Table 6.11: Initial and final ranges of SWAT model parameters used in calibration

Parameter	Definition	Initial parameter	Final parameter
ESCO	Soil evaporation compensation factor	0-1 ^(a)	0.100
SURLAG	Surface runoff lag time [days]	0-10 (*)	1.00
GWQMN	Threshold water depth in the shallow aquifer for flow [mm]	0.00-5000 ^(a)	35-90
SOL_AWC_SCL	Soil available water capacity for sand-loam-clay [mm/mm]	-50-50 ^(b)	0.08-0.17
SOL_AWC_SL	Soil available water capacity for sand-loam [mm/mm]	-50-50 ^(b)	0.07-0.17
SOL_AWC_LS	Soil available water capacity for loamy-sand [mm/mm]	-50-50 ^(b)	0.08-0.12
SOL_AWC_CL	Soil available water capacity for clay-loamy [mm/mm]	-50-50 ^(b)	0.13-0.16
SOL_AWC_L	Soil available water capacity for Loam [mm/mm]	-50-50 ^(b)	0.02-0.17
SOL_AWC_C	Soil available water capacity for Clay [mm/mm]	-50-50 ^(b)	0.13-0.17
RECHRG_DP	Deep Aquifer percolation fraction [-]	0-1 ^(a)	0.20
GW_REVAP	Groundwater "revap" coefficient [-]	0.02-0.20 ^(a)	0.15
GW_DELAY	Groundwater delay [days]	0-500 ^(a)	35.0-90.0
ALPHA_BF	Baseflow alpha factor [days]	0-1 ^(a)	0.042-0.100

Method of changing parameter value: ^a for changing by value and ^b by percentage

 Table 6.12: Final values of CSC curve numbers (CN₂) used for each landuse type

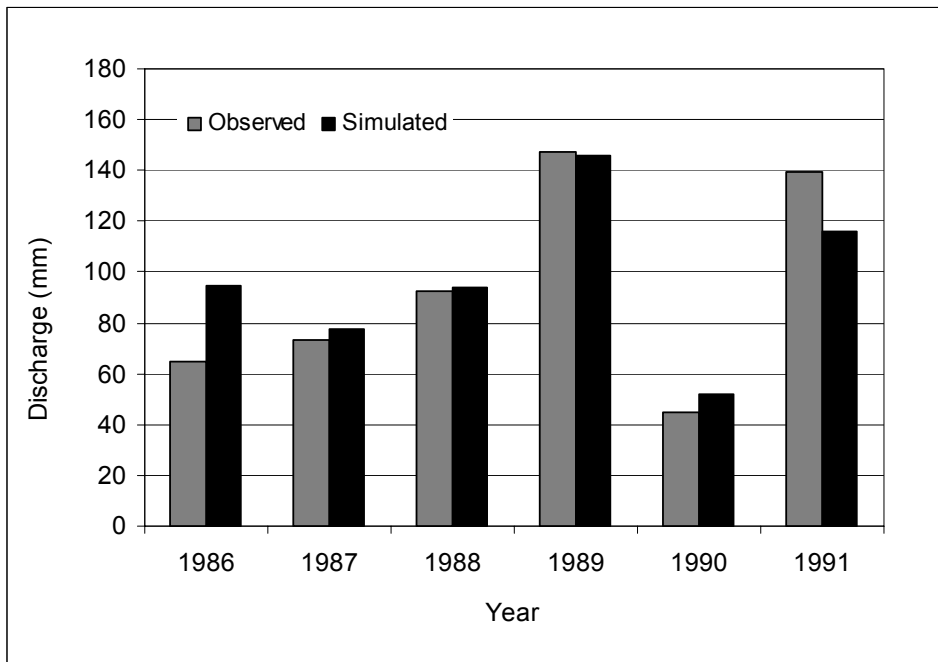
Land-use code	Name	CN ₂ value
SAVA	Savannah	64.00
BSVG	Barren/Sparsely vegetated	62.50
GRAS	Grassland	65.50
FOEB	Evergreen broadleaf forest	53.50
CRWO	Cropland/Woodland	56.50
FOMI	Mixed forest	55.0
WEHB	Herbaceous wetland	61.0
WEWO	Wooded Wetland	76.0

In order to calibrate the surface runoff and the baseflow, the streamflow for Nawuni was separated into the baseflow and surface runoff components using an

automated baseflow separation filter (section 6.5). The results indicate that baseflow constitutes about 64 % of the streamflow in the White Volta Basin.

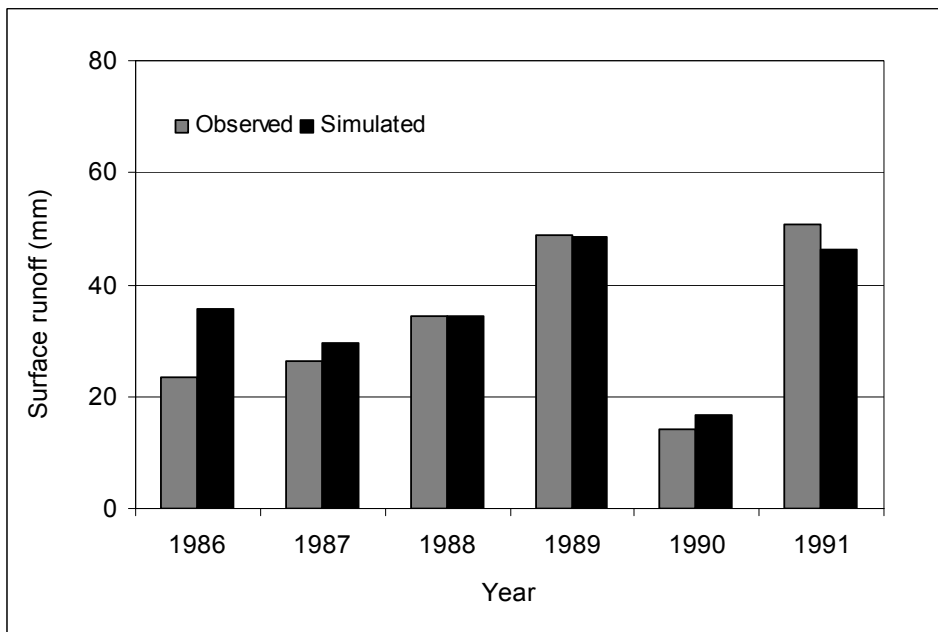
The calibration results show good agreement between simulated and observed annual discharge, surface runoff and baseflow (Figures 6.10, 6.11 and 6.12), with coefficient of determination (R^2) higher than 0.80, Nash-Sutcliffe model efficiency (NSE) greater than 0.80 and index of agreement (IA) higher than 0.90. The difference between the observed- and simulated-mean annual discharge, surface runoff and baseflow are all under 7 % (discharge-3.2 %; surface runoff-6.8 %; and baseflow-2.6 %). In four of the 6 year calibration period, SWAT slightly overestimated the annual discharge, surface runoff and baseflow.

The monthly calibration show significant improvement in the goodness-of-fit measures compared to the annual calibration (Figure 6.12). A better correlation between simulated and observed discharge was obtained for the monthly calibration compared to the annual (annual- R^2 : 0.85; monthly- R^2 : 0.93; annual-NSE: 0.83; monthly- NSE: 0.92). The difference between the simulated and observed mean monthly discharge was 3.1 %, which is similar to the value obtained for the annual discharge. Generally, SWAT overestimated the high flows (5 out of 6 years) and underestimated the low flows (4 out of 6 years). Compared to the annual and monthly calibrations, the daily calibration had the lowest correlation between simulated and observed discharge (Figure 6.13), with R^2 of 0.77, NSE of 0.68, and IA of 0.93. However, the model goodness measures meet the recommended minimum values ($R^2 = 0.60$ and $NSE = 0.50$) for the calibration to be acceptable. Again, SWAT overestimated the high flows and underestimated the low flows, frequently with zero daily flow during part of the dry season (January, February and March).



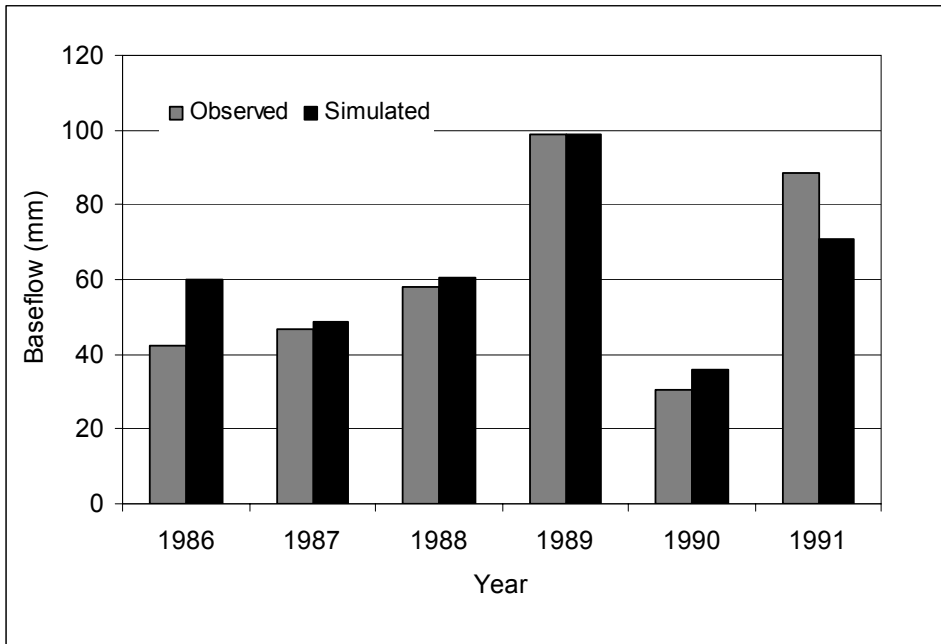
Mean		Standard deviation		Goodness-of-fit measures		
Observed	Simulated	Observed	Simulated	R ²	NSE	IA
93.63	96.62	37.96	29.38	0.85	0.83	0.94

Figure 6.10 Observed and simulated annual discharge and statistics at Nawuni (90,856 km²)



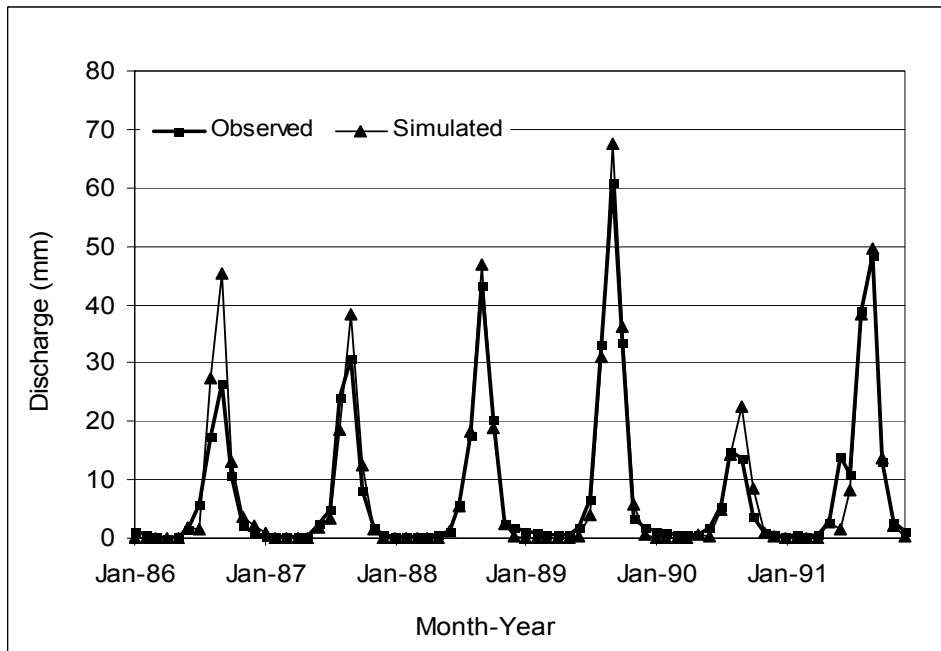
Mean (mm)		Standard deviation		Goodness-of-fit measures		
Observed	Simulated	Observed	Simulated	R ²	NSE	IA
33.01	35.22	13.31	10.58	0.88	0.83	0.95

Figure 6.11 Observed and simulated annual surface runoff and statistics at Nawuni (90,856 km²)



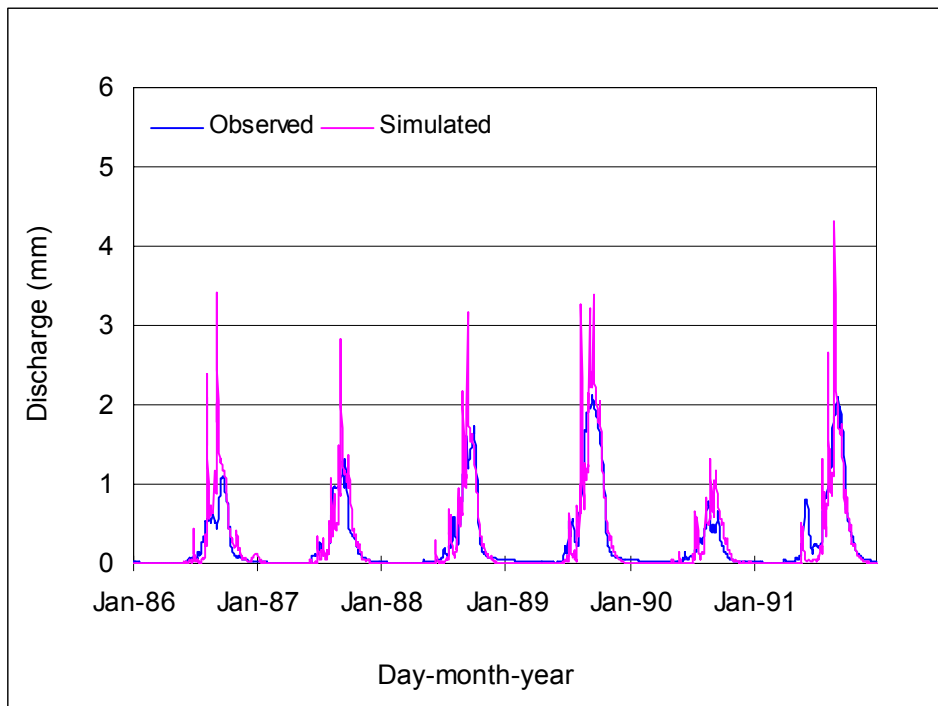
Mean (mm)		Standard deviation		Goodness-of-fit measures		
Observed	Simulated	Observed	Simulated	R ²	NSE	IA
60.80	62.36	24.70	19.70	0.84	0.82	0.97

Figure 6.12 Observed and simulated total annual baseflow and statistics at Nawuni (90,856 km²)



Mean (mm)		Standard deviation		Goodness-of-fit measures		
Observed	Simulated	Observed	Simulated	R ²	NSE	IA
7.77	8.01	12.84	14.49	0.93	0.92	0.98

Figure 6.13 Observed and simulated total monthly discharge and statistics at Nawuni (90,856 km²)



Mean (mm)		Standard deviation		Goodness-of-fit measures		
Observed	Simulated	Observed	Simulated	R ²	NSE	IA
0.26	0.26	0.45	0.53	0.77	0.68	0.93

Figure 6.14 Observed and simulated daily discharge and statistics at Nawuni (90,856 km²)

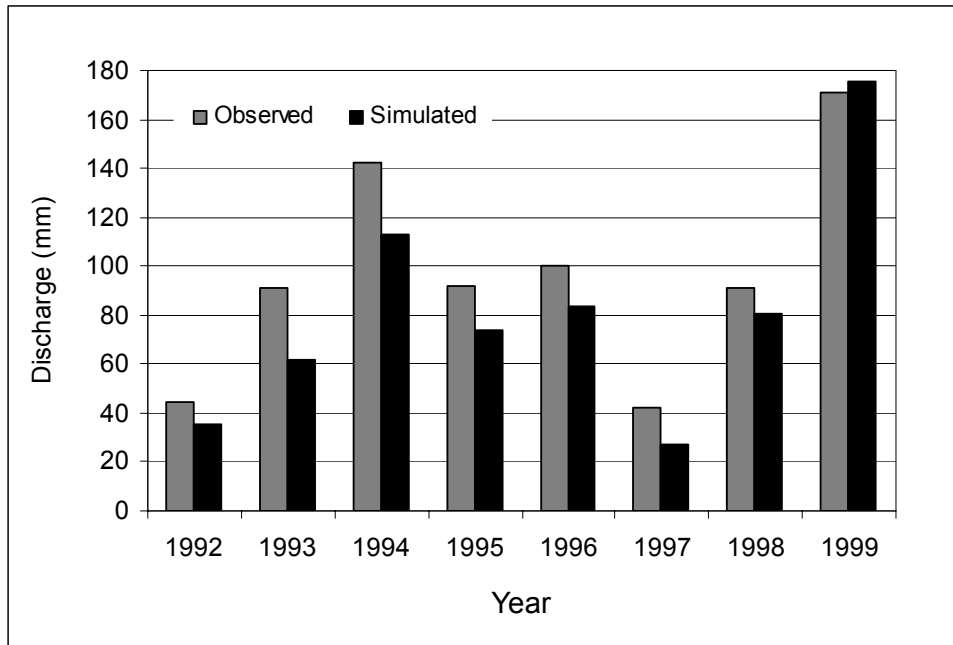
6.7.4 Model validation

The calibrated White Volta SWAT model was validated by using it to predict the hydrological quantities in the study area for a period other than the calibration period and without any further change in the model input parameters. The model was validated for the period 1992-1999.

As shown by the goodness-of-fit measures, the simulated and observed annual discharge, surface runoff and baseflow were in good agreement (Figures 6.15, 6.16, and 6.17), with R², NSE and IA higher than 0.90, 0.70, and 0.90, respectively. However, the differences in the mean values of the flows are rather high (discharge-15.8 %; surface runoff-18 %; and baseflow-13 %). This is due to the fact that the model was unable to simulate the low flows well enough. It constantly underestimated the annual discharge, surface runoff and baseflow in the entire validation period except for the annual baseflow in 1999, which was overestimated. The underestimation of the low flows

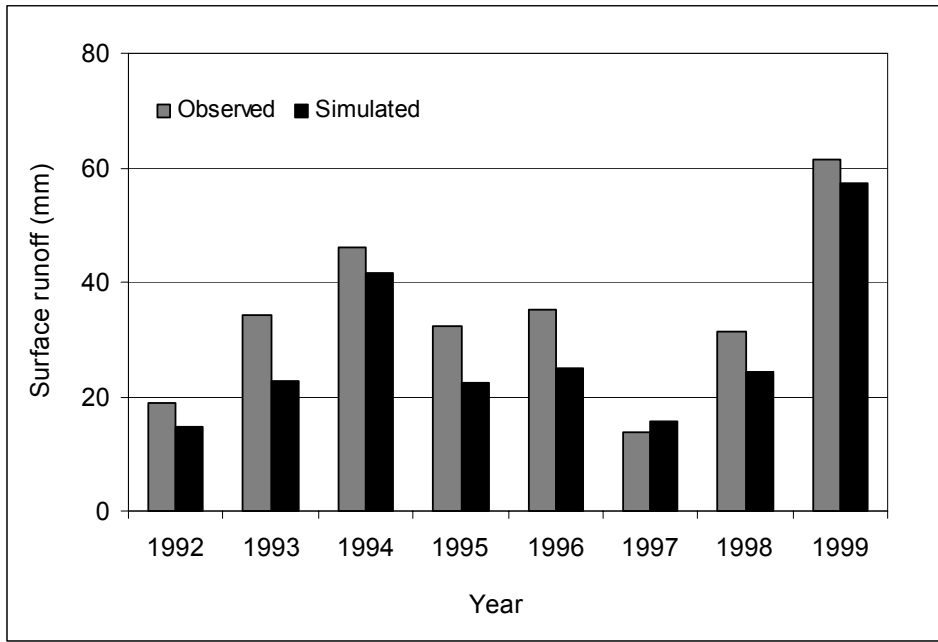
could be due to more than one aquifer contributing to baseflow in the basin, a situation not handled in SWAT at present.

Similar to the monthly calibration, the monthly validation results show a better correlation between the simulated and observed monthly discharge (Figure 6.18). The model goodness-of-fit measures were all higher than 0.90. However, the model mainly underestimated both the high and low flows resulting in about 15 % differences between the simulated and observed mean monthly discharge. The daily validation shows a good agreement between the simulated and observed daily discharge (Figure 6.19), although the model goodness-of-fit measures were lower compared to those obtained in the annual and monthly validations.



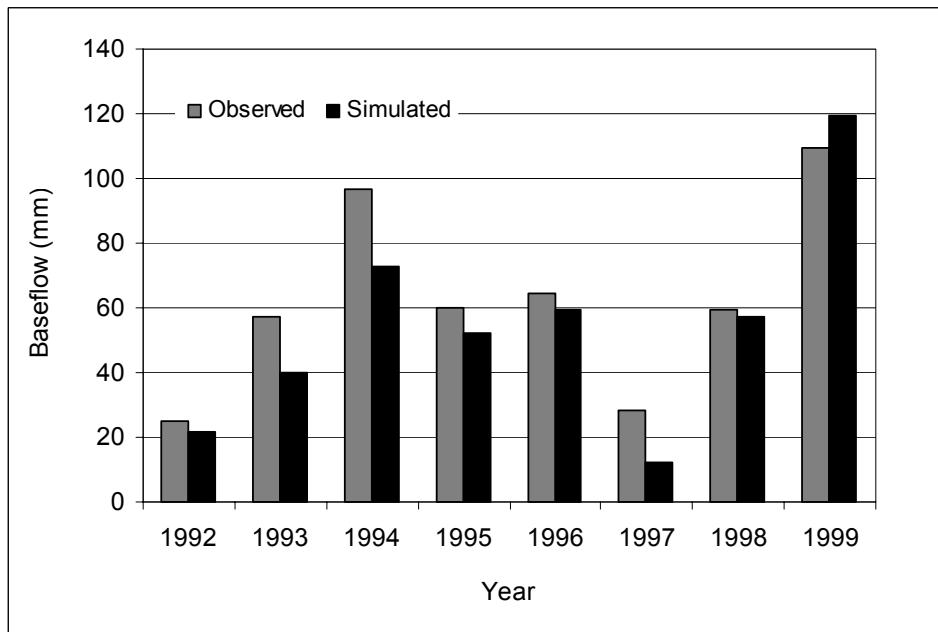
Mean (mm)		Standard deviation		Goodness-of-fit measures		
Observed	Simulated	Observed	Simulated	R ²	NSE	IA
96.75	81.45	41.00	43.64	0.94	0.80	0.91

Figure 6.15 Observed and simulated total annual discharge and statistics at Nawuni (90,856 km²)



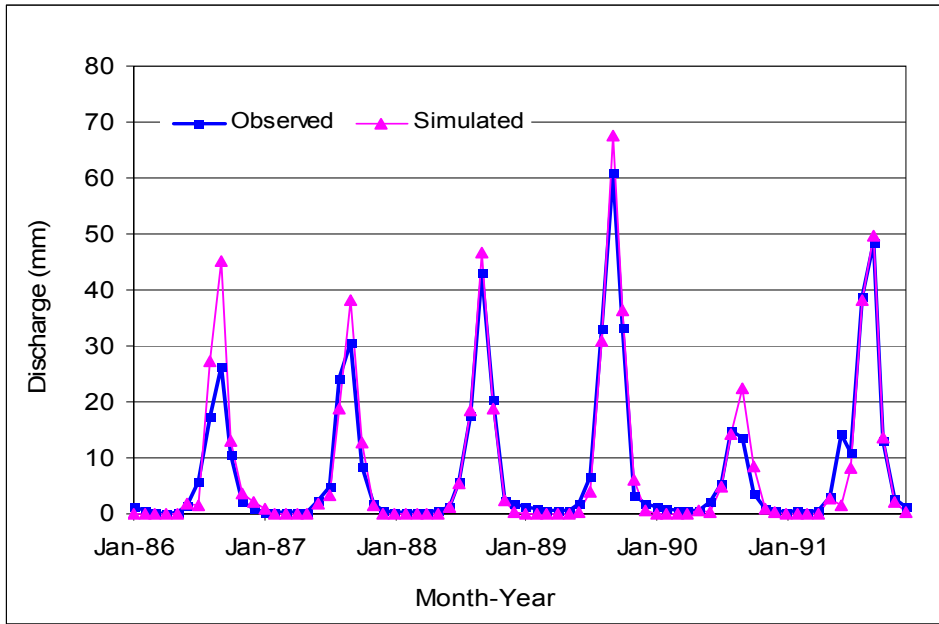
Mean (mm)		Standard deviation		Goodness-of-fit measures		
Observed	Simulated	Observed	Simulated	R ²	NSE	IA
34.18	27.91	13.90	13.45	0.91	0.71	0.93

Figure 6.16 Observed and simulated total annual surface runoff and statistics at Nawuni (90,856 km²)



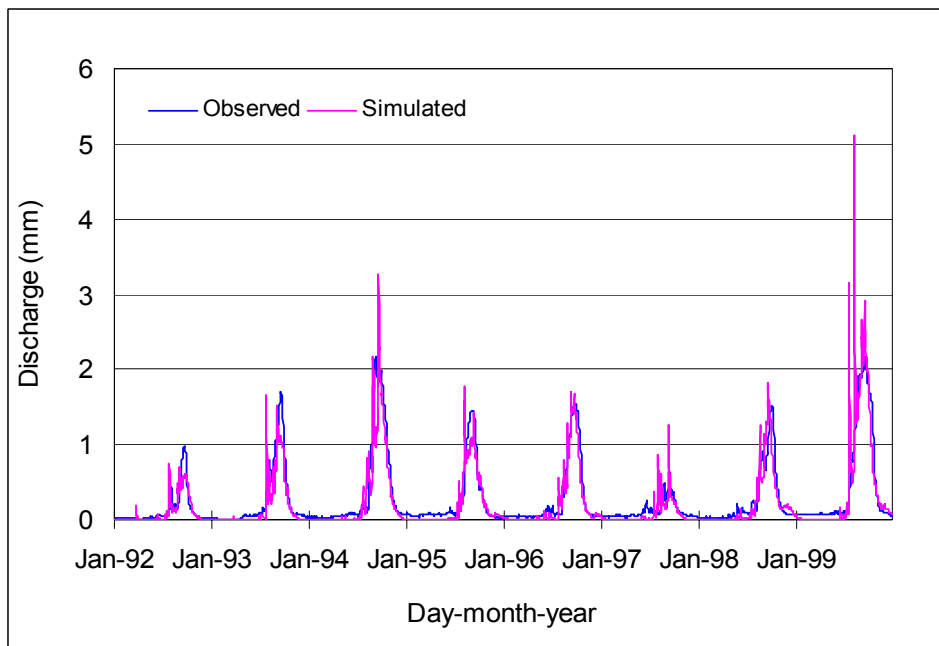
Mean (mm)		Standard deviation		Goodness-of-fit measures		
Observed	Simulated	Observed	Simulated	R ²	NSE	IA
62.58	54.31	27.33	28.02	0.90	0.77	0.95

Figure 6.17 Observed and simulated annual baseflow and statistics at Nawuni (90,856 km²)



Mean (mm)		Standard deviation		Goodness-of-fit measures		
Observed	Simulated	Observed	Simulated	R ²	NSE	IA
8.01	6.79	12.99	12.62	0.95	0.94	0.98

Figure 6.18 Observed and simulated monthly discharge and statistics at Nawuni (90,856 km²)



Mean (mm)		Standard deviation		Goodness-of-fit measures		
Observed	Simulated	Observed	Simulated	R ²	NSE	IA
0.26	0.22	0.45	0.46	0.80	0.78	0.94

Figure 6.19 Observed and simulated daily discharge and statistics at Nawuni (90,856 km²)

Clearly, the calibration and validation results show that the SWAT model performed very well in simulating the annual, monthly and daily discharge as well as the annual surface runoff and baseflow in both the calibration and validation periods. This indicates that the final values of the model-sensitive parameters selected at calibration represent those parameters in the study area. It can therefore be concluded that the SWAT model built for the White Volta Basin realistically reproduces the hydrological flows in the basin and can, therefore, be used for future impact studies.

6.7.5 Annual water balance

The mean annual water balance in the study area was estimated with the SWAT model for the calibration and validation periods. There were slight differences in the values of the mean annual water balance for the two periods (Table 6.13).

Table 6.13: Mean annual values of the water balance of the White Volta Basin at calibration (1986-1991) and validation (1992-1999)

Parameter	Mean values at calibration (mm)	Mean values at validation (mm)
Precipitation	842.50	805.40
Surface runoff	33.26	25.81
Groundwater flow (Baseflow)	62.23	54.67
Lateral flow	0.65	0.65
Shallow aquifer recharge	154.55	139.34
Deep aquifer recharge	38.64	34.83
Actual evapotranspiration (AET)	598.60	606.80
Change in soil water storage	-45.43	-56.70

For the calibration period, about 73 % of the mean annual precipitation that occurs in the study area evapotranspires. This value is slightly higher (75 %) for the validation period. The annual discharge for the calibration period was estimated to be 11 % of the annual precipitation and consisted of 4 % surface runoff and 7 % baseflow. For the validation period, the simulated discharge was 10 % of the annual rainfall, and the surface runoff and baseflow components were respectively 3 % and 7 % of the annual rainfall. Similar discharge, surface runoff and baseflow values have been obtained in

previous studies in other parts of the Volta basin and in neighboring basins in Ghana (Table 6.14).

Statistics of the water balance show that for both the calibration and validation periods, the baseflow had the highest annual variability (Table 6.15). This was closely followed by the surface runoff. The annual variations in rainfall and actual evapotranspiration were relatively very low. Friesen et al. (2005) obtained similar values for the entire Volta basin.

Table 6.14: The water balance in the Volta Basin in West Africa and neighboring basins in Ghana (HAPS, 2006)

Study area and country	Rainfall	Actual evapotranspiration	Runoff coefficients (% of rainfall)			Source
			Total runoff	Surface runoff	Baseflow	
Atankwidi catchment (Ghana)	910-1138	789-798	10-17	-	-	1
Southern Voltaian Sedimentary Basin (Ghana)	1400	1027	13	-	-	2
Volta River Basin (West Africa)	1002	893	11	6	5	3
	1200	-	10	-	-	4
	1009	918	8	-	-	5
Pra River Basin (Ghana)	1170-1490	1170-1490	6-9	0.6-1	3.4-4.5	6

(1): Martin, 2005; (2): Acheampong, 1996; (3): Friesen et al., 2005; (4) Shahin, 2002; Andreini et al., 2000; (6): Darko and Krasny

Table 6.15: Statistics of the water balance in the White Volta Basin

		Rainfall	AET	Baseflow	Surface runoff	Discharge
Calibration	Mean	842.50	598.60	62.23	33.26	94.98
	CV	0.07	0.04	0.35	0.33	0.33
Validation	Mean	805.40	606.80	54.67	25.81	79.73
	CV	0.09	0.06	0.43	0.36	0.39

The temporal dynamics of the mean annual precipitation and potential evapotranspiration of the study area as simulated in SWAT are consistent with the general trend in that part of the Volta basin. Precipitation in the study area has a mono-modal pattern and peaks in August (Figure 6.20). The mean annual rainfall amount generally increases across the basin, from the north to the south (Figure 6.21). The potential evapotranspiration (PET) is high throughout the year with maximum values

recorded in March, April and May. The mean monthly PET exceeds the mean monthly rainfall in 9 of the 12 months.

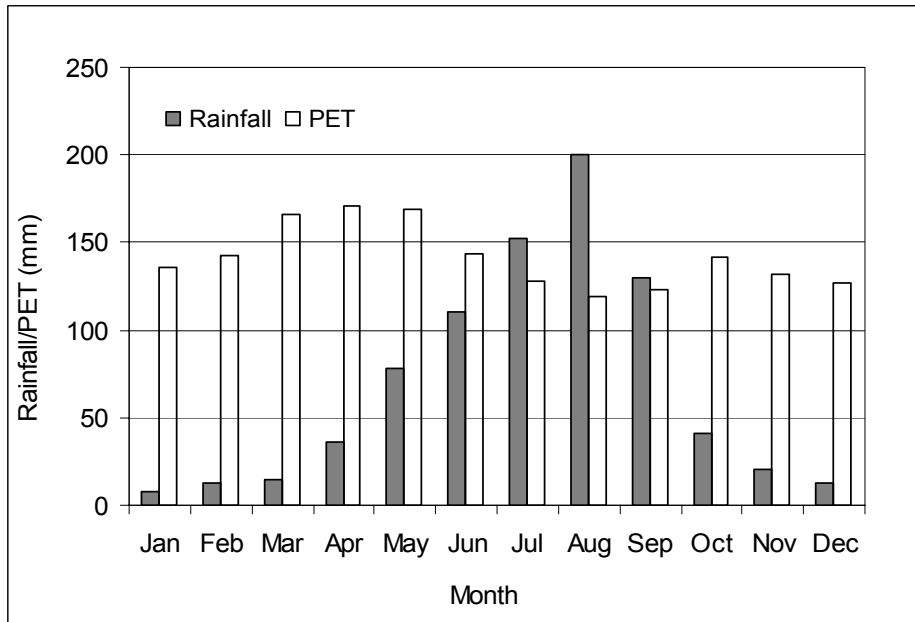


Figure 6.20 Temporal dynamics of mean rainfall and potential evapotranspiration (PET) in the White Volta Basin (from SWAT model: 1980-2001)

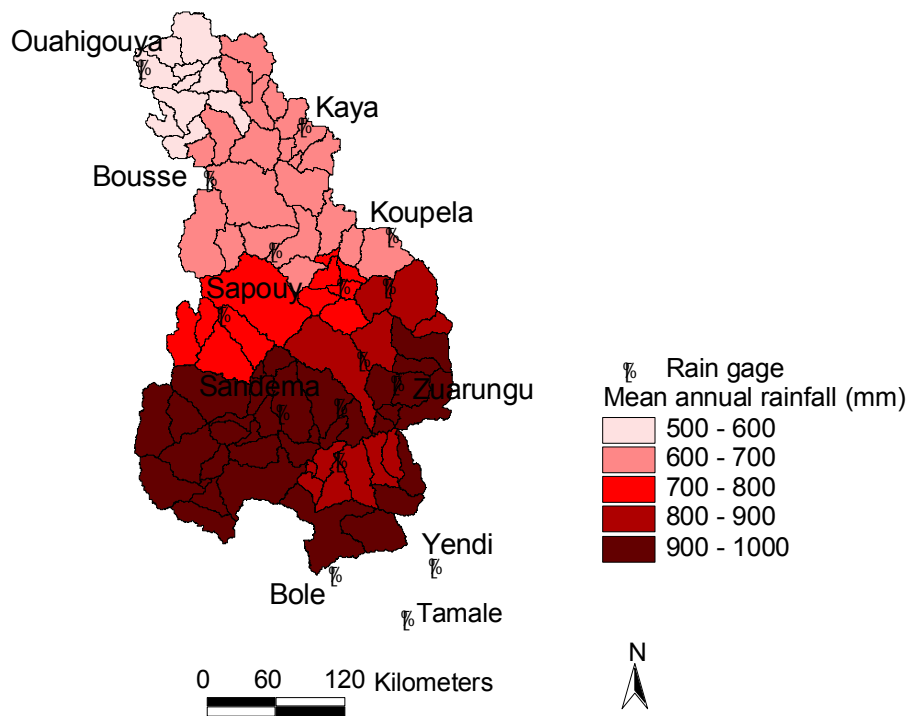


Figure 6.21 SWAT modeled distribution of mean annual rainfall in the White Volta Basin (1980-1999)

6.7.6 Distribution of surface runoff and baseflow

The spatial distribution of the 20 year (1980-1999) mean annual surface runoff and baseflow (shallow groundwater recharge) was simulated for the study area using the calibrated SWAT model. Most of the surface runoff and baseflow in the study area are generated in the south of the basin (Figures 6.22 and 6.23). This could be attributed to the trend in rainfall and potential evapotranspiration among other factors. Precipitation in the basin increases from north to south, while potential evapotranspiration decreases. The combined effects of the variation in the two climate parameters between the north and south of the basin strongly influences the spatial distribution of the baseflow and surface runoff, with more flows generated in the south than in the north.

6.7.7 SWAT recharge estimates

In SWAT, the baseflow is the shallow groundwater contribution to the river discharge (section 6.2.8) and can reasonably be taken to be the groundwater recharge to the shallow aquifer. Therefore, the mean annual recharge to the shallow groundwater in the White Volta Basin as simulated in SWAT is 7 % of the mean annual rainfall (section 6.7.5). This recharge value is similar to those obtained with the chloride mass balance (8.3 %) and the water table fluctuation (7-8 %) methods in parts of the White Volta basin (chapters 4 and 5). This recharge value is also similar to the 5 % recharge value estimated for the whole Volta basin by Friesen et al. (2005) using a rainfall-runoff model based on the Thornthwaite-Mather storage model. The authors estimated the recharge from the baseflow component of the discharge, which they defined as runoff from the groundwater reservoirs or aquifers that, in turn, are filled by groundwater recharge from the root zone.

Comparing spatial distribution of groundwater recharge in the north-eastern part of Ghana (Upper East Region) in the White Volta Basin, based on the SWAT model, chloride mass balance, and water table fluctuation methods, there appear to be much agreement regarding areas of high groundwater recharge. These areas are essentially the middle part of the Region, around Gowrie, Bongo, Tongo, and Datuku. There is also a general agreement that the western part of the Region receives more recharge than the east.

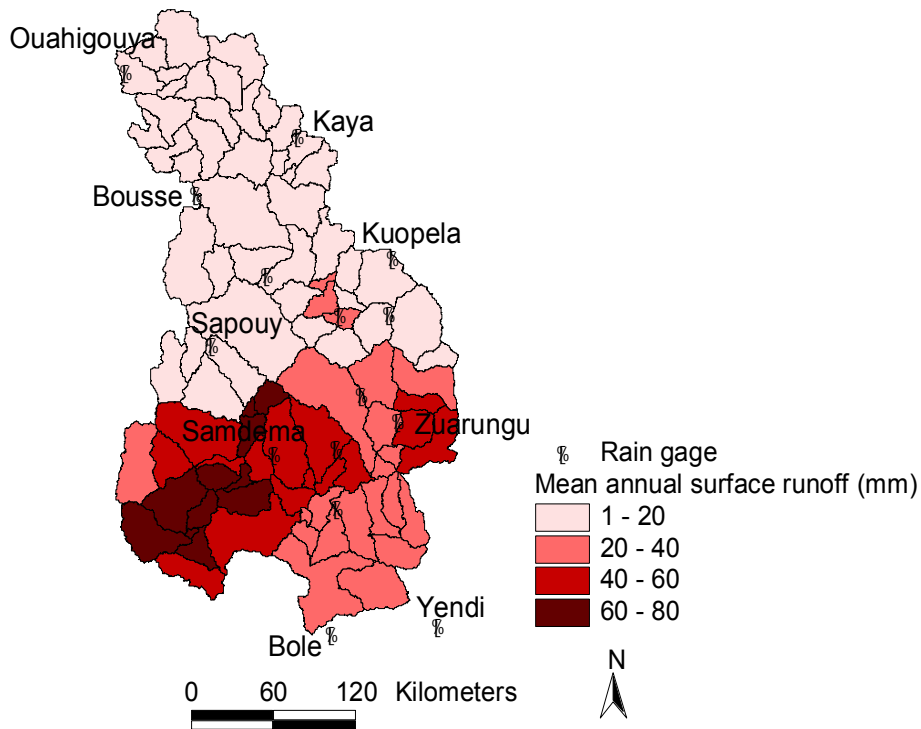


Figure 6.22 SWAT modeled distribution of mean annual surface runoff in the White Volta River Basin (1980-1999)

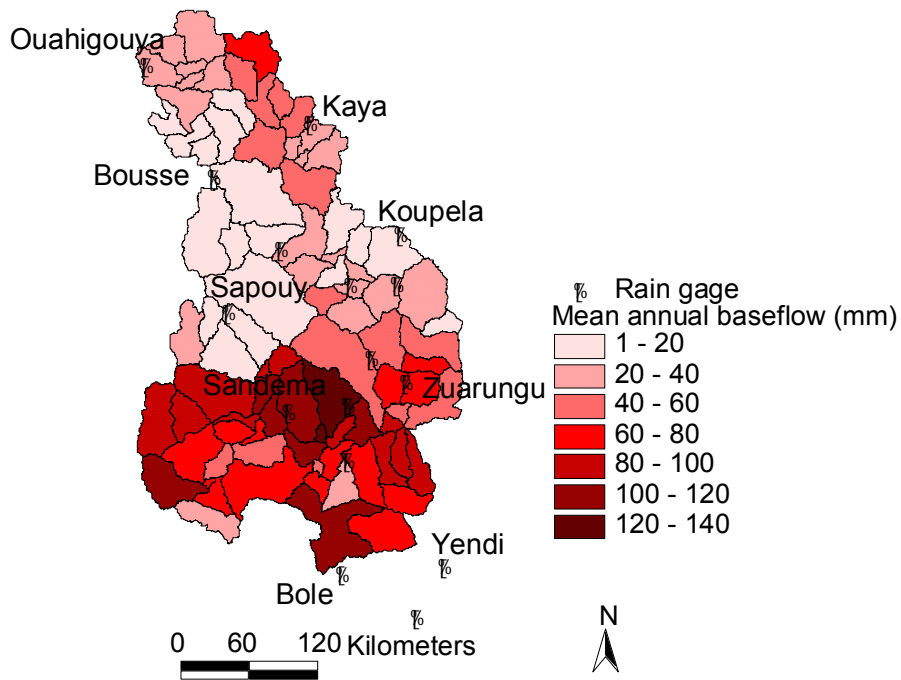


Figure 6.23 SWAT modeled distribution of mean annual baseflow (shallow groundwater recharge) in the White Volta River Basin (1980-1999)

7 IMPACTS OF FUTURE CLIMATE CHANGE ON WATER RESOURCES

7.1 Introduction

The impacts of future climate change on water resources can be studied using a hydrological model that is driven with the output from general circulation models (also known as global climate models when used for climate projections) (GCMs). GCMs are a class of computer-driven models that are based on the integration of a variety of fluid dynamical, chemical, and sometimes biological equations. They are used for weather forecasting, understanding climate and projecting climate change (Thorpe, 2005). Three types of GCMs can be distinguished: atmospheric global climate models (AGCMs), oceanic global climate models (OGCMs) and the atmosphere-ocean coupled GCMs (AOGCMs), which are the most complex models. The AOGCMs consist of AGCM, coupled with OGCM. Several AOGCMs exist for simulating the present and projecting the future climate series. Examples of AOGCMs are, HADCM, GFDL, CM2.X, and ECHAM).

The spatial resolution of GCMs (typically 250 km) is often too coarse for direct application in hydrological modeling at local or regional scale. This is because regional scale climate is greatly influenced by atmospheric processes, topography and land-sea distribution, which are not well represented in global models because of their coarse resolution (Storch et al., 1993). In simulating the hydrology of a basin, a good representation of the climate, more particularly rainfall, is of utmost importance, since misrepresentation can greatly affect the values of the hydrological variables. GCMs exhibit a much larger spatial scale (grid-point area) than is usually needed for impact studies in hydrology. This can result in inconsistencies in the frequency statistics, such as the exceedance of a threshold for heavy rainfall (Busche et al., 2005, Sintondji, 2005; Osborn and Hulme, 1997).

To overcome the coarse resolution of GCMs, two major techniques have been developed to downscale the output of GCMs to meso- or regional-scale. These are dynamical downscaling and statistical downscaling. Dynamical downscaling uses regional climate models (RCMs) to simulate higher resolution (typically 50 km) physical processes that are consistent with large scale climate projection from a GCM (Mearns et al., 2004). RCMs take their boundary and sea-surface conditions from

GCMs. The high resolution of RCMs make them more appropriate for resolving small-scale features of topography and land use, which have a major influence on climate parameters such as rainfall in climate models. Also, the high resolution of RCMs is ideal to capture the variability of regional rainfall. Examples of RCMs include REMO, PRECIS and MM5.

Statistical downscaling uses statistical relationships between the regional climate and selected large-scale parameters (Goodess et al., 2005, cited in Schmidli et al., 2005). These relationships are empirical and are applied using the predictor fields from GCM in order to construct scenarios (Schmidli et al., 2005). Examples of statistical downscaling methods are weather generators (Wilby et al., 2004). The dynamical and statistical downscaling techniques are both based on certain assumptions that are very difficult to verify and are, therefore, associated with some uncertainty (Schmidli et al., 2005).

7.2 Climate change scenarios of MM5/ECHAM4

In this study, climate series (present and future) simulated with the GCM ECHAM4 and downscaled using the regional climate model MM5 (Mesoscale Model) were used to evaluate the impacts of climate change on water resources in the White Volta river basin. The ECHAM4/MM5 climate series were obtained from the GLOWA-Volta project of the Center for Development Research (ZEF), Germany. The MM5 is a community mesoscale model that was developed in cooperation with the Pennsylvania State University (PSU) and the National Center for Atmospheric Research (NCAR), USA. It is a non-hydrostatic or hydrostatic (Version 2 only), terrain-following sigma-coordinate model designed to simulate or predict mesoscale and regional-scale atmospheric circulation (Grell et al., 1995). Like all regional models, MM5 requires initial and lateral boundary conditions to run.

In the case of the GLOWA-Volta project runs of MM5, the initial and lateral boundary conditions were derived from ECHAM4, which was run from 1860 to 2100 based on the IS92a future climate scenario, and was calibrated using the 0.5° x 0.5° gridded monthly observational dataset from the East Anglia Climate Research Unit (CRU), UK. The effects of sulphate aerosols were not considered, as they are known to be the largest sources of error within the IS92a scenario. The IS92a has an underlying

assumption of an annual increase in CO₂ of 1 %, resulting in a doubling of CO₂ in 90 years (May and Rockner, 2001; cited in Jung, 2006). Compared to the new SRES scenarios, with regard to CO₂ emissions, the IS92a scenario could be considered as intermediate (Jung, 2006). Two time slices of 10 years each (1991-2000 and 2030-2039) simulated with ECHAM4 for the West African region were downscaled with the MM5 for the Volta Basin. The climate series of the time slice 1991-2000 were taken to be the present (baseline) climate condition, while those of the 2030-2039 time slice were used as future climate series. The MM5 was calibrated with long-term observed mean climate data. Details of the ECHAM4 and MM5 setup and simulations can be obtained in Jung (2006) and Kunstmann and Jung (2003).

Results of the GLOWA-Volta climate studies show good agreement in mean annual, monthly and seasonal temperatures between ECHAM4-simulated climate and the CRU dataset for the period 1961-1990. There was, however, a slight overestimation of temperature by ECHAM4 for the Saharan region in the wet season and for southern West Africa in the dry season. For the same period, ECHAM4 rainfall amounts are comparable to the CRU data, but the maximum values are generally low (Jung, 2006). A perfect agreement was obtained between the MM5 simulated mean monthly temperatures and the observed. However, the model underestimated temperatures in the dry season nearly everywhere in the Volta Basin. The correlation obtained between MM5 simulated mean monthly rainfall and the observed was much weaker compared to the temperature. There was a strong underestimation of rainfall (up to 80 %) along the coast and an overestimation in the Sahel zone (10-30 %) (Jung, 2006). However, the MM5-simulated rainfall shows a temporal trend consistent with the annual observed rainfall cycle (Figure 7.1).

A comparison of MM5- and ECHAM4-simulated temperature and rainfall revealed a pronounced positive deviation in the MM5 temperature values from those of ECHAM4, but the change in temperature between the present and future time slices were found to be nearly the same for both models (Jung, 2006). The rainfall amounts simulated in MM5 were lower compared to those of ECHAM4 but showed improvement in spatial representation. Over the Volta Basin, the MM5 gave an overall increase of 44.7 mm (5.1 %) in the mean annual rainfall between the two time slices and a mean temperature increase of 1.2°C (Jung, 2006).

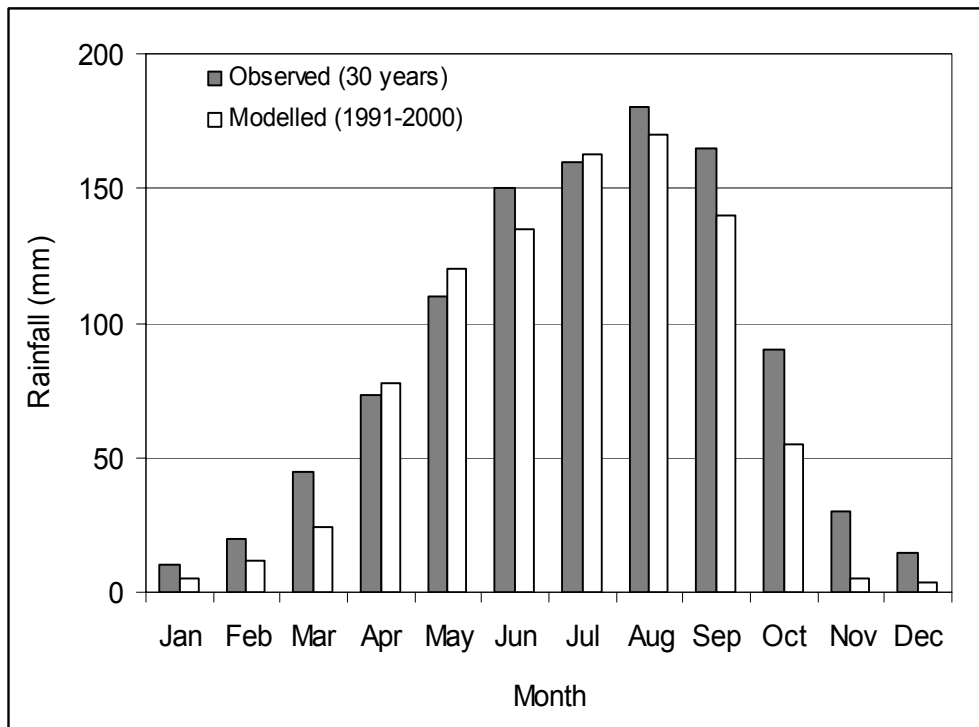


Figure 7.1 MM5-simulated mean monthly rainfall versus long-term observed mean monthly rainfall in the Volta River Basin (after Jung, 2006)

7.3 Frequency statistics of MM5 and observed rainfall series

Rainfall is a very important input parameter for any hydrological modeling because it is the main source of moisture input to the hydrological cycle. Therefore, before using any rainfall data for impact studies in hydrology, it is important not only to ensure that the data represent the study site by way of the annual amounts and temporal distribution, but also to ensure that the frequency statistics of the data, such as the exceedance of a threshold for heavy rainfall, are consistent with the long-term mean observed rainfall.

To assess the reliability of the MM5 future climate scenario for the evaluation of the impacts of climate change on water resources in the White Volta basin, the MM5-simulated mean rainfall for the present time slice (1991-2000) obtained for the basin weather stations are compared to the 30 year (1971-2000) mean observed rainfall for the stations. The results of the comparison for the Ouahigouya weather station, for example, show a good correlation between the observed and MM5-simulated monthly rainfall, with a coefficient of determination of 0.83. However, the MM5 strongly overestimated the rainfall from April to July and underestimated it from August to November, though to a lesser extent (Figure 7.2). The results also show that the MM5 simulated rainfall pattern is slightly shifted towards the start of the rainfall season, with

the highest rainfall amount occurring in July instead of August, as is the case with the observed rainfall. In addition, much of the rainfall occurs in the first half of the rainfall season for the MM5 climate series, which is a deviation from the observed. The mean annual value of the MM5-simulated rainfall (834.5 mm) is considerably higher than that of the observed (681.8 mm).

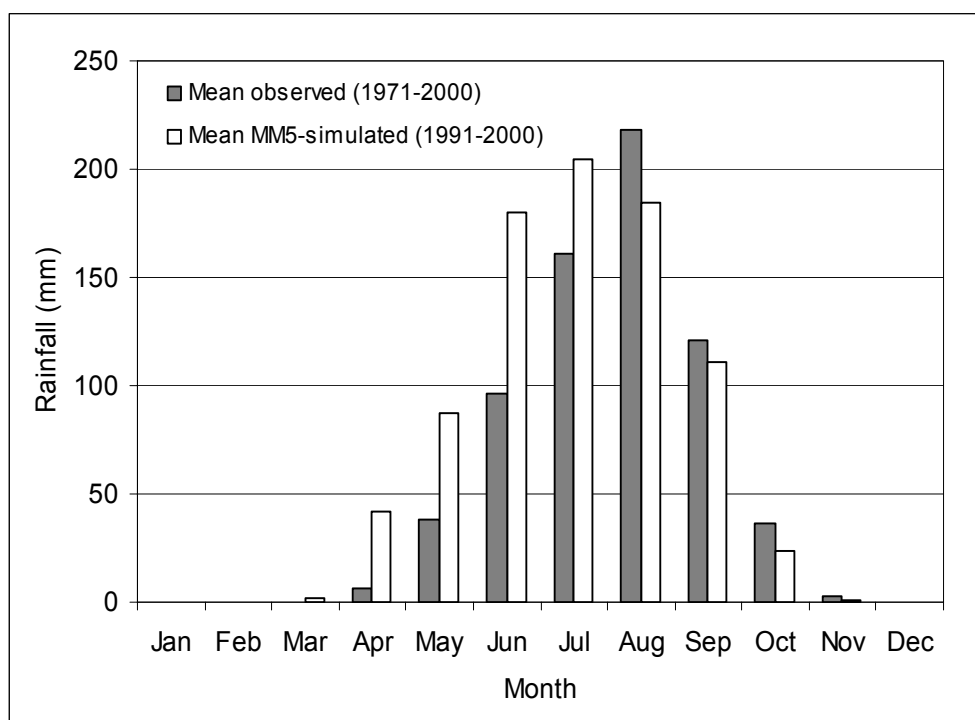


Figure 7.2 MM5-simulated (mean over 10 years) compared to the observed (mean over 30 years) monthly rainfall at Ouahigouya weather station in the White Volta Basin. Data source (Direction de la Météorologie Nationale, Burkina Faso, and Jung, 2006)

A comparison of the observed and MM5-simulated daily rainfall events was also done for the Ouahigouya station. The results demonstrate that the MM5 overestimated the high daily rainfall events (50 mm or more) and generally underestimated the low rainfall events, except for those in the range of 1-5 mm and less than 1 mm (Figure 7.3). A major reason for the deviation of the MM5-simulated rainfall from the observed is that the MM5 data assigned to the weather station are the mean of gridded (9-km resolution) rainfall and not site specific as obtained with the observed data and required for modeling in SWAT. Similar deviations of MM5-simulated daily rainfall intensity from the observed were found for most of the other weather stations

used for the SWAT modeling in the White Volta Basin. Therefore, the MM5 daily rainfall data were not suitable for direct use in SWAT.

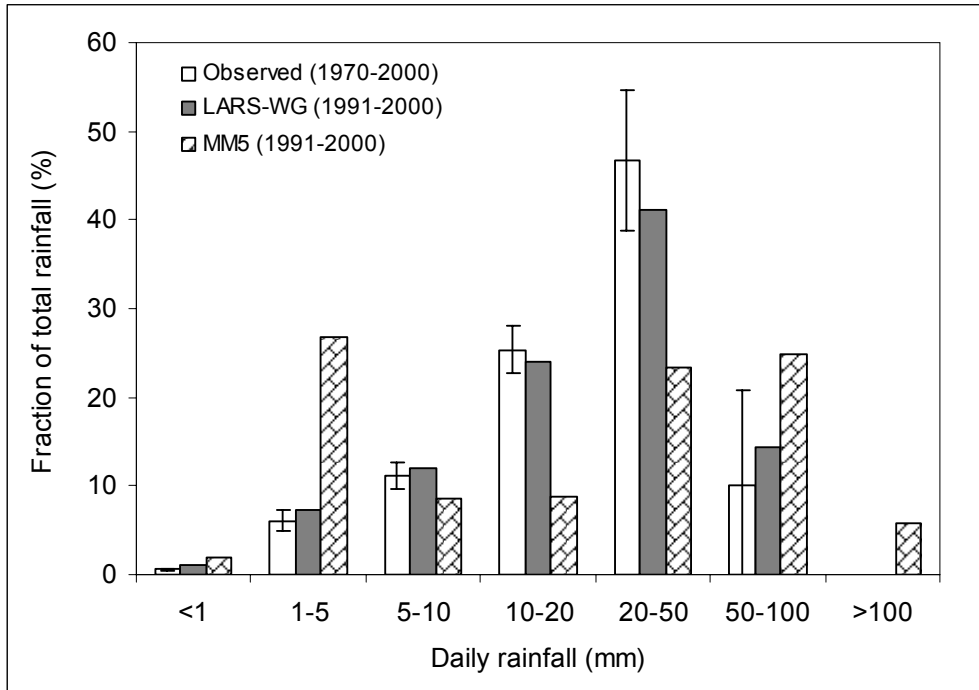


Figure 7.3 MM5-simulated (mean over 10 years) and LARS-WG-generated (mean over 95 years after 5 realizations) compared to observed (mean over 30 years including standard deviation) rainfall at Ouahigouya weather station in the White Volta Basin

To obtain station-specific data for use in SWAT, the Long Ashton Research Station Weather Generator (LARS-WG) was used to generate daily climate series with similar statistics as the observed data. LARS-WG is a stochastic weather generator which was first developed in Budapest in 1990 (Racsko et al., 1991). It can be used for simulation of daily climate data at a single site under current and future climate conditions (Semenov et al., 1998). Three distinct steps described in detail by (Semenov and Barrow, 2002) were followed in generating station-specific climate series with the LARS-WG for the weather stations in the White Volta Basin. First, LARS-WG was calibrated with 30 years observed climate data (Rainfall and temperature) to determine their statistical characteristics. Second, LARS was validated by generating 100 years of synthetic weather data and comparing their statistical characteristics to that of the observed data to find out if there were any significant differences. Third, LARS-WG was used to generate 95 years synthetic climate data that have the same statistical

characteristics as the observed data but differing on day to day basis. Five realizations of generated climate series were obtained based on different random seeds. The resulting LARS-WG data are the mean of the 5 realizations.

Compared to the MM5-simulated, the LARS-WG-generated rainfall series better represent the daily rainfall events within the 30-year observed period (Figure 7.3). A higher correlation ($R^2 = 0.95$) is obtained between the observed monthly rainfall and the generated compared to the simulated. Similarly, there is high agreement in daily rainfall events and monthly correlations between the observed and the generated climate series for the other weather stations in the basin.

7.4 Water balance based on observed and generated climate series

The water balance of the White Volta Basin was simulated with the calibrated SWAT model based on the observed and the LARS-WG-generated climate series and the results compared. This was done to quantify the deviations of the generated climate series from the observed by way of the impact on the water balance. Quantifying deviations in the water balance resulting from the LARS-WG-generated present climate series can provide a means for checking the reliability of the generated future climate series for impact analysis. Two SWAT simulations of the water balance were run based on 15 years of observed climate series and 95 years of generated climate series. The results of the 2 simulations were then compared.

The pattern of distribution of monthly rainfall in the White Volta Basin is maintained by the generated series, with the highest monthly rainfall recorded in August, which is consistent with the observed (Figure 7.4). However, the generated series underestimated the monthly rainfall from January to June and overestimated it from July to December. The mean annual rainfall of the generated series is slightly higher than that of the observed by about 3 % (Table 7.1). The monthly actual evapotranspiration (AET) follows the same trend as the rainfall, but the mean annual value was found to be 6 % lower than the observed. Except for the months of June, July and September, the mean monthly discharge of the generated series had very good agreement with the observed, with just about 3 % difference in the mean annual values as a result of a small overestimation by the generated series. The biggest deviation was obtained with the mean annual surface runoff, which was overestimated with the

generated climate series. Except for the AET, the water balance simulated with the generated climate series shows less variability in the mean annual values than the observed (Table 7.2).

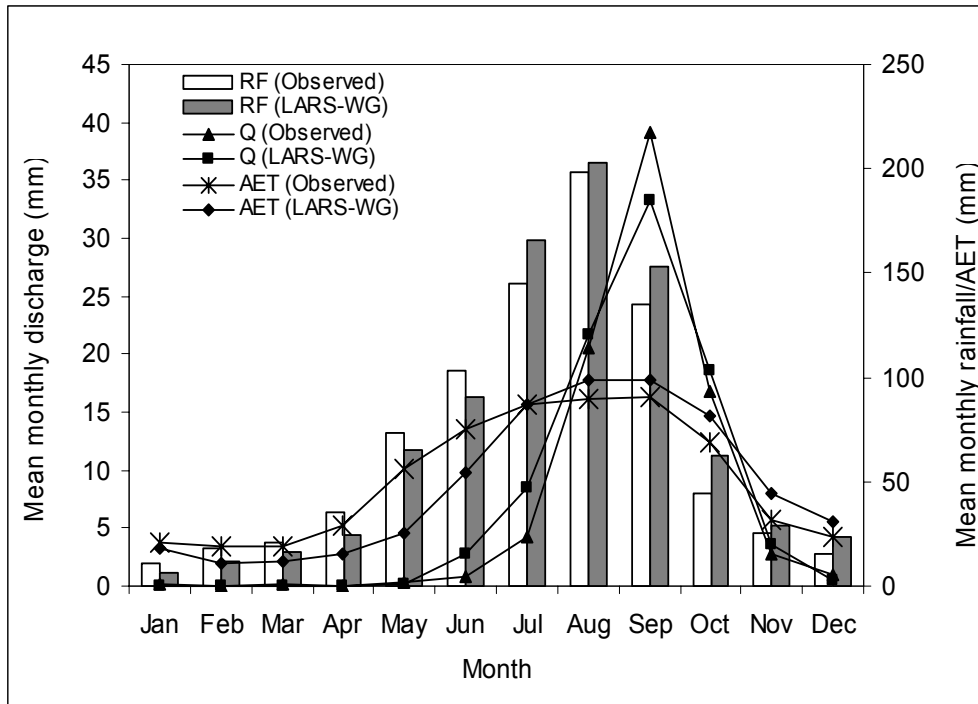


Figure 7.4 SWAT-simulated mean monthly water balance of the White Volta Basin based on observed (15 years) and LARS-WG-generated (95 years) climate series. (RF-rainfall; Q-discharge; and AET-actual evapotranspiration)

On the whole, the water balance of the White Volta Basin as simulated with the generated climate series is consistent with the observed, except for a few over- and under-estimations. The pattern of monthly distribution of the water balance variables is in high agreement with the observed; the mean annual values of the water balance simulated with the two climate series show only a slight variation, which is largely within the standard of deviation. The frequency statistic of the daily event given by the generated series is identical with the observed (Table 7.2). Based on the above results, the LARS-WG-generated future climate series was assumed to be reliable for evaluating the impact of future climate change in the White Volta Basin.

Table 7.1: Comparison of mean annual water balances simulated in SWAT based on observed (mean over 15 years) and LARS-WG-generated (mean over 95 years) climate series

Scenario	Simulation period (Years)	Rainfall (mm)	AET ^a (mm)	Discharge (mm)	Surface runoff (mm)	Baseflow (mm)
Observed series	15	825	611	86	29	57
Generated series	95	851	576	89	35	55
Percent change		3	-6	3	15	-4

^a Actual evapotranspiration

Table 7.2: Coefficients of variation of the annual water balance simulated in SWAT based on observed (mean over 15 years) and LARS-WG-generated (mean over 95 years) climate series

Scenario	Rainfall	AET	Discharge	Surface runoff	Baseflow
Observed series	0.09	0.06	0.41	0.36	0.45
Generated series	0.08	0.06	0.27	0.31	0.25

7.5 Impacts of future climate change scenario on water resources

To evaluate the impact of future climate change on the water resources (discharge, surface runoff and baseflow), a baseline or present scenario was needed to form the basis of comparison of the future simulated water resources. Since the results of the simulated water balance based on the LARS-WG-generated climate series had a very good correlation with that of the observed series, the simulated water balance based on the generated climate series was taken to be the baseline. The mean annual and monthly future water balance were then simulated in SWAT using station-specific future climate series (mean over 95 years at 3 realizations) generated with LARS-WG and reflecting the MM5-simulated monthly changes between the present (1991-2000) and future (2030-2039) climate conditions.

The results of the simulated future water balance show important increases in the mean annual rainfall, discharge, surface runoff and baseflow (Table 7.3; Figures 7.5, 7.6 and 7.7). The rainfall had the lowest increase in the mean annual value from the present (1991-2000) 851 mm to the future (2030-2039) 904 mm, representing an increase of about 6 % in a 40-year period. The future mean annual discharge shows a far higher mean annual increase of 33 % in response to the relatively small increase in the annual rainfall. This could be attributed to the non-linear response of the discharge to

rainfall in the basin. The surface runoff had the highest future increase (37 %). The baseflow show a slightly lower increase (29 %) in the future annual value compared to the surface runoff. However, this increase is very important for the development and management of the shallow groundwater resource in the basin. The future annual rainfall, discharge, surface runoff and baseflow, all show increases in the coefficient of variation, with the future rainfall exhibiting an annual variability twice that of the present (Table 7.4).

Table 7.3: SWAT-simulated mean annual water resources for the present and future (both, mean over 95 years) climate scenarios in the White Volta River Basin (90, 856 km²)

Scenario	Simulation period	Rainfall (mm)	Discharge (mm)	Surface runoff (mm)	Baseflow (mm)
Present (baseline)	1991-2000	851	89	35	55
Future (Sce_2030-2039)	2030-2039	904	118	48	71
Percent change		6	33	37	29

Table 7.4: Coefficients of variation of the simulated mean annual present and future (both, mean over 95 years) water resources in the White Volta River Basin (90, 856 km²)

Scenario	Rainfall	Discharge	Surface runoff	Baseflow
Present (baseline)	0.08	0.27	0.31	0.25
Future (Sce_2030-2039)	0.14	0.41	0.46	0.40

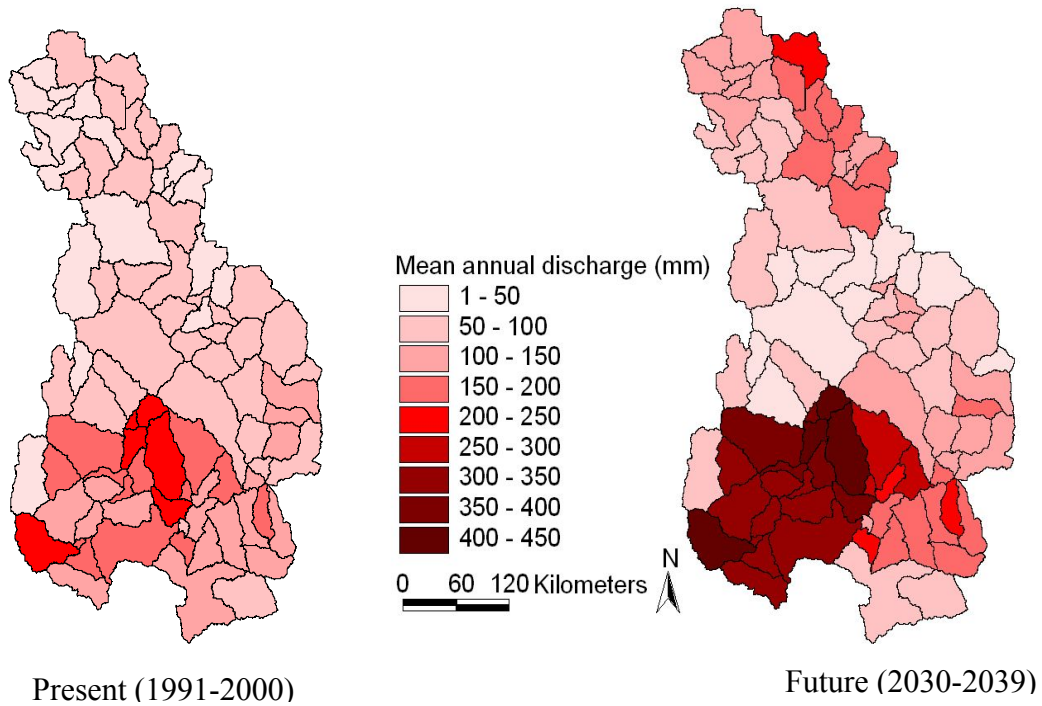


Figure 7.5 SWAT-simulated mean annual discharge under present and future climate conditions (mean over 95 years in both cases) in the White Volta River Basin

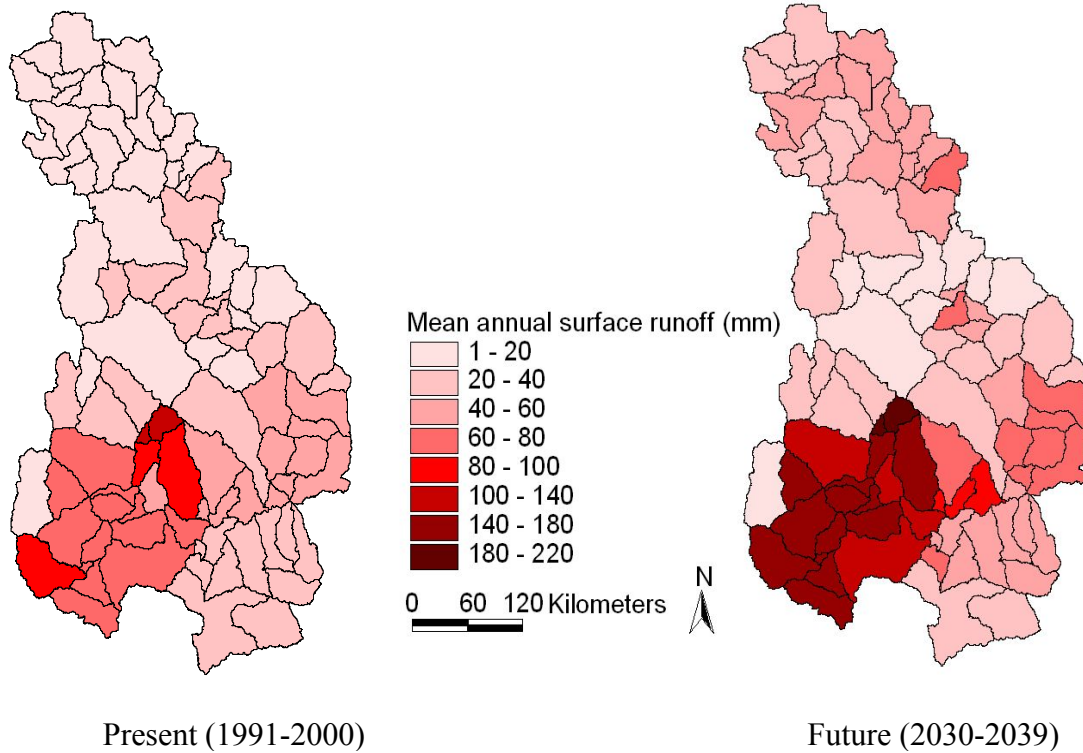


Figure 7.6 SWAT-simulated mean annual surface runoff under present and future climate conditions (mean over 95 years in both cases) in the White Volta River Basin

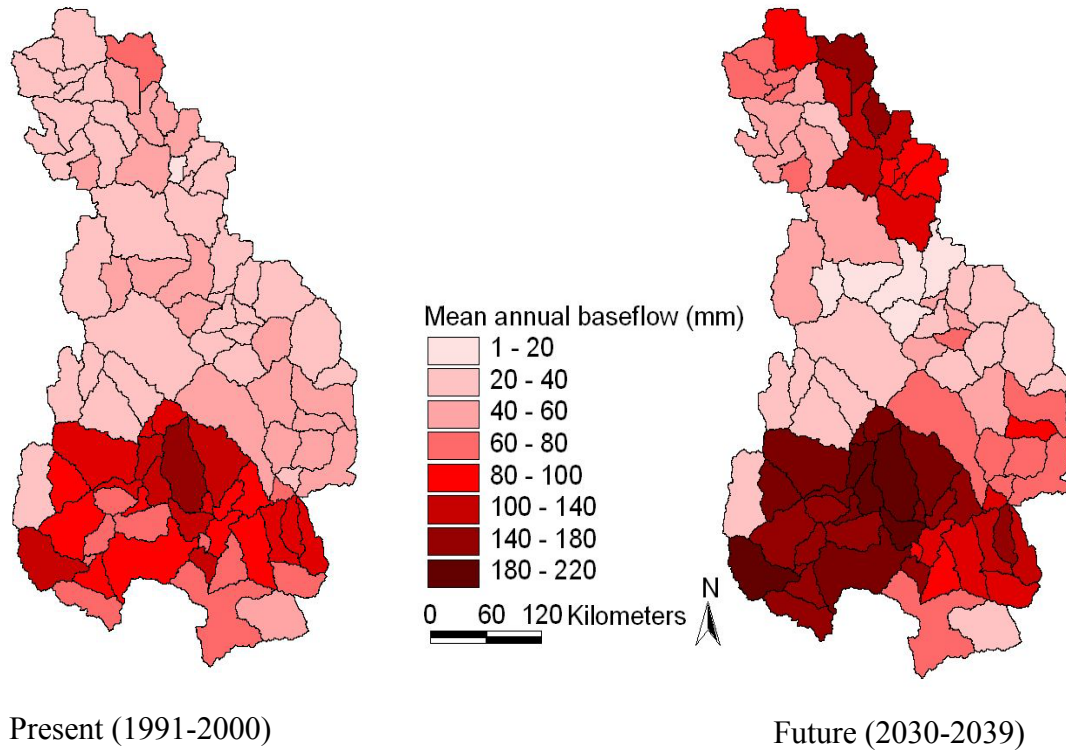


Figure 7.7 SWAT-simulated mean annual baseflow (shallow groundwater recharge) under present and future climate conditions (mean over 95 years in both cases) in the White Volta River Basin

The pattern of monthly distribution of the rainfall and discharge in the basin for the future scenario is largely identical to that of the present scenario, except for increases in the monthly quantities and a slight shift in the rainfall pattern of the future scenario (Figure 7.8). Generally, there is a reduction in the monthly rainfall amount in the first half of the rainfall season up to July, which is compensated for by increases in the second half of the season from August to December. Except for the months of September and October, the future monthly surface runoff does not differ significantly in pattern and amount from that of the present. However, there is a shift of the peak monthly rainfall from August to September (Figure 7.9). The future baseflow shows increases for all months of the year.

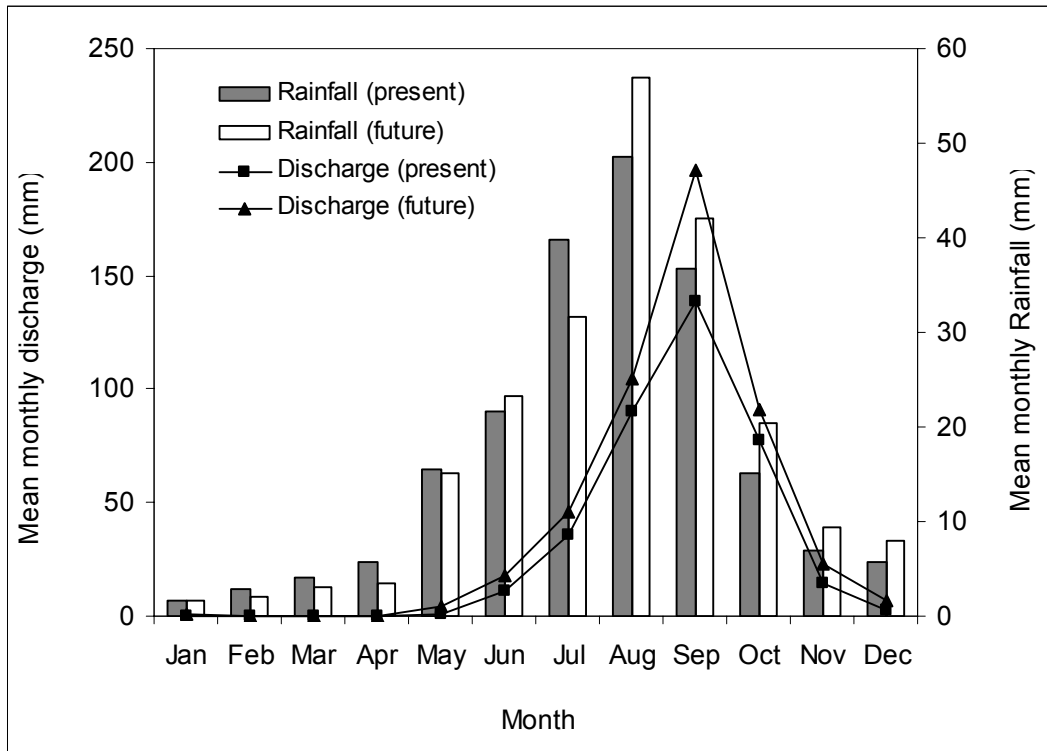


Figure 7.8 SWAT-simulated present (1991-2000) and future (2030-2039) mean monthly rainfall and discharge in the White Volta river basin.

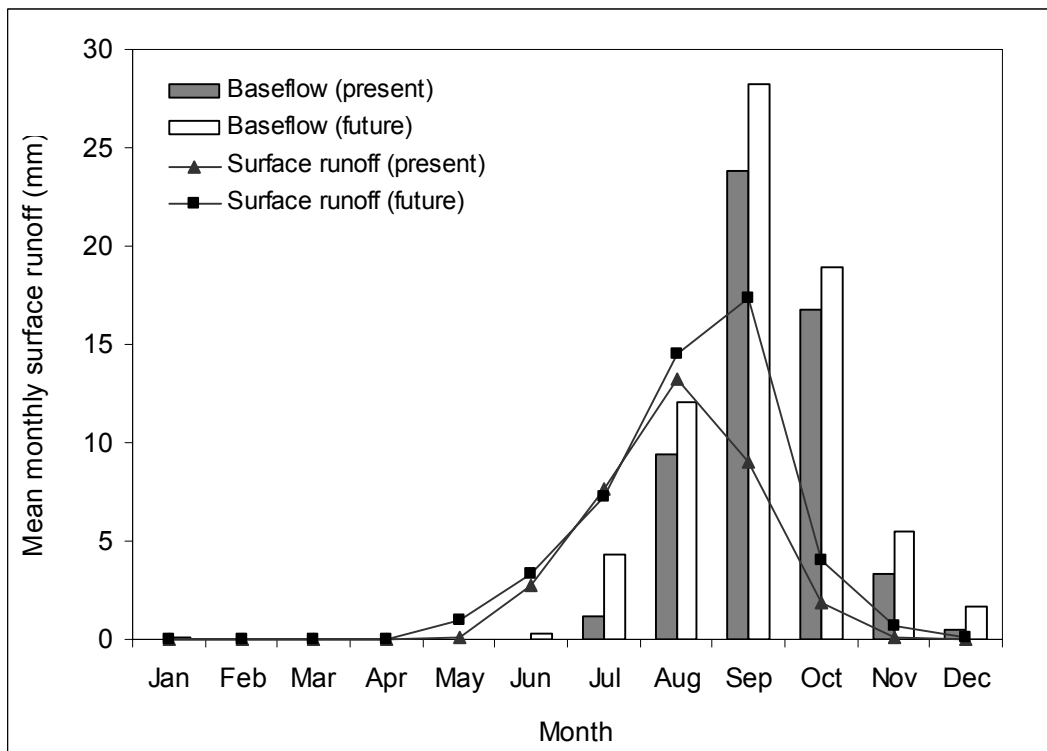


Figure 7.9 SWAT-simulated present (1986-1999) and future (2030-2039) mean monthly surface runoff and baseflow in the White Volta river basin.

7.6 Comparison of study results with previous studies

The marked increase in the future simulated annual discharge obtained in this study for the White Volta Basin is similar to what has been obtained for the entire Volta Basin in the ADAPT project (Andah et al., 2003). The ADAPT project investigated the impact of climate change on the hydrology of the Volta basin using the Water Evaluation And Planning System (WEAP) to simulate future water resources based on the A2 and B2 SRE forcing scenarios. The A2 and B2 scenarios were developed for two future time slices, i.e., 2020-2039 and 2070-2099, using the GCM HADCM3 and were statistically downscaled to have the same statistics as the historic (1961-1990) climate series in the basin. Climate data (precipitation and temperature) for the period 1961-1990 were obtained from the East Anglia Climate Research Unit (CRU) and were used for calibrating the HADCM3.

Results of the HADCM3 projected future climate series for the Volta basin suggest increases in both precipitation and temperature in the two time slices under the two SRE scenarios (Table 7.5). Slightly higher increases in precipitation, 8 and 10 % for the scenarios A2 and B2, respectively, are projected for the time slice 2020-2039, compared to the 6 and 9 % increases for the 2070-2099 time slice. In the case of the temperature, the reverse is true.

Table 7.5: Climate change projections of HADCM3 and statistics, based on the SRE A2 and B2 scenarios (Modified from Andah et al., 2003)

Scenario	Period	Rainfall (mm)			Temperature (°C)		
		Mean	Standard deviation	Coefficient of variation	Mean	Standard deviation	Coefficient of variation
SRE A2	1961-1990	1079	115	0.11	27.3	0.5	0.02
	2020-2039	1161	105	0.09	28.5	0.5	0.02
	2070-2099	1147	123	0.11	31.8	0.8	0.03
SRE B2	1961-1990	1079	117	0.11	27.3	0.5	0.02
	2020-2039	1181	144	0.12	28.4	0.5	0.02
	2070-2099	1173	118	0.10	30.4	0.5	0.02

The results of the ADAPT project show an important increase in the discharge for all the future climate change scenarios simulated with the WEAP (Table 7.6). The A2 and B2 scenarios of the time slice 2020-2039 are of particular interest because of the

similarity they have with this study by way of their time slice and the magnitude of increase in the future discharges. The ADAPT project obtained increases of 27 and 34 % in the mean annual discharge for the A2 and B2 scenarios, respectively, for 2020-2039 as a result of the relatively lower increases in rainfall. This was attributed to the non-linear relationship between the discharge and rainfall in the Volta basin (Andah et al., 2003).

Table 7.6: Mean annual inflow into Lake Volta (taken to be the outlet of the Volta Basin) together with standard deviation and coefficient of variation of the respective simulation periods for Hadley A2 and B2 (Modified from Andah et al., 2003)

Scenario	Time slice	Mean discharge (km ³)	Percent change (%)	Standard deviation	Coefficient of variation
Historical	1961-1990	32.8 (82)	-	17.1	0.52
HA2	2020-2039	41.6 (104)	27	14.0	0.34
HB2	2020-2039	43.8 (110)	34	15.4	0.35
HA2	2070-2099	37.2 (93)	13	19.9	0.54
HB2	2070-2099	44.0 (110)	34	17.6	0.40

NB: Figures in brackets are discharge in mm; the Volta Basin covers 400,000 km²

Another study of interest for comparison purposes is the climate change impact studies done by Jung (2006) in the Volta Basin. Jung used future climate series of the IS92a climate change scenario simulated in ECHAM4 and downscaled with MM5. The same scenario was used for the White Volta basin in this study. The point of departure, however, is that Jung used the MM5 future climate series (2030-2039) directly in the hydrological model (WaSiM) for the impact simulation, whereas in this study the MM5 data were used to drive a stochastic weather generator to produce station specific data with identical statistics as that of the observed.

For the future simulated discharge, Jung (2006) obtained an increase of nearly 5 % over that of the baseline (1991-2000) for the entire Volta Basin. This increase is much smaller compared to the 27 and 34 % increases for the SRE A2 and B2 scenarios obtained by Andah et al. (2003) for the same Volta Basin. Obviously, the two studies differ greatly in terms of the GCM and the climate scenarios selected as well as the downscaling method used and may be responsible for the differences in the results.

Similar to the findings of this study, the results of Jung (2006) for Nawuni in the White Volta Basin show increases in all the water resources (rainfall, discharge, surface runoff, and baseflow) (Table 7.7). The surface runoff has the highest increases as found in this study, although much higher increase was obtained in the study by Jung. The increase in the annual discharge obtained in this study is twice the value obtained by Jung. The baseflow is also twice. Possible reasons for the deviation in the two study results could be due to differences in (i) the way the future climate series were processed before used, (ii) hydrological models used and (iii) model calibration periods.

Table 7.7: Comparison of the mean annual increases (%) of selected water balance variables, between the baseline simulation (1991-2000) and the future (2030-2039) simulation, at Nawuni in the White Volta Basin

Source	Rainfall	Discharge	Surface runoff	Baseflow
Study	6	33	37	29
Jung, 2006	5	15	57	13

8 CONCLUSIONS AND RECOMMENDATIONS

8.1 Introduction

The White Volta Basin is one of the major sub-basins of the Volta River Basin of West Africa. On the whole, the basin has enough water resources to meet current demands. However, there are many challenges including high spatial and intra-annual variability in rainfall, global climate change, deforestation, land degradation, and high population growth rate. These challenges put immense pressure on the water resources. The basin experiences a prolonged dry season of 7 months when many rivers and streams dry up. As a result, surface water supplies are unreliable and insufficient to meet the water demands for socio-economic development in many places in the basin, thereby making groundwater sources the preferred and most cost-effective means of supplying water to the largely rural and dispersed population in the basin.

Exploitation of groundwater in the White Volta Basin has increased substantially in recent times and can lead to depletion and degradation if not properly managed, particularly in areas where the resource could be affected by over-exploitation, contamination and climate change. A basic prerequisite for efficient and sustainable management of groundwater is the understanding of the recharge process. This study estimates the amount and spatial distribution of groundwater recharge at different spatial scales in the White Volta Basin using the chloride mass balance, water table fluctuation, and hydrological modeling techniques. In addition, the study evaluates the impact of future climate change on the shallow groundwater recharge. The conclusions and recommendations of this study are summarized below.

8.2 Chloride mass balance method for estimating groundwater recharge

The chloride mass balance (CMB) method is widely used for estimating recharge in arid and semi-arid regions. In this study, the method was applied in the north-eastern part of Ghana (Upper East Region of Ghana) within the White Volta Basin in 2006. The results show that recharge to the groundwater in the Upper East Region ranged from 3 to 19 % of the long-term mean annual rainfall and averaged 8 %. Weaknesses of the CMB method as applied in this study include the non-existence of data on dry atmospheric deposition of chloride and direct runoff, as well as long-term data on total chloride deposition.

8.3 Water table fluctuation method for estimating groundwater recharge

The water table fluctuation (WTF) method requires data of specific yield and changes in the water table over time. It is best suited for areas with distinct periods of recharge. The use of the method is not restricted by the presence of preferential flow paths at a study site. The WTF method was applied in the south of the White Volta Basin (White Volta Basin of Ghana) in 2006 and 2007 to quantify groundwater recharge and to analyze the fluctuations in the water table. Findings from water table monitoring show high annual and spatial variations in the water table rise, with a range of 1240-5000 mm in 2006, and 1600-6800 mm in 2007. For a mean increase of 50 % in rainfall between 2006 and 2007, a mean increase of 35 % was obtained for the water table rise. Findings from the recharge estimation for the two study years show that the mean groundwater recharge in the White Volta Basin is 8 % and 7 % of the mean annual rainfall for 2006 and 2007, respectively.

The main limitation of this method is the difficulty in obtaining specific yield values that are representative of the aquifer materials in the study area. Besides the specific yield limitation, there are only a few wells for monitoring water table data, which affects the reliability of the recharge estimates.

8.4 Hydrological modeling and recharge estimation with SWAT

The Soil and Water Assessment Tool (SWAT) model has been calibrated (1986-1991) and validated (1992-1999) for the White Volta Basin at Nawuni. A pre-calibration impact analysis of the number of sub-basin and hydrologic response units (HRUs) on discharge, generally shows that the higher the number of sub-basins and HRUs, the higher the number of rain gages and land-use classes used by the model for simulating the discharge. Consequently, the simulated discharge is more accurate, however, the effect an increased number of sub-basins and HRUs has upon the accuracy of the discharge is limited. In a basin like the White Volta, due to a limited amount of diversity in landuse types, the potential for improved accuracy due to an increase in the number of HRUs is not significant.

The calibration and validation results show that the SWAT model performed very well in reproducing the annual, monthly and daily discharge, and the annual surface runoff and baseflow. The monthly calibration shows the best agreement between

simulated and observed discharge with coefficient of determination (R^2) of 0.93 (annual- $R^2=0.85$; daily- $R^2=0.77$), and Nash-Sutcliffe model efficiency (NSE) of 0.93 (annual-NSE=0.83; daily-NSE=0.68). Also, there is a very good correlation between the simulated and observed annual surface runoff ($R^2=0.84$; NSE=0.82) and baseflow ($R^2=0.88$ and NSE=0.83). The validation results show equally good agreement between the simulated and observed discharge ($R^2>0.80$; NSE>0.78), annual surface runoff ($R^2=0.91$; NSE=0.71), and annual baseflow ($R^2=0.90$; NSE=0.77). Generally, SWAT overestimated the high flows and underestimated the low flows. The underestimation of the low flows could be due to more than one aquifer contributing to baseflow in the basin, a situation not handled in SWAT at present.

The simulated water balance in SWAT shows that about 11 % of the annual precipitation in the White Volta Basin becomes discharge, which consists of 4 % surface runoff and 7 % baseflow. In SWAT, the baseflow is the shallow groundwater recharge, which is 7 % of the annual rainfall. Compared to rainfall, actual evapotranspiration, and surface runoff, the shallow groundwater recharge experiences the highest annual variability.

8.5 Impacts of future climate change on water resources

The climate series of the regional climate model MM5, which is downscaled from ECHAM4 simulation of the IS92a scenario, is found to be unsuitable for direct use with SWAT for evaluating climate change impacts on the water resources in the study area. Using Ouahiagouya weather station as an example, it is shown that the MM5 overestimated the mean annual precipitation by about 22 %; the highest monthly rainfall shifted from August to July; the frequency statistics of the daily rainfall are not consistent with the observed; and the MM5 rainfall series are the mean of gridded rainfall, and not station-specific as required by the SWAT model. The weather generator LARS-WG was, therefore, used to generate station-specific mean daily climate series with the same statistics as for the observed data and reflected the MM5 forecasted changes in the monthly rainfall.

Comparison of the SWAT-simulated water balance using the recent time (1991-2000) LARS-WG-generated climate series and the observed reveals a high correlation between the two, except for a few over- and underestimations. The

frequency statistic of the daily rainfall events and the pattern of monthly distribution of the water balance variables (rainfall, actual evapotranspiration, discharge, surface runoff and baseflow) are consistent with the observed, with only a slight variation in the mean annual values. Using the simulated water balance based on the generated climate series in the recent time period as the basis for comparison, the results of the simulated future (2030-2039) water balance show important increases in the rainfall, discharge, surface runoff, and the baseflow.

8.6 Final conclusions

The chloride mass balance, water table fluctuation and the hydrological model SWAT were used in this study to estimate the amount and spatial distribution of the groundwater recharge at 3 different spatial scales in the White Volta Basin. Findings from the three methods show that annual recharge to the groundwater in the basin is about 7 % of the annual rainfall. This figure is expected to increase by about 33 % in the future (2030-2039) as a result of future climate change in the basin.

8.7 Recommendations

Accurate estimation of the groundwater recharge is very important for sustainable planning of the groundwater resource. The accuracy of the groundwater recharge estimation in the White Volta Basin could be improved through further research.

The chloride mass balance is a relatively easy method for estimating the groundwater recharge and provides long-term recharge information. However, the method requires long-term data of wet and dry atmospheric deposition, rainfall, surface runoff and chloride concentration in groundwater. At present, data on dry atmospheric deposition and long-term data on wet deposition are non-existent in the study area. A continuous monitoring of chloride deposition is needed to provide long-term data for a more reliable estimation of the long-term recharge. Also, the number of wells from which groundwater samples were taken and analyzed for use with the CMB method can greatly influence the recharge estimate. It is, therefore, recommended to sample a more representative number of wells for chloride analysis in order to have recharge estimates that are more representative and reliable.

To a large extent, recharge estimates from the water table fluctuation method depend on the specific yield values used in calculating them. Currently, there are no data on the exact specific yield of the aquifer materials in the study area. Available data on well-pumping tests are not useful for determining specific yield values, because the test periods are too short. Selecting specific yield values from literature can result in wide ranges of estimated recharge, which may not be good for sustainable planning of the groundwater resource. Further research is needed to determine the exact specific yield values of aquifer materials in the entire Volta Basin. Another way of dealing with this issue is to make the specific yield one of the mandatory aquifer parameters to be estimated during pumping tests on wells constructed in the basin.

Similar to any other hydrological model, the quality of the output of the SWAT model is as good as the quality of the input climate data, e.g., rainfall and temperature, and the quality of the discharge data used for the calibration and validation of the model. Climate records from some of the weather stations in the White Volta Basin have missing data, which were filled by the weather generator in SWAT. Although there are many river gages in the basin, discharge records of most of the stations are unreliable and data is frequently missing. A few sub-basins of interest for studying water resources on a small scale should be selected and monitored continuously to provide high-quality hydrological data such as discharge for large-scale hydrological studies that support decision making on water resources in the basin. Due to the uncertainties associated with climate forecast and downscaling, it is recommended to use climate model ensembles and multiple future climate scenarios, e.g., best- and worst-case scenarios, in hydrological impact studies in order to understand the range of impacts that can be expected.

REFERENCE

- Abraham LZ, Roehrig J, Chekol DA (2007) Calibration and validation of SWAT Hydrologic model for Meki Watershed, Ethiopia. Tropentag 2007. University of Kassel-Witzenhausen and University of Göttingen. October 9-11, 2007
- Acheampong SY (1996) Geochemical evolution of the shallow groundwater system in the Southern Voltaian Sedimentary Basin of Ghana. PhD dissertation, University of Nevada, Reno
- Adjei-Gyapong T, Asiamah RD (2000) The interim Ghana soil classification system and its relation with the World Reference Base for Soil Resources. In: FAO, 2000. Quatorzième Réunion du Sous-Comité ouest et centre africain de corrélation des sols pour la mise en valeur des terres. ISBN 92-5-204803-0
- Afinowicz JD, Munster CL, Wilcox BP (2005) Modeling effects of brush management on the rangeland water budget: Edwards Plateau, Texas. *J. American Water Resour. Assoc.* 41 (1): 181-193
- Agyekum WA, Darko PK, Dapaah-Siakwan S (2006) Annual summary of groundwater monitoring in the White Volta River Basin. Water Research Institute. Accra, Ghana
- Allen RG, Pereira LS, Raes D, Smith M (1998) Crop Evapotranspiration, Guideline for Computing Crop Water Requirements. FAO Irrigation and Drainage Paper 56. FAO Rome, Italy
- Amani A (2001) Assessment of precipitation and resources variability across the Sahelian region. In: Gash JHC, Odada EO, Oyebande L and Schulz RE (eds) Report of the International Workshop on Africa's Water Resources. Nairobi, 26-30 October 1999 (BAHC)
- Amisigo BA (1996) Modelling riverflow in the Volta Basin of West Africa: A data-driven framework. PhD Thesis. Ecology and Development Series No. 34. ZEF Bonn. Cuvillier Verlag, Göttingen
- Amuzu AT (1975) A survey of the water quality of the River Densu. WRRRI Technical Report. Accra, Ghana
- Andah AI (1993) Groundwater Utilization for small-scale Irrigation in the Accra Plains: Kponkpo and Ablekuma pilot schemes. Water Resources Research Institute (C.S.I.R). Accra, Ghana
- Andah EI, van de Giesen N, Biney CA (2003) Water, climate, food, and environment in the Volta Basin. Adaptation strategies to changing environments. Contribution to the ADAPT project
<http://www.weap21.org/downloads/ADAPTVolta.pdf>
- Andreini M, van de Giesen NC, van Edig A, Fosu M, Andah W (2000) Volta basin water balance. ZEF discussion papers on development policy. No. 21. Bonn, Germany
- Apambire WB (1996) Groundwater geochemistry and the genesis and distribution of groundwater fluoride in the Bolgatanga and Bongo districts, Ghana. MSc Thesis. Carleton University, Ottawa, Ontario, Canada
- Arabi M, Govindaraju RS, Hantush MM (2006) Cost-effective allocation of watershed management practices using a genetic algorithm. *Water Resour. Res.* 42.W10429, doi:10.1029/2006WR004931
- Arnell NW (1999) Climate change and global water resources, *Glob. Environ. Change - Human Policy Dimens.*, 9, S31-S49

- Arnell NW, Liu C (2001) Hydrology and Water Resources. In: McCarthy JJ, Osvaldo FC, Neil AL, David JD and Kasey SW (eds) *Climate Change 2001: Impacts, Adaptation and Vulnerability*. Cambridge, Royaume-Uni: Cambridge University Press for the Intergovernmental Panel on Climate Change
- Arnold JG, Allen PM (1999) Automated methods for estimating baseflow and ground water recharge from streamflow records. *Journal of the American Water Resources Association* 35(2): 411-424
- Arnold JG, Allen, PM (1996) Estimating hydrological budgets for three Illinois watersheds. *J. Hydrol.*, 176: 57-77
- Arnold JG, Allen PM, Bernhardt G (1993) A comprehensive surface groundwater flow model. *J. Hydrol.* 142:47-69
- Arnold J, Allen PM, Muttiah R, Bernhardt G (1995) Automated base flow separation and recession analysis technique. *Groundwater*, Vol. 33, No. 6. November-December
- Arnold JG, Muttiah RS, Srinivasan R, Allen PM (2000) Regional estimation of base flow and groundwater recharge in the Upper Mississippi river basin. *J. Hydrology* 227:21-40
- Arnold JG, Srinivasan R, Muttiah RS, Allen PM (1999) Continental scale simulation of the hydrologic balance. *Journal of American Water Resour. Assoc.* 35 (5), 1037-1051
- Ayeneu T, Alemayehu T, Kebede S (2006) *Environmental Isotopes and Hydrochemical Studies as Applied to Water Resources Assessment in Central and Southern Afar and Adjacent Highlands*. Ethiopian Science and Technology Agency. Unpublished Report of the International Atomic Energy Agency Project (ETH/8/008). Addis Ababa, Ethiopia. 128pp
- Bannermann RR, Ayibotele NB (1984) Some critical issues with monitoring crystalline rock aquifers for groundwater management in rural areas, *Challenges in African Hydrology and Water Resources*. IAHS Publ. No. 144, 47-56, IAHS Press, Wallingford
- Barry B, Obuobie E, Andreini M, Andah W and Pluquet M (2005) *The Volta river basin. Comprehensive assessment of water management in agriculture. Comparative study of river basin development and management*. Draft http://www.iwmi.cgiar.org/assessment/research_projects/river_basin_development_and_management/projects_locations/volta_river_burkina_faso_ghana.htm.
- Beekman, HE, Gieske A, Selaolo, ET (1996) GRES: Groundwater recharge studies in Botswana 1987-1996. *Botswana. J. of Earth Sci.*, Vol. III: 1-17
- Beekman HE, and Xu Y (2003) Review of Groundwater Recharge Estimation in Arid and Semi-Arid Southern Africa. In: Xu Y and Beekman HE (eds) *Groundwater recharge estimation in Southern Africa*. UNESCO IHP Series No. 64, UNESCO Paris. ISBN 92-9220-000-3
- Benneh G, Agyepong GT, Allotey JA (1990) *Land degradation in Ghana*. Food production and rural development division. Commonwealth Secretariat, Marlborough House. Pall Mall. London
- Bougairé F (2006) *Processus de creation de l'autorite du bassin de la Volta*. Presentation at the 4th World Water Forum. Mexico City, Mexico, 18th March, 2006. <http://www.inbo-news.org/wwf-4/ft2-29/comms/Burkina-faso.pdf>

- Bourouai F, Grizzetti B, Granlund K, Rekolainen S, Bidoglio G, (2004) Impact of climate change on the water cycled and nutrient losses in a Finnish catchment. *Clim. Change* 66(1-2): 109-126
- Bourouai F, Benabdallah S, Jrad A, Bidoglio G (2005) Application of the SWAT model on the Medjerda River basin (Tunisia). *Phys. Chem. Earth* 30(8-10): 497-507
- Bredenkamp DB, Botha L T, van Tonder GJ, van Rensburg HJ (1995) Manual on Quantitative Estimation of Groundwater Recharge and Aquifer Storativity. Report TT 73/95. Water Research Commission, Pretoria. 419pp
- Busche H, Hiepe C, Diekkrüger B (2005) Modelling the effects of land use and climate change on hydrology and soil erosion in a sub-humid African Catchment. *Proceedings of the 3rd International SWAT Conference 2005*, pp434-443
- Chand R, Hodlur GK, Prakash MR, Mondal NC, Singh VS (2005) Reliable natural recharge estimates in granitic terrain. *Current science*, 88 (5)
- Chekol DA (2006) Modelling of Hydrology and Soil Erosion of Upper Awash River Basin. PhD Thesis, University of Bonn: 233pp
- Christiaens K, Feyen J (2002) Use of sensitivity and uncertainty measures in distributed hydrological modeling with an application to the MIKE SHE model. *Water Resources Research*, 38(9), doi: 10.1029/2001WR000478
- Cimmery V (2007) User guide for SAGA
<http://switch.dl.sourceforge.net/sourceforge/saga-is/SAGA>
- Codjoe SNA (2004) Population and land use/cover dynamics in the Volta River Basin of Ghana, 1960-2010. PhD Thesis. Ecology and Development Series, No. 15. Cuvillier Verlag Göttingen. 184pp
- Conan C, de Marsily G, Bourouai F, Bidoglio G (2003) A long-term hydrological modelling of the upper Guadiana river basin (Spain). *Phys. Chem. Earth* 28(4-5): 193-200
- Crosbie RS, Binning P, Kalma JD (2005) A time series approach to inferring groundwater recharge using the water table fluctuation method. *Water Resources Research* 41 (1), 1–9
- Darko PK, Krasny J (2003) Regional transmissivity distribution and groundwater potential in hard rocks of Ghana, in Krasny, Hrkal, Bruthans (Edts): *Groundwater in fractured rocks*, 45-46, Prag
- Dapaah-Siakwan S, Gyau-Boakye P (2000) Hydrogeologic Framework and Borehole Yields in Ghana, *Hydrogeology Journal*, 8, 405-416
- Delin GN, Healy RW, Lorenz DL, Nimmo JR (2006) Comparison of local- to regional-scale estimates of ground-water recharge in Minnesota, USA. *Journal of Hydrology*, Volume 334, Issues 1-2, 20 February 2007, Pages 231-249
- DGH (Direction Générale des l'Hydraulique) (2001) "Etat des Lieux des Ressources en Eau du Burkina Faso et de leur Cadre de Gestion." Ouagadougou: Ministère de l'Environnement et de l'Eau
- Di luzio M, Srinivasan R, Arnold JG, Neitsch SL (2002) ArcView interface for swat2000 user's guide, Grassland, soil and water research laboratory – Agricultural Research Service, Texas, US
- Duan Q, Sorooshian S, Gupta VK (1992) Effective and efficient global optimisation for conceptual rainfall-runoff models, *Water Resour. Res.* 28(4): 1015-1031
- Edmunds WM, Fellmann E, Goni IB, Prudhomme C (2002) Spatial and temporal distribution of groundwater recharge in northern Nigeria, *Hydrogeology Journal*, 10, 205-215

- El-Nasr A, Arnold JG, Feyen J, Berlamont J (2005) Modelling the hydrology of a catchment using a distributed and a semi-distributed model. *Hydrol. Process.* 19(3): 573-587
- FAO (2003) Aquastat: <ftp://ftp.fao.org/agl/aglw/aquastat/aquatat2003.xls>
- FAO (1995) Digital soil map of the world and derived soil properties (CDROM) food and Agriculture Organization of the United Nations. FAO
- FAO (1997) Irrigation potential in Africa: A basin approach. FAO Land and Water Bulletin 4
- FAO-UNESCO (1974) FAO-UNESCO soil map of the World. Vol. I Legend. UNESCO, Paris, 59 pp
- FAO-UNESCO (1994) Soil map of the world - Revised Legend. Technical paper 20. Roma: FAO; Wageningen, the Netherlands: ISRIC
- Foster SSD (1988) Quantification of groundwater recharge in arid regions: a practical view for resource development and management. In: Simmers I (Ed) Estimation of natural groundwater recharge. Reidel publishing company, Dordrecht, The Netherlands pp323-338
- Freeze RA, Cherry JA (1979) Groundwater. Prentice Hall, Englewood, New Jersey.
- Friesen J, Andreini M, Andah W, Amisigo B, van de Giesen N (2005) Storage capacity and long-term water balance of the Volta Basin, West Africa. IAHS Publication no. 296: 138-145
- Gassman PW, Reyes MR, Green CH, Arnold JG (2007) The Soil and Water Assessment Tool: Historical development, applications, and future research directions, *Trans. ASABE*, 50(4), 1211-1250
- Gee GW, Hillel D (1988) Groundwater recharge in arid regions: review and critique of estimation methods. *Hydrol. Process.* Vol. 2:255-266
- Gee GW, Zhang ZF, Tyler SW, Albright WH, Singleton MJ (2004) Chloride-mass-balance for predicting increased recharge after land-use change. University of California, University of California
<http://repositories.cdlib.org/lbnl/LBNL-55584>
- Geirnaert W, Groen M, van der Sommen JJ (1984) Isotopes studies as a final stage in groundwater investigations on African shield. Challenges in African hydrology and water resources. IAH publication. 144
- Ghana Statistical Service (2002) 2000 Population and housing census. Summary report on final results. Medialite Co. Ltd. Accra
- Gonfiantini R, Frölich K, Araguás-Araguás L, Rozanski K (1998) Isotopes in groundwater hydrology. p. 203–246. In: C. Kendall and J. McDonnell (ed.) Isotope tracers in catchment hydrology. Elsevier Sci., Amsterdam
- Gieske ASM (1992) Dynamics of groundwater recharge: a case study in semi-arid eastern Botswana. PhD Thesis, Vrije Universiteit, Amsterdam, 289 pp
- Gikas GD, Yiannakopoulou T, Tsihrintzis VA (2005) Modeling of nonpoint-source pollution in a Mediterranean drainage basin. *Environ. Model. Assess.* 11(3): 219-233
- Githui FW (2007) Assessment of impacts of climate change on runoff: River Nzoia catchment, Kenya. Book of abstracts, 4th International SWAT conference, UNESCO-IHE Institute for Water Education, Delft, The Netherlands. July 4-6, 2007

- Gosain AK, Rao S, Srinivasan R, Reddy NG (2005) Return-flow assessment for irrigation command in the Palleru River basin using SWAT model. *Hydrol. Process.* 19(3): 673-682
- Govender M, Everson CS (2005) Modelling streamflow from two small South African experimental catchments using the SWAT model. *Hydrological Processes*, 19: 683-692
- Grell GA, Dudhia J, Stauffer DR (1995) A Description of the Fifth-Generation Penn State/NCAR Mesoscale Model (MM5); NCAR technical note; NCAR/TN-398+STR
- Grizzetti B, Bouraoui F, de Marsily G (2005) Modeling nitrogen pressure in river basins: A comparison between a statistical approach and the physically-based SWAT model. *Physics and Chemistry of the Earth* 30(8-10): 508-517
- Groen J, Schuchmann JB, Geirnaert W (1988) The occurrence of high nitrate concentration in groundwater in villages in northwestern Burkina Faso. *Journal of African Earth Sciences*, 7, 999-1009
- Gupta BL, Gupta A (1999) *Engineering hydrology*. Standard publishers distributors. Delhi. 380pp
- Gyau-Boakye P (2001) Sources of Rural Water Supply in Ghana, *Water International*, 26, 1, 96-104
- Gyau-Boakye P, Tumbulto JW (2006) Comparison of rainfall and runoff in the humid south-western and the semiarid northern savannah zone in Ghana. *African Journal of Science and Technology. Science and Engineering Series Vol. 7, No. 1*, pp. 64-72
- Hall DW, Risser DW (1993) Effects of agricultural nutrient management on nitrogen fate and transport in Lancaster County, Pennsylvania. *Water Resource Bulletin* 29, 55-76
- Hao FH, Zhang XS, Yang ZF (2004) A distributed nonpoint-source pollution model: Calibration and validation in the Yellow River basin. *J. Environ. Sci.* 16(4): 646-650
- HAPS (2006) Hydrological assessment of the Northern Regions of Ghana: A bibliographical review of selected papers. CIDA, WRC, SNC-LAVALIN International
- Hargreaves GL, Hargreaves GH, Riley JP (1985) Agricultural benefits for Senegal River Basin. *J. Irrig. And Drain. Engr.* 111(2):113-124
- Hargreaves GH, ZA Samani (1985) Reference crop evapotranspiration from temperature. *Applied Engineering in Agriculture* 1:96-99
- Healy RW, Cook PG (2002) Using groundwater levels to estimate recharge. *Hydrogeol. J.* 10:91-109
- Heppner CS, Nimmo JR (2005) A computer program for predicting recharge with a master recession curve: US Geological Survey Scientific Investigations Report 2005-5172, 8p
- Hiepe C, Diekkrüger B (2007) Modelling soil erosion in a sub-humid tropical environment at the regional scale considering land use and climate change. Book of abstracts, 4th International SWAT conference, UNESCO-IHE Institute for Water Education, Delft, The Netherlands. July 4-6, 2007
- Holvoet K, van Griensven A, Seuntjens P, Vanrolleghem PA (2005) Sensitivity analysis for hydrology and pesticide supply towards the river in SWAT. *Phys. Chem. Earth* 30(8-10): 518-526

- Houston, JFT (1982) Rainfall and recharge to dolomite aquifer in a semi-arid climate at Kabwe, Zambia. *J. Hydrol.* 59, pp173–187
- Huisman JA, Breuer L, Frede HG (2004) Sensitivity of simulated hydrological fluxes towards changes in soil properties in response to land use change. *Phys. Chem. Earth* 29(11-12): 749-758
- IPCC (2001) *Climate Change 2001: The scientific basis*. Eds. J. T. Houghton, Y. Ding, M. Nogua, D. Griggs, P. Vander Linden, K. Maskell, Cambridge Univ. Press., Cambridge, U.K
- Jha M, Gassman PW, Secchi S, Arnold J (2006) Upper Mississippi River Basin modelling system part 2: Baseline simulation results. In: *Coastal Hydrology and Processes* (Eds. V.P. Singh and Y.J. Xu), pp.117-126. Water Resources Publications, Highland Ranch, CO
- Johnson AI (1967) Specific yield compilation of specific yields for various materials. U.S. Geological survey. Water-Supply paper 1662-D, 74pp
- Johnston CD (1987) Preferred water flow and localized recharge in a variable regolith. *J. Hydrol.* 94, 129 -142
- Joubert AM, Hewitson BC (1997) Simulating present and future climates of southern Africa using general circulation models. *Prog Phys Geog* 21:51–78
- Jung G (2006) *Regional Climate Change and the Impact on Hydrology in the Volta Basin of West Africa*. Doctoral thesis. IMK-IFU. Garmisch-Partenkirchen
- Kang MS, Park SW, Lee JJ, Yoo KH (2006) Applying SWAT for TMDL programs to a small watershed containing rice paddy fields. *Agric. Water Mgmt.* 79(1): 72-92
- Key RM (1992) An introduction to the crystalline basement of Africa. In: *The hydrogeology of crystalline basement aquifers in Africa*, EP Wright, WG Burgess. Geological Society Special Publication 66: 29-57
- Kirchner R, van Tonder GJ, Lukas E (1991) Exploitation potential of Karoo aquifers. WRC Project no. 170/1/91. Water Research Commission, Pretoria
- Kortatsi BK (1994) Groundwater utilization in Ghana, in: *Future Groundwater Resources at Risk (Proceedings of the Helsinki Conference)* IAHS Publ. No. 222, 149-156, IAHS Press, Wallingford
- Kunstmann H, Jung G (2003) Investigation of feedback mechanisms between soil moisture, land use and precipitation in West Africa; IAHS publications no. 280; *Water Resources Systems - Water Availability and Global Change*
- Landmann T, Herty C, Dech S, Schmidt M, Vlek PLG (2007) Land cover change analysis within the GLOWA Volta Basin in West Africa using 30-meter Landsat data snapshots, in: *Proceedings of the Geoscience and Remote Sensing Symposium, 2007. IGARSS 2007. IEEE International Conference, July 31 2007-Aug. 4 2007. Page(s):c24-c26, Barcelona, Spain*
- Lane LJ (1983) Transmission Losses. P.19-1–19-21. In *Soil Conservation Service. National engineering handbook, section 4: hydrology*. U.S. Government Printing Office, Washington, D.C
- Larsen F, Owen R, Dahlin T, Mangeya P (2001) A preliminary analysis of the groundwater recharge to the Karoo formations, mid-Zambezi basin, Zimbabwe. 2nd WARFSA Symposium: IWRM: Theory, Practice Cases; Cape Town, 30-31 Oct. 2001
- Larsson I (1984) Groundwater in hard rocks. UNESCO, Project 8.6 of the Hydrological Programme, 228 p

- Le Barbé L, Lebel T (1997) Rainfall climatology of the HAPEX-Sahel region during the years 1950-1990. *J. Hydrol.* Vol. 188-189:43–73
- Lenhart T, Eckhardt K, Fohrer N, Frede HG (2002) Comparison of two different approaches of sensitivity analysis, *Phys. Chem. Earth*, 27, p645–654
- Lerner DN (1997) Groundwater recharge. In: Saether OM & de Caritat P (eds) *Geochemical processes, weathering and groundwater recharge in catchments*. AA Balkema, Rotterdam. p109-150
- Lerner DN (2003) Surface Water - Groundwater Interactions in the Context of Groundwater Resources. In: Xu Y and Beekman HE (eds) *Groundwater recharge estimation in Southern Africa*. UNESCO IHP Series No. 64, UNESCO Paris
- Lerner DN, Issar AS, Simmers I (1990) *Groundwater recharge. A guide to understanding and estimating natural recharge*. International contributions to hydrogeology. Verlag Heinz Heise. 8
- Lerner DN, Yang Y, Barrett MH, Tellam JH (1999) Loadings of non-agricultural nitrogen in urban groundwater. Impacts of urban growth on surface and ground waters (Proc. IAHS symposium HS5, Birmingham, July 1999). IAHS publ. 259, 117-123
- Livestock Planning and Information Unit (LPIU)-Ministry of Food and Agriculture (2004) *Projected livestock population (for 1997-2007)*. Accra
- Lloyd JW (1986) A review of aridity and groundwater. *Hydrol. Process.* Vol.1, p63-78
- Loheide II SP, Butler JJ, Gorelick SM (2005) Estimation of groundwater consumption by phreatophytes using diurnal water table fluctuations: A saturated-unsaturated flow assessment. *Water resources research*, vol. 41, 2005, 1 of 14
- Martin N (2005) *Development of a water balance for the Atankwidi catchment, West Africa - A case study of groundwater recharge in a semi-arid climate*. Doctoral thesis. University of Göttingen
- Martin N, van de Giesen N (2005) Spatial distribution of groundwater use and groundwater potential in the Volta River basin of Ghana and Burkina Faso. *IWRA Water International* Vol. 30 (2):239-249
- McNamara JP (2005) *An assessment of the potential for using water and chloride budgets to estimate groundwater recharge in granitic, mountain environments*. Final report
- Mearns LO, Giorgi F, Whetton P, Pabon D, Hulme M, Lal M (2004) *Guidelines for use of climate scenarios developed from regional climate model experiments*, Tech. rep., Data Distribution Centre of the IPCC
- Meinzer OE (1923) *The occurrence of groundwater in the United States with a discussion of principles*. US Geol. Surv Water-Supply Pap 489, 321 pp
- Ministry of Works and Housing (1998) *Water Resources Management Study, Information 'Building Block' Study. Part II, Volta Basin System, Groundwater Resources*. Accra: Ministry of Works and Housing
- Monteith JL (1965) *Evaporation and Environment*. Symp. Soc. Expl. Biol. 19, 205-234.
- Morris MD (1991) *Factorial sampling plans for preliminary. Computational experiments*. *Technometrics* 33(2), 161-174
- Morris DA, Johnson AI (1967) *Summary of hydrologic and physical properties of rock and soil materials as analyzed by the Hydrologic Laboratory of the U.S. Geological Survey*, U.S. Geol. Surv. Water-Supply Paper 1839-D, 42p. Nash, J.E., and Sutcliffe, J.V. (1970). *River Flow forecasting through conceptual models. Part I – A discussion of principles*. *J. Hydrol.* 10:282-290

- Moussa R (2008) Significance of the Nash-Sutcliffe efficiency measure for linear rise and exponential recession in event based flood modelling. *Geophysical Research Abstracts*, Vol. 10, EGU2008-A-08369, 2008 SRef-ID: 1607-7962/gra/EGU2008-A-08369 EGU General Assembly 2008
<http://www.fao.org/DOCREP/005/Y3948F/y3948f00.htm#toc>
- Nachabe MH (2002) Analytical expressions for transient specific yield and shallow water table drainage, *Water Resour. Res.*, 38(10), 1193, doi: 10.1029/2001WR001071
- Nash JE, Sutcliffe JV (1970) River Flow forecasting through conceptual models. Part I: A discussion of principles. *J. Hydrol.* 10:282-290
- Ndomba PM, Mtalo FW, Killingtveit A (2005) The Suitability of SWAT model in sediment yield modelling for ungauged catchments: A case study of Simiyu river basin catchments, Tanzania. *Proceedings of the 3rd International SWAT conference, Zurich, 2005*
- Neitsch SL, Arnold JG, Kiniry JR, Williams JR, King KW (2002) *Soil and Water Assessment Tool (SWAT) Theoretical Documentation, Version 2000*, Grassland Soil and Water Research Laboratory, Blackland Research Center, Texas Agricultural Experiment Station, Texas Water Resources Institute, Texas Water Resources Institute, College Station, Texas, 506pp
- Neitsch SL, Arnold JG, Kiniry JR, Srinivasan R, Williams JR (2002) *Soil and Water Assessment Tool (SWAT) User's Manual, Version 2000*, Grassland Soil and Water Research Laboratory, Blackland Research Center, Texas Agricultural Experiment Station, Texas Water Resources Institute, Texas Water Resources Institute, College Station, Texas, 472pp
- Neitsch SL, Arnold JG, Kiniry JR, Srinivasan R, Williams JR (2005) *Soil and Water Assessment Tool Input/Output File Documentation, Version 2005*. Temple, Tex.: USDA-ARS Grassland, Soil and Water Research Laboratory. Available at: www.brc.tamus.edu/swat/doc.html. Accessed on 06.01. 2008
- Nelson RG, Ascough II JC, Langemeier MR (2005) Environmental and economic analysis of switchgrass production for water quality improvement in northeast Kansas. *J. Environ. Mgmt.* 79(4): 336-347
- Niasse M, Afouda A, Amani A (Eds) (2004) *Reducing West Africa's Vulnerability to Climate Impacts on Water Resources, Wetlands and Desertification. Elements for a Regional Strategy for Preparedness and Adaptation*. IUCN, Gland (Switzerland) and Cambridge (UK)
- Nicks AD (1974) Stochastic generation of the occurrence, pattern, and location of maximum amount of daily rainfall. p154-171. In: *Proc. Symp. Statistical Hydrology, Aug.-Sept. 1971, Tuscon, AZ*. U.S. Department of Agriculture, Misc.Publ. No. 1275
- Nkotagu H (1996) Application of environmental isotopes to groundwater recharge studies in a semi-arid fractured crystalline basement area of Domoda, Tanzania, *Journal of African Earth Sciences*, 22, 4, 443-457
- Nyagwambo NL (2006) *Groundwater recharge estimation and water resources assessment in a tropical crystalline basement aquifer*. PhD thesis. UNESCO-IHE, TUDelft. AA Balkema Publishers

- Obuobie, E and Barry, B. 2004. Groundwater Socio-Ecology of Ghana. IWMI-OPEC funded groundwater project studies in selected Sub-sahara African countries. Ghana country report. IWMI Ghana. 41pp
- Odada EO (2006) Freshwater resources of africa: major issues and priorities. Global Water News, No. 3. http://www.gwsp.org/downloads/GWSP_NL3_Internet.pdf
- Ofori-Sarpong E (1983) The drought of 1970-1977 in Upper Volta. In : Singapore J. Trop. Geo. 4, S. 53-61
- Oguntunde PG (2004) Evapotranspiration and complementarity relations in the water balance of the Volta Basin: field measurements and GIS-based regional estimates. Ecology and development series No. 22. ZEF Bonn. Cuvillier Verlag Göttingen
- Opoku-Ankomah Y (2000) Impacts of Potential Climate Change on River Discharge in Climate Change Vulnerability and Adaptation Assessment on Water Resources of Ghana. Water Research Institute (CSIR), Accra. Ghana
- Opoku-Ankomah Y, Dembélé Y, Ampomah BY, Somé L (2006) Hydro-political assessment of water governance from the top-down and review of literature on local level institutions and practices in the Volta Basin. Colombo, Sri Lanka. International Water Management Institute. 36p. IWMI Working Paper 111. www.iwmi.cgiar.org/pubs/working/WOR111.pdf
- Osborn TJ, Hulme M (1997) Development of a relationship between station and grid-box rainday frequencies for climate model evaluation, J. Climate, 10, 1885-1908
- Palacky GJ, Ritsema IL, De Jong SJ (1981) Electromagnetic prospecting for groundwater in Precambrian terrains in the Republic of Upper Volta. Geophysical Prospecting vol. 29, pp932-955
- Prickett TA (1965) Type-curve solution to aquifer tests under water-table conditions. Ground Water 3:5-14
- Priestley CHB, Taylor RJ (1972) On the assessment of surface heat flux and evaporation using large-scale parameters. Mon. Weather. Rev.100:81-92.
- Racsko P, Szeidl L, Semenov M (1991) A serial approach to local stochastic weather models. Ecological Modelling 57, 27-41
- Ritchie JT (1972) Model for predicting evaporation from a row crop with incomplete cover. Water Resour. Res. 8:1204-1213
- Rodgers C, van de Giesen N, Laube W, Vlek PLG, Youkhana E (2007) The GLOWA Volta project: A framework for water resources decision-making and scientific capacity building in a transnational West African Basin. In: E. Craswell, M. Bonell, D. Bossio, S. Demuth, and N. van de Giesen (Editors), Intergrated assessment of water resources and global change (A north-south analysis). Springer, p.295-313
- Rosenthal WD, Srinivasan R, Arnold JG (1995) Alternative River Management using a Linked GISHydrology Model, Transactions of the American Society of Agricultural Engineers, 38(3), 783-790
- Rushton KR (1988) Numerical and conceptual models for recharge estimation in arid and semi-arid zones. In: Simmers I (ed) Estimation of natural groundwater recharge. Reidel publishing company, Dordrecht, The Netherlands. 223-238
- Rushton KR (1997) Recharge from permanent water bodies. In: I. Simmers (Editor), Recharge of Phreatic Aquifers in (Semi) Arid Areas. A.A. Balkema, Rotterdam, p215-255

- Rushton KR, Ward C (1979) The estimation of groundwater recharge. *J. Hydrol.* 41:345-361
- Saleh A, Arnold JG, Gassman PW, Hauck LM, Rosenthal WD, Williams JR, McFarland AMS (2000) Application of SWAT for Upper North Bosque River Watershed. *Trans. ASAE* 45(3): 1077-87
- Sami K, Hughes DA (1996) A comparison of recharge estimates to a fractured sedimentary aquifer in South Africa from a chloride mass balance and an integrated surface-subsurface model. *J. Hydrol.* 179, pp111–136
- Sandwidi WJP (2007) Groundwater potential to supply population demand within the Kompienga dam basin in Burkina Faso. PhD Thesis. Ecology and Development Series, No. 54. Cuvillier Verlag Göttingen. 160pp
- Sanford W (2002) Recharge and groundwater models: An overview. *Hydrogeol. J.*, 10: 110-120
- Sangrey DA, Harrop-Williams KO, Klaiber JA (1984) Predicting groundwater response to precipitation. *ASCE J. Geotech. Eng.* 110(7): 957-975
- Santhi C, Arnold JG, Williams JR, Dugas WA, Srinivasan R, Hauck LM (2001) Validation of the SWAT Model on a Large River Basin with Point and Nonpoint Sources, *Journal of the American Water Resources Association*, Vol. 37, No. 5, 1169-1188pp
- Scanlon BR, Healy RW, Cook PG (2002) Choosing appropriate techniques for quantifying groundwater recharge. *Hydrogeology Journal* (2002) 10:18–39. DOI 10.1007/s10040-0010176-2. <http://dx.doi.org/10.1007/s10040-001-0176-2>
- Scanlon BR, Keese K, Reedy RC, Simunek J, Andraski BJ (2003) Variations in flow and transport in thick desert vadose zones in response to paleoclimatic forcing (0–90kyr): field measurements, modeling, and uncertainties. *Water Resources Research* 39: 1179, DOI: 1110D1029/2002WR001604
- Schmidli J, Frei C, Vidale PL (2005) Downscaling from GCM precipitation: A benchmark for dynamical and statistical downscaling methods, *Int. J. Climatol.*, accepted
- School J, Abbaspour KC (2006) Calibration and uncertainty issues of a hydrological model (SWAT) applied to West Africa. *Advances in Geosciences*, 9: 137–143.
- School J, Abbaspour KC, Srinivasan R, Yang H (2008) Estimation of freshwater availability in the West African sub-continent using the SWAT hydrologic model *Journal of Hydrology*. 2008(352):30-49
- Semenov MA, Brooks RJ, Barrow EM, Richardson CW (1998) Comparison of the WGEN and LARS-WG stochastic weather generators in diverse climates. *Climate Research* 10, 95-107
- Semenov MA, Barrow EM (2002) LARS-WG: A stochastic weather generator for use in climate impact studies. Version 3.0. User manual <http://www.rothamsted.ac.uk/mas-models/download/LARS-WG-Manual.pdf>
- Servat E, Paturol JE, Lubès H, Kouamé B, Ouedraogo M, Masson JM (1997) Climatic variability in humid Africa along the Gulf of Guinea, Part I: Detailed analysis of the phenomenon in Côte d'Ivoire, *Journal of Hydrology*, 191, 1-15
- Shahin M (2002) Hydrology and water resources of Africa. Water Science and Technology library. Kluwer academic publisher, Dordrecht, Netherlands. 659p
- Simmers I (ed) (1988) Estimation of natural groundwater recharge. NATO ASI series. Series C: mathematical and physical sciences. D. Reidel publishing company, Dordrecht, The Netherlands, 510pp

- Sintondji L (2005) Modelling of process rainfall-runoff in the Upper Quémé catchment area (Terou) in a context of climate change: extrapolation from the local scale to a regional scale. PhD Thesis. Shaker Verlag, Aachen, Germany
- Smedley PL (1996) Arsenic in rural groundwater in Ghana. *Journal of African Earth Sciences* 22 (4): 459-470
- Soil Conservation Service (1972) Section 4: Hydrology. In: National Engineering handbook. SCS
- Soil Conservation Service Engineering Division (1986) Urban hydrology for small watersheds. U.S. Department of Agriculture, Technical release 55
- SONABEL (2003) Barrage de la KOMPIENGA. Informations hydrologiques et énergétiques de 1988 à 2002. Division hydraulique KOMPIENGA
- Sophocleous M (1985) The role of specific yield in ground-water recharge estimations: A numerical study: *Ground Water*, v. 23, no. 1, p 52-58
- Sophocleous MA, Schloss JA (2000) Estimated Annual Groundwater Recharge. <http://www.kgs.ukans.edu/HighPlains/atlas/atrch.htm>, Lawrence, Kansas
- Srinivasan R, Arnold JG (1994) Integration of a basin-scale water-quality model with GIS. *Water Resources Bulletin* 30(3):453-462
- Stone WJ (1992) Paleohydrologic implications of some deep soil water chloride profiles, Murray Basin, South Australia. *J. Hydrol.* 132:201-223
- Storm B (1988) Modeling of saturated flow and the coupling of surface and subsurface flow. In: D.S. Bowles and P. E. O'Connell (eds). *Recent Advances in the Modeling of hydrologic systems*, 185-2003. 1991 Kluwer Academic Publishers. Printed in the Netherlands
- Sumioka SS, Bauer, HH (2004) Estimating groundwater recharge from precipitation on Whidbey and Camano Islands, Island County, Washington, Water Years 1998 and 1999. Water-Resources Investigations Report 03-4101, Version Number 1.20, August 2004. U.S. Geological Survey
- Taylor JC, van de Giesen N, Steenhuis TS (2006) West Africa: Volta Discharge Data Quality Assessment and Use. *Journal of the American Water Resources Association (JAWRA)* 42(4):1113-1126
- Thierry D (1990) Analysis of long duration piezometric records from Burkina Faso to determine aquifer recharge, in D.N. Lerner, A.S. Issar, I. Simmers (Eds.): *Groundwater Recharge-A guide to understanding and estimating natural recharge; International Contributions to Hydrogeology*, 8, International Association of Hydrogeologists. Heise, Hannover
- Thorpe AJ (2005) Climate change prediction. A challenging scientific problem. A paper produced on behalf of the Institute of Physics, London, UK
http://www.ncas.ac.uk/publications/iop_thorpe_climate_change_prediction.pdf
- Tindall JA, Kunkel JR (1999) *Unsaturated Zone Hydrology for Scientists and Engineers*, Prentice Hall
- Tripathi MP, Panda RK, Raghuwanshi NS (2003) Identification and Prioritisation of Critical Subwatersheds for Soil Conservation Management using the SWAT Model. *Biosystems Engineering* (2003) 85(3):365-379, doi:10.1016/S1537-5110(03)00066-7
- UNESCO (2004) *Water resources in the OSS (Observatory of the Sahara and the Sahel) countries: evaluation, use and management*
- UNESCO (2007) *White Volta (Ghana)*. http://portal.unesco.org/science/en/ev.php-URL_ID=3755&URL_DO=DO_PRINTPAGE&URL_SECTION=201.html

- U.S. Geological Survey (2008) Groundwater recharge. Accessed on August 21, 2007, at http://water.usgs.gov/ogw/gwrp/activities/gw_recharge.html
- UNEP (2002) State of the environment and policy retrospective: 1972-2002. In: Global environment outlook 3: past, present and future retrospectives. Accessed on December 17, 2007, at <http://www.grid.unep.ch/geo/press.htm>
- UN-Water/Africa (2006) African water development report 2006, Economic Commission for Africa, Addis Ababa, Ethiopia
- van de Giesen NC, Andreini M, van Edig A, Vlek PLG (2001) Competition for water resources of the Volta basin. Regional Management of Water Resources. Proceedings of a symposium held during the Sixth IAHS. Scientific Assembly at Maastricht, the Netherlands, July 2001. IAHS Publ. no. 268. 2001
- van der Sommen JJ, Geirnaert W (1988) On the continuity of aquifer systems on the crystalline basement of Burkina Faso. In: Simmers I (ed) Estimation of natural groundwater recharge. Reidel publishing company, Dordrecht, The Netherlands. 29-45
- van Griensven A, Meixner T (2006) Methods to quantify and identify the sources of uncertainty for river basin water quality models, *Water Sci. Technol.*, 53(1), 51-59
- van Griensven A, Francos A, Bauwens W (2002) Sensitivity analysis and auto-calibration of an integral dynamic model for river water quality, *Water Science and Technology*, 45(5), 321-328
- von Storch H, Zorita E, Cubasch U (1993) Downscaling of global climate change estimates to regional scales: An application to Iberian rainfall in wintertime. - *J. Climate* 6: 1161-1171
- Wardrop and Associates Limited (1977) CIDA Ghana Upper Region Water Supply Project, Phase 1, Hydrogeological report based on 1460 well supplies, Canada International Development Agency
- Water Research Institute (2002) Info Water. Quarterly Newsletter of the CSIR Water Research Institute. Volume 1, Issue 1. June 2002
- VBRP (2002) Volta Basin Research Project water resources management GIS maps on the Volta Basin. Accra, Ghana
- Wilby RL, Charles SP, Zorita E, Timbal B, Whetton P, Mearns LO (2004) Guidelines for use of climate scenarios developed from statistical downscaling methods. http://www.ipcc-data.org/guidelines/dgm_no2_v1_09_2004.pdf
- Williams JR (1995) Chapter 25: The EPIC model. p. 909-1000. In V.P. Singh (ed). Computer models of watershed hydrology. Water Resources Publications, Highlands Ranch, CO
- Williams JR, Hann RW (1973) HYMO: Problem-oriented language for hydrologic modeling-User's manual. USDA, ARS-S-9
- Wood WW, Sanford WE (1995) Chemical and isotopic methods for quantifying ground-water recharge in a regional, semi-arid environment; *Ground Water*, 33 (3), p458-468
- WRI (2003) Watersheds of Africa: Water Resources eAtlas Land Cover and Use Variables: A19 Volta. World Resources Institute
- WRRI/DANIDA (1993) Rural drinking water supply and sanitation project in the Volta Region: Inventory and assessment of potential for hand dug wells in the Volta region, Ghana. WRI project report, Accra, Ghana

References

- Wu K, Xu YJ (2006) Evaluation of the applicability of the swat model for coastal watersheds in southeastern Louisiana. *Journal of the American water resources association* 42 (5), 1247 - 1260
- Xu Y, van Tonder GJ (2001) Estimation of recharge using a revised CRD method. *Water SA*, Vol. 27, No. 3, pp. 341-343
- Xu Y, Beekman HE (Eds) (2003) *Groundwater recharge estimation in Southern Africa*. UNESCO IHP Series No. 64, UNESCO Paris. ISBN 92-9220-000-3

ACKNOWLEDGEMENTS

This thesis has been realized by the grace and mercy of the Almighty God. I will be forever thankful to Him for his provision, protection and guidance during my stay in Bonn.

I want to sincerely thank Prof. Dr. Bernd Diekkrüger, vice chair of the department of Geography, University of Bonn, for the interest he had in my thesis from the beginning of my PhD studies and for providing me with the needed scientific support and supervision to realize this thesis. I am very grateful to him. I also want to thank Prof. Dr. Barbara Reichert, Steinmann Institute, University of Bonn, for the time and efforts she put into this thesis as the second supervisor. I am grateful for all her support. I am grateful to Prof. Dr. Andreas Hense, Meteorology Institute, University of Bonn and Prof. Dr. Richard Sikora, Faculty of Agriculture, University of Bonn, for their roles as members of my PhD committee.

I acknowledge the invaluable contribution, inspiration and advice I received from Dr. Charles Rodgers, formally at the Center for Development Research (ZEF), Bonn, during the proposal development and field research stages of this thesis.

I am grateful for the academic, logistics and social support I received ZEF throughout my academic work in Bonn. I am very pleased with the education I received from ZEF and the invaluable learning experiences made available to me have expanded and strengthened my research skills. In particular, I am grateful to Prof. Dr. Paul L.G. Vlek, Director of ZEFc, for the invaluable inspiration and encouragement I received from him. I would also like to thank Dr. Günther Manske, academic coordinator at ZEF, for his assistance with academic issues and for organizing lively gatherings like barbeques and parties that fired up my social life. A special thank you to Mrs. Rosemary Zabel, Administrative Assistant, ZEF, for the invaluable administrative support she gave me during my stay in Bonn. She has been extremely helpful and I sure will remember her for a long time to come.

My PhD studies could not have been possible but for the financial support from the German Federal Ministry for Economic Cooperation and Development (BMZ) via the German Academic Exchange Services (DAAD) and the German Technical Cooperation (GTZ), and the German Federal Ministry of Education and Research via the GLOWA Volta project. I am highly grateful to these institutions for their generosity.

I want to thank the International Water Management Institute (IWMI) Ghana for providing me with an office space during the field research phase of this thesis.

A large number of individuals helped me in one way or the other to realize this thesis and their efforts are worth acknowledging. Thanks go to Henning Busche and Claudia Hiepe (GLOWA IMPETUS project) and Dilnesaw Chekol (formally GLOWA Volta project), who assisted me in solving some of the difficulties I encountered with the SWAT model used in this thesis. I acknowledge the assistance received from Dr. Wilson Agyare, Kwame Nkrumah University of Science and Technology, Ghana, and Dr. Mathias Fosu, Savannah Research Institute, Ghana, regarding soil sampling during my field research. Special thanks to the GLOWA Volta team in Ghana (Dr. Boubacar Barry, Daniel Ofori, Benjamin Haywood, David Kwesi Orchard, Eli Sokpli and Salisu Adams) for the logistic support I received from them during the field research stage of this thesis.

Last but not least, I want to thank Mr. William Agyekum, Water Research Institute, Ghana, for working with me regarding water level monitoring in the White Volta river basin of Ghana.

Finally, my sincere thanks go to my family and friends who supported me immensely with their prayers and encouragements.